Role of DDB2 in senescence and EMT

BY

NILOTPAL ROY

M.Sc, University of Calcutta, 2006

THESIS

Submitted as partial fulfillment of the requirements
for the degree of Doctor of Philosophy in Biochemistry and Molecular Genetics
in the graduate college of the
University of Illinois at Chicago, 2012

Chicago, Illinois

Defense committee:

Pradip Raychaudhuri, Chair and Advisor
Nissim Hay, Biochemistry and molecular genetics
Karen Colley, Biochemistry and molecular genetics
Vadim Gaponenko, Biochemistry and molecular genetics
Bin He, Microbiology and immunology

I am dedicating this thesis to my parents and Prof. Raychaudhuri, without whom this work would never have been accomplished.

ACKNOWLEDGEMENTS

I am greatly indebted to my thesis advisor Dr. Pradip Raychaudhuri for his exceptional support, mentorship and encouragement during the years of my PhD.

I would like to thank all my committee members- Dr. Nissim Hay, Dr. Karen Colley, Dr. Vadim Gaponenko and Dr. Bin He for their valuable suggestions regarding my thesis project.

I thank my entire family for their outstanding support, especially my parents- Debasish and Krishna Roy and my wife, Shivani.

TABLE OF CONTENTS

TABLE OF CONTENTS (Continued)

CHAPTER PAGE

LIST OF FIGURES

LIST OF FIGURES (CONTINUED)

LIST OF ABBREVIATIONS

CPD	Cyclobutane Pyrimidine dimers
CSA	Cockayne syndrome A
CSB	Cockayne syndrome B
Cul4a	Cullin4a
DAPI	4,6-diamidino-2-phenylindole
DCFDA	2,7-dicholorofluorescein diacetate
DDB1	Damaged DNA binding protein 1
DDB2	Damaged DNA binding protein 2
GG-NER	Global genomic nucleotide excision repair
TC-NER	Transcription coupled nucleotide excision repair
IP	Immunoprecipitation
IR	Ionizing radiation
MEF	Mouse embryonic fibroblast
NER	Nucleotide excision repair
RT-PCR	Reverse transcription polymerase chain reaction
UV	Ultra violet
WT	Wild type
XPE	Xeroderma Pigmentosum group E
XPC	Xeroderma Pigmentosum group C
ROS	Reactive oxygen species
SOD	Superoxide dismutase
PEITC	Phenethyl Isothiocyanate

LIST OF ABBREVIATIONS (continued)

ChIP	Chromatin Immunoprecipitation
6-4PP	(6-4) pirimidone photodimers (6-4 photoproducts)
EMT	Epithelial to mesenchymal transition

SUMMARY

I have studied the role of Damaged DNA binding protein 2 (DDB2) as a tumor suppressor. DDB2 is a DNA repair protein that is involved in the repair of UV induced DNA damage lesions, cyclobutane pyrimidine dimers and 6-4 photoproducts. Consistent with that DDB2-/- mice exhibit increased skin tumorigenesis in response to UV irradiation. These mice also develop spontaneous malignant tumor at a high frequency. My work revealed two new tumor suppressor functions of DDB2: a role in senescence and as an inhibitor of epithelial to mesenchymal transition (EMT). These new tumor suppressor functions are related to the role of DDB2 as a transcriptional repressor. I showed that DDB2 deficient cells do not undergo premature senescence after culture shock, exogenous oxidative stress, oncogenic stress or DNA damage. The deficiency in senescence results from lack of ROS accumulation. Further investigation revealed that DDB2 causes ROS accumulation by epigenetically inhibiting expression of two important anti-oxidant genes, MnSOD and Catalase. These findings were further substantiated in mice by using CCl4 induced liver fibrosis and UV induced skin carcinogenesis. As an extension of my work on delineating tumor suppressive role of DDB2, I investigated the role of DDB2 in colon cancer, as reduced DDB2 expression correlates with aggressive progression of colon carcinoma. Loss of DDB2 expression increases tumorigenecity of colon cancer cells in vitro and in vivo. A closer analysis attributed this increased tumorigenecity phenotype to a regulation of EMT and resistance to anoikis. Further findings indicated that the EMT regulation by DDB2 is related to

transcriptional repression of VEGF, Snail1 and Zeb1. Concordantly, DDB2 deficient colon carcinoma cells are more metastatic. Thus, loss of DDB2 expression results in a deficiency in senescence and increased EMT leading to an aggressive cancer progression. Hence, targeting DDB2 expression would be beneficial from therapeutic perspective. Towards that, I have used a naturally occurring compound Phenethyl Isothiocyanate (PEITC) to elevate expression of DDB2 and inhibit tumorigenesis in mice. Together, my observation provide new insights on the role of DDB2 as a tumor suppressor through its regulation of senescence and metastasis related to EMT. Also, my work shows how DDB2 can be therapeutically targeted for the treatment of colon cancer.

1.INTRODUCTION

1.1 DDB2 IS MUTATED IN XERODERMA PIGMENTOSUM GROUP E (XPE)

Xeroderma Pigmentosum is a rare autosomal hereditary disorder characterized by hypersensitivity to sunlight and predisposition to skin tumor development upon exposure to Ultraviolet light (UV)[1]. The UV rays in sunlight causes variety of DNA damage lesions such as cyclobutane pyrimidine dimers (CPD) and 6-4 photoproducts (6-4 PPs). Cell constantly repairs these damages to prevent accumulation of unwanted mutations. Nucleotide excision repair (NER) is a particularly important mechanism by which cell is able to repair aforementioned UV induced DNA damage lesions (Fig. 1) [2]. NER is a multi-step process requiring involvement of several proteins. Xeroderma Pigmentosum is a genetic defect in which NER enzymes are mutated resulting deficiency in the repair pathway, leading to high frequency skin carcinoma development upon UV exposure [3, 4]. Based on somatic cell fusion experiments 8 complementation groups (XPA, XPB, XPC, XPD, XPE, XPF, XPG AND XPV) for XP have been characterized. XPA through XPG encode proteins directly involved in NER. Unlike these Xeroderma Pigmentosum variants, XP-V cells execute normal NER but are defective in the replication of UV damaged DNA. Later studies revealed DNA polymerase eta as the XPV gene product [5].

The XPE gene encodes Damaged DNA binding protein 2 (DDB2), the smaller subunit of the damaged DNA binding protein DDB. DDB is a heterodimeric protein complex that possesses a very high affinity for CPDs and 6-4 PPs. DDB recognizes UV damaged DNA as well as DNA damage caused by Cisplatin, abasic sites and single

stranded DNA [1]. The DDB1 gene is strongly conserved among the eukaryotes. Homologs of DDB1 are found in the plant *Arabidopsis thaliana*, the slime mold *Dictyostelium discoideum*, the fission yeast *Schizosaccharomyces pombe*, fruit fly *Drosophila melanogaster* and the nematode *Caenorhabditis elegans*. However, homologs of human DDB2 are found only in other mammals. DDB2 amino acid sequences between human and mice are only 73% identical. DDB2 is expressed ubiquitously in human tissue with higher expression in testes, liver, kidney, corneal endothelium and lower expression in brain, skin, lung, muscle and heart.

Cells from individuals suffering from XPE exhibit deficient NER [6, 7]. The NER defect can be restored in XPE cells by microinjection of purified DDB, demonstrating that DDB, and thus DDB2, is necessary to carry out efficient NER [8]. The cDNAs encoding the DDB complex were isolated, cloned and characterized. DNA sequencing analysis revealed that DDB2 is mutated in the XPE patients. These individuals have mutation in DDB2 that leads to single amino acid substitution or c-terminal truncation. Naturally occurring mutants of DDB2 carry single amino acid substitution in the DDB2 WD motif, a short motif of approximately 40 amino acids involved in protein- protein interaction often terminating in Tryptophan- Aspartic Acid (Trp-Asp) dipeptide.

To characterize the role of DDB2 in NER, several labs generated mice lacking DDB2 expression. Consistent with the phenotype of XPE patients, DDB2-/- mice are predisposed to UV induced skin carcinoma formation [9-11]. It is noteworthy that,

of all the XP groups, XPE subgroup patients exhibit mildest phenotype with regard to sun sensitivity. [1]. Enhanced expression of DDB2 in mice reduced UV induced skin carcinogenesis by both delaying the onset of tumor development and by attenuating the number of tumor occurrence in each mouse [11]. This provides further evidence that DDB2 is necessary to inhibit UV induced skin carcinogenesis. Interestingly, the DDB2-/- mice also develop spontaneous malignant tumor at a very high frequency. Tumors are of wide spectrum with frequent incidence of hematopoietic neoplasms and lymphomas [10, 12].

1.2 ROLE OF DDB2 IN NER

DDB2, along with DDB1, associates with Cul4a, an E3 ligase of Ubiquitin mediated proteasomal degradation pathway. Cul4 utilizes WD40-like repeat containing proteins as an adapter molecule. DDB2, also a WD40 repeat containing protein, acts as a substrate receptor molecule for Cul4a E3 ligase complex, in which DDB1 serves as the linker protein [13]. Interestingly, XPE mutants are unable to bind to Cul4a suggesting role of the Cul4a-DDB2 complex in NER [14]. The well-characterized targets of Cul4a-DDB1-DDB2 complex are XPC, p21 and DDB2, which are all involved in the repair pathway further underscoring the importance of the protein ubiquitination activity of DDB2 [15-17].

The precise role DDB2 plays in NER is a point of controversy. There are several models. Many of the suggested models involve the role of DDB2 in protein ubiquitination. Initial reports suggested that DDB2 recruits DDB1 to the nucleus and

Figure 1: Model depicting the factors involved in global genomic NER and transcription coupled NER.
TC-NER and GG-NER involves three steps: 1) Damage recognition 2) Opening of helix containing DNA damage lesion 3) Repair synthesis and ligation

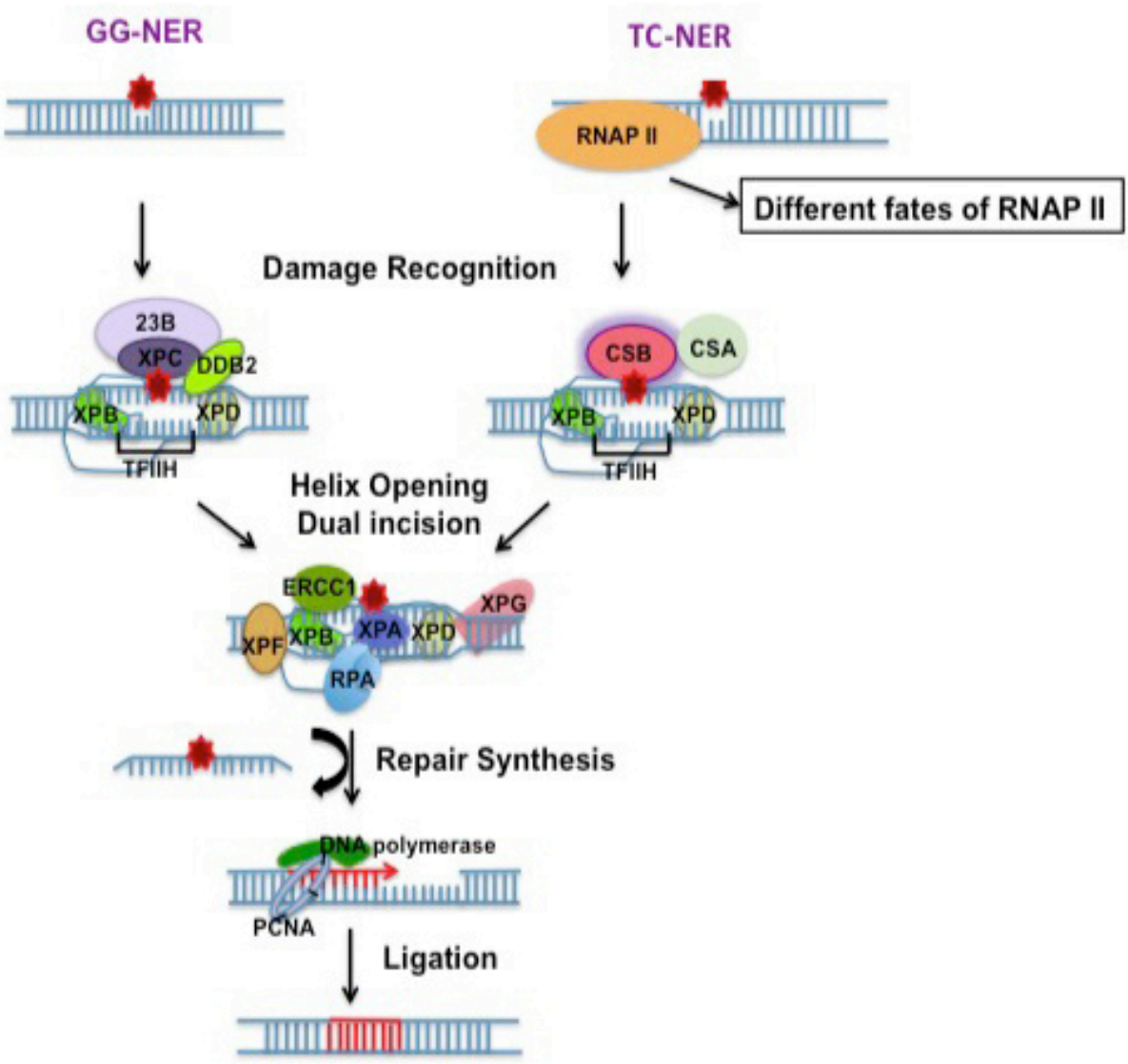
GG-NER
TC-NER
RNAP II
Different fates of RNAP II
Damage Recognition
23B
XPC
DDB2
XPB
XPD
TFIIH
CSB
CSA
XPB
XPD
TFIIH
Helix Opening
Dual incision
ERCC1
XPG
XPF
XPB
XPA
XPD
RPA
Repair Synthesis
DNA polymerase
PCNA
Ligation

recognizes the UV induced DNA damage lesions [18-20]. Following damage recognition, the Cul4a-DDB1-DDB2 complex recruits XPC at the damage site and ubiquitinates XPC [17]. DDB2 itself also gets ubiquitinated in the process. Ubiquitination of DDB2 results loss of its DNA binding activity followed by proteasomal-mediated degradation. However, XPC ubiquitination potentiates its binding to the DNA and activates the repair process [17]. Other studies also linked the DNA repair activity of DDB2 to its protein ubiquitination function. For example, the Cul4a-DDB1-DDB2 complex has been shown to mono-ubiquitinate histones (H2A, H3 and H4) at the DNA damage site, modulating the chromatin structure to help the repair factors gain access to the lesion [21, 22]. Moreover, H3/ H4 ubiquitination has been found also to play an important role in recruiting XPC to the damaged chromatin [22]. DDB2 was reported also to associate with histone acetyl transferase CBP/ p300 [23]. Moreover, DDB2 was found also to be a component of histone acetylating transcriptional co-activator STAGA complex [24], which possesses chromatin-remodeling activity. A recent report suggested that DDB2 plays role in chromatin decondensation at UV induced DNA lesion independent of the protein ubiquitination activity [25]. DDB2 was found to attenuate the density of core histones in the chromatin containing UV induced DNA damage lesions. This function of DDB2 is ATP dependent and involves poly(adenosine diphosphate [ADP]-ribose) polymerase 1. However, no genetic evidence is available for these models.

Ataxia telangiectasia mutated kinase (ATM) and Ataxia telangiectasia RAD3 –related

Figure 2: Model depicting role of DDB2 in NER.
Cul4a-DDB1-DDB2 complex results ubiquitin mediated proteasomal degradation of p21 and p53S18 resulting low-level accumulation of p21, a condition conducive to repair synthesis.

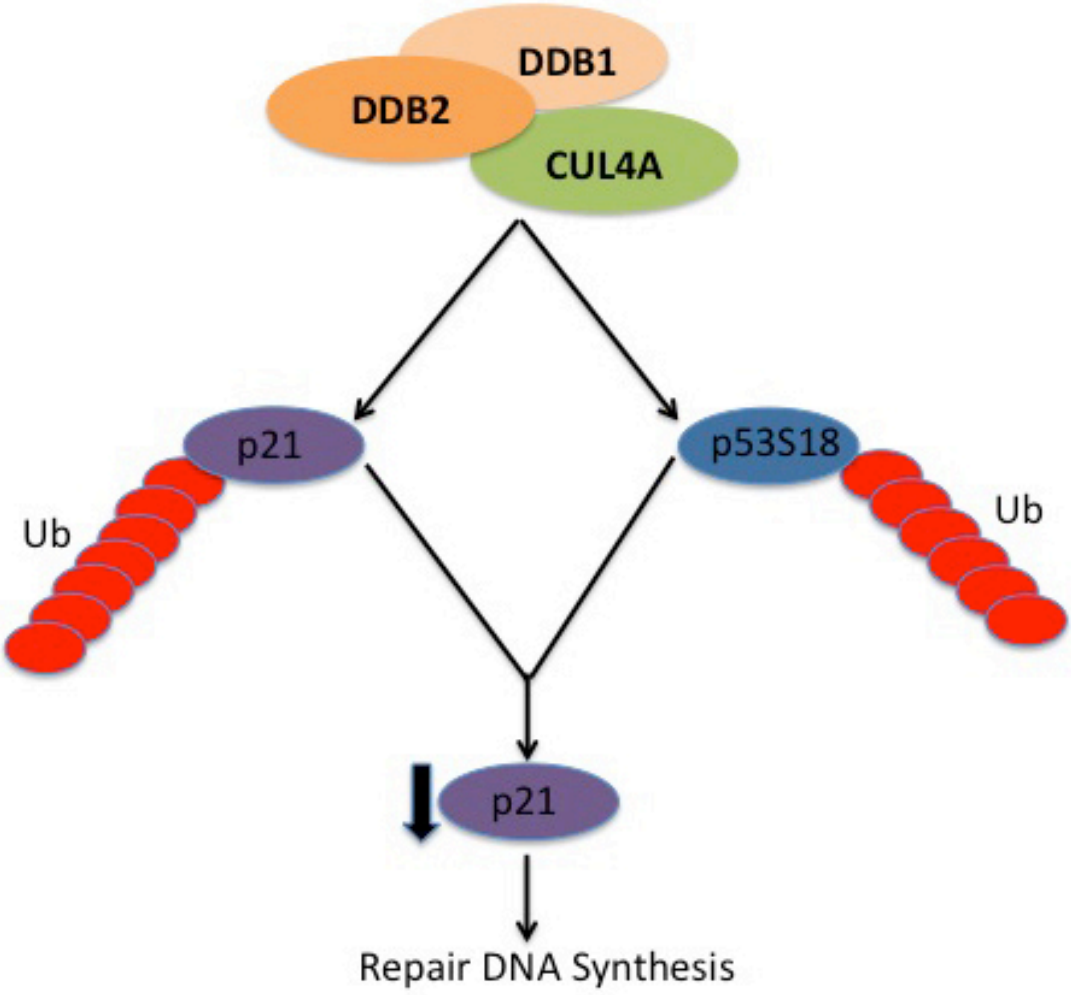
DDB1
DDB2
CUL4A
p21
p53S18
Ub
Ub
p21
Repair DNA Synthesis

kinase (ATR) are activated following DNA damage and recruited to the damaged DNA lesion [26]. Activated ATM and ATR phosphorylate downstream effector p53 at residues Ser15 in human/ Ser18 in mouse [27]. Ser18 phosphorylation in mouse does not augment the stability of p53, but rather renders p53 transcriptionally more active [28]. In low dose UV irradiated cells, DDB2 keeps p53 Ser18P level low, but does not regulate the cellular level of total p53 [29]. DDB2 mediated degradation of p53 Ser18P involves the ubiquitin mediated proteasome pathway. DDB2 imports DDB1 from the cytoplasm to the nucleus following low dose UV. The DDB1-DDB2 complex in association with Cul4a causes proteolysis of p53 Ser18P. By degrading p53Ser18P, DDB2 regulates the level of p21, which is a direct transcriptional target of p53 following DNA damage [30]. Moreover, DDB2 regulates p21 at the protein level through its ability to induce proteolysis of p21 [16]. p21 has been reported to impede DNA repair by sequestering proliferating cell nuclear antigen (PCNA), an important factor for repair synthesis. PCNA acts as a DNA clamp to recruit DNA polymerase δ onto the DNA. Thus, by attenuating expression of p21, DDB2 ensures efficient DNA repair activity. In the absence of functional DDB2 expression, high-level p21 sequesters PCNA and inhibits the repair synthesis function. In agreement with that, deletion of p21 in the DDB2-/- background eliminated the repair deficiency of DDB2-/- cells. These observations provide clear genetic evidence for a role of DDB2 in the global genomic NER pathway through its regulation of p21 (Fig. 2).

1.3 REGULATION OF DDB2

DDB2 is a p53-regulated gene in human [31]. Following UV irradiation, p53 transcriptionally activates DDB2 expression [32]. Further studies identified a p53 response element in the promoter region of DDB2. Interestingly, DDB2 was reported also to regulate p53 expression directly [33]. Hence, a positive feed back loop between DDB2 and p53 was suggested, where p53 activates DDB2 expression and DDB2 regulates activation of p53. However, in murine cells there is no p53 response element in the DDB2 promoter region even though the mouse DDB2 gene shares significant sequence identity with the human gene [32]. Accordingly, p53 failed to transactivate DDB2 expression following UV irradiation in murine cells.

p38MAPK has been shown to regulate DDB2 expression [34]. Moreover, p38MAPK has been suggested to facilitate NER following UV irradiation through phosphorylation of Histone H3 at serine 10 and subsequent alteration of chromatin structure. That study also indicated that p38MAPK is involved in UV-induced serine phosphorylation of DDB2. Phosphorylation of DDB2 leads to ubiquitin mediated proteasomal degradation. Degradation of DDB2 allows subsequent recruitment of critical pre-incision NER factor XPC and TFIIH. Interestingly, an earlier study reported that c-Abl tyrosine kinase phosphorylates DDB2 and inhibits its activity [35]. However, IR, but not UV augments the tyrosine kinase activity of c-Abl. Hence, the physiological significance of this regulation is unclear.

DDB2 is a cell cycle regulated gene. It is present at a low level in growth arrested primary human fibroblasts. Following serum addition, DDB2 level peaks at the G1/S boundary[15]. The cell cycle regulation of DDB2 partly involves post-transcriptional mechanism. It is degraded in S phase by the Cul4a-DDB1 complex. Interestingly, DDB2 also associates with COP9 signalosome complex, which participates in proteolysis through ubiquitin-proteasome pathway [36, 37].

Analysis of transcriptional regulatory region of DDB2 revealed core promoter region associated with cell cycle regulating/ regulated genes: no TATA box, a G/C rich region, a NF-1 element and multiple Sp1 elements [38]. Furthermore, an active E2F element was also identified on the DDB2 promoter.

1.4 INVOLVEMENT OF DDB2 IN APOPTOSIS

Recent studies also implicated DDB2 in biochemical pathways other than DNA repair. The spontaneous tumor development with DDB2-/- mice strongly suggested other important tumor suppressor functions of DDB2. In agreement with that, DDB2 was found to be an important mediator of apoptosis following DNA damage [16, 39]. The XPE cells were found to be deficient in UV mediated apoptosis response [9]. Later studies revealed that the DDB2 deficient MEFs or human carcinoma cells are resistant to apoptosis induced by a variety of agents, including IR, chemotherapeutic drugs and E2F1 [16]. Also, keratinocytes from the DDB2-/- mice are resistant to UV induced apoptosis. Further studies revealed that the apoptosis promoting function of DDB2 is linked to its ability to regulate expression of p21. p21 has been shown to

Figure 3: Role of DDB2 in apoptosis.
DNA damage results p53 mediated up-regulation of DDB2. DDB2 in turn results ubiquitin mediated proteasomal degradation of p21. Low p21 level allows the cell to undergo apoptosis.

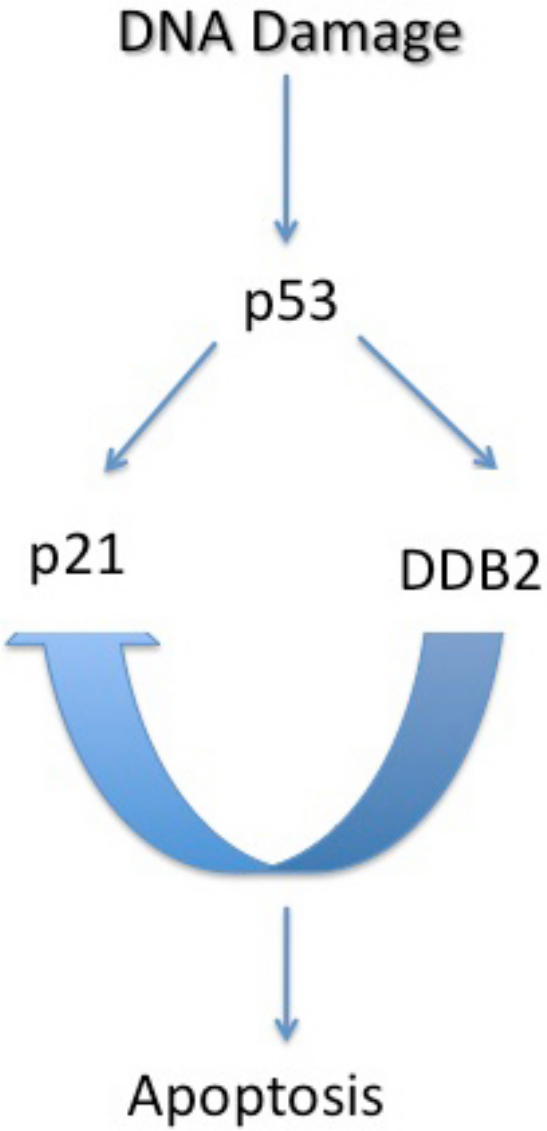
DNA Damage
p53
p21
DDB2
Apoptosis

exhibit anti-apoptotic effect by multiple mechanisms [40]. One mechanism involves p21 mediated inhibition of S phase progression. p21 may also inhibit apoptosis by interacting with pro-apoptotic molecules pro-caspase 3, caspase 8, ASK1. In the DDB2-/- cells there is high-level accumulation of p21 , which inhibits the apoptosis response (Fig. 3). In agreement with that the DDB2-/- p21-/- cells show efficient apoptosis response after DNA damage. DDB2 has also been implicated in augmenting apoptosis response by chemotherapeutic drug Cisplatin through attenuation of anti-apoptic protein Bcl-2 expression [41]. In contrast, one study implicated DDB2 in protecting against UV induced apoptotic response by up-regulation of anti-apoptotic protein cFLIP [42].

As a part of my thesis research, I observed that DDB2 plays a very important role during oxidative stress induced cellular senescence. Below, I have included an introduction to cellular senescence.

1.5 OXIDATIVE STRESS AND SENESCENCE

Cellular senescence is defined by the irreversible inability of the cell to divide. Senescent cells generally undergo growth arrest at G1 phase of the cell cycle, though they are metabolically active [43]. In contrast to quiescent cells, which undergo reversible cell cycle arrest at G0 phase, senescent cells essentially undergo permanent cell cycle arrest. Except for a few experimental manipulations, general physiological stimuli fail to restore cell division in senescent cells. When grown in cell culture medium, human diploid fibroblasts undergo 60 to 80 population

doublings, after which they cease proliferation and enter into the stage of replicative senescence characterized by enlarged and flattened morphology, increased granularity, and enhanced senescence-associated β-galactosidase (SA-β-Gal) activity [44]. Telomere is a region of repetitive nucleotide sequence at the end of the chromosome that protects chromosomes from deterioration and end-fusion with neighboring chromosomes. With the proliferation of somatic cells, there is a gradual loss of telomere sequences. The progressive loss of telomere length contributes to induction of senescence in normal cells. Dysfunctional telomere causes activation of DNA damage checkpoint response that triggers downstream effector proteins to induce senescence. Senescent human fibroblasts display molecular markers characteristic of DNA double stranded break, such as phosphorylated H2AX; DNA damage checkpoint factors 53BP1, MDC1 and NBS1 [43]. Furthermore, there is activation of DNA damage checkpoint proteins Chk1 and Chk2 that further supports the notion that telomere dysfunction initiates a DNA damage response that leads to senescence. In contrast, cancer cells maintain their immortality by up-regulating expression of the telomere-maintaining enzyme telomerase. Also, expression of oncoproteins in pre-senescent cells inactivates p53 and Rb, two critical regulators of senescence. Thus, cancer cells circumvent the process of senescence to become immortalized.

Senescence can be triggered also by external stimuli, such as oncogene, DNA damage, oxidative stress or culture shock (Fig. 4) [45, 46]. This type of telomere

Figure 4: Critical pathways regulating senescence.
Senescence can be triggered by different internal and external stimuli. These stimuli induce expression of p16INK4a and/or p19Arf that targets downstream effector molecules such as p53 and Rb to induce senescence response.

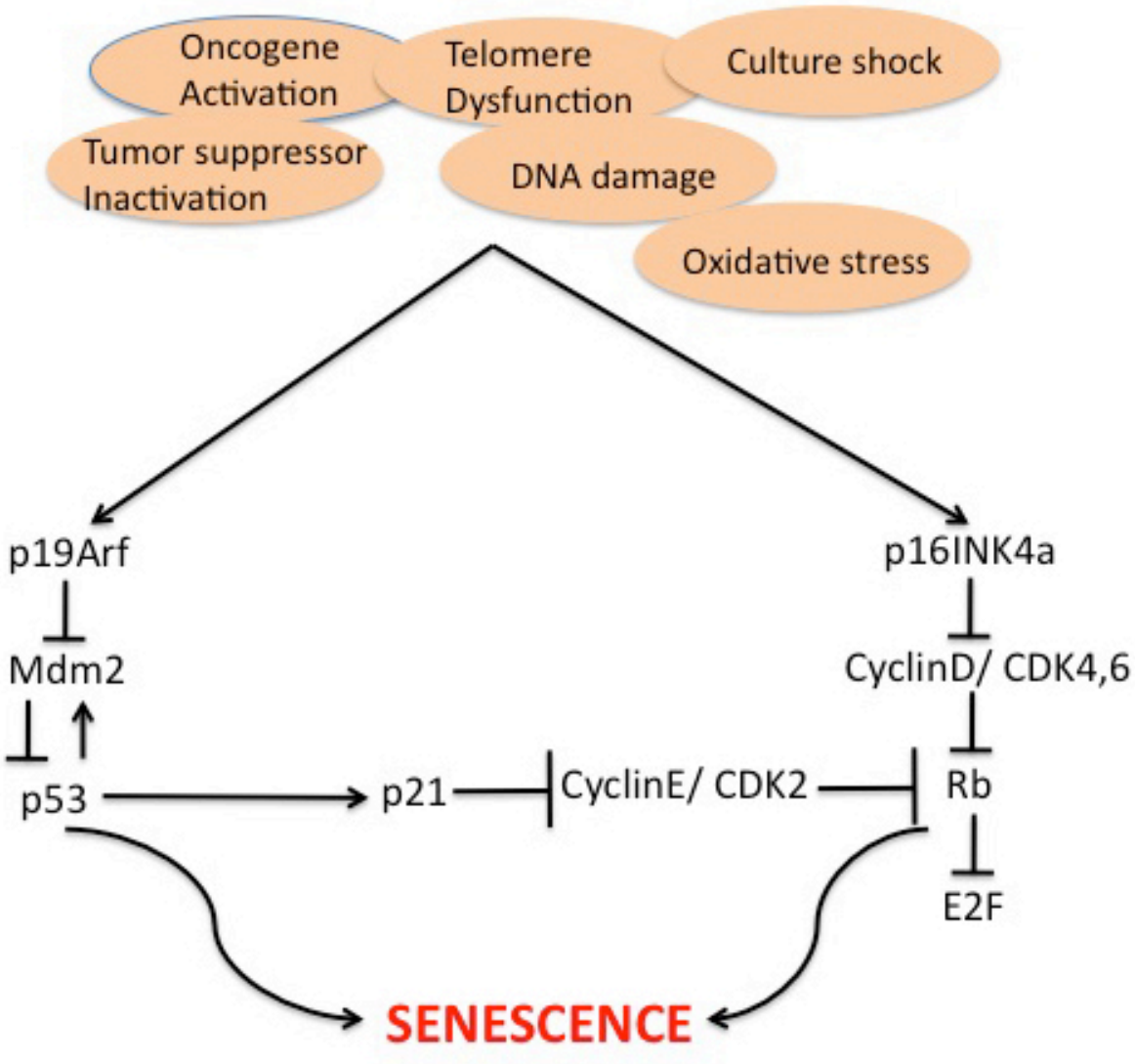
Oncogene Activation
Telomere Dysfunction
Culture shock
Tumor suppressor Inactivation
DNA damage
Oxidative stress
p19Arf
p16INK4a
Mdm2
CyclinD/ CDK4,6
p53
p21
CyclinE/ CDK2
Rb
E2F
SENESCENCE

independent senescence has been termed premature senescence, which recapitulates molecular features of replicative senescence (Fig. 4) [47]. Premature senescence can result from adverse culture condition, commonly known as culture shock. For example, MEFs can be cultured for limited number of passages before they succumb to senescence. Studies revealed that supra-physiological oxygen concentration at the cell culture condition induces premature senescence response in MEFs [45]. In agreement with that, when cultured under physiological oxygen concentration, MEFs exhibit longer life span. Consistent with this, oxidative stress results cessation of replication in human cells cultured in vitro [48]. Premature senescence can be induced by oncogenes as well. For example, oncogenic RasV12 induces premature senescence of primary murine cells [49]. But, inactivation of p53 or its upstream activator p19Arf abrogates ability of RasV12 to induce senescence [49, 50]. In human cells, inactivation of p16Ink4a is sufficient to bypass oncogene-induced senescence [51]. One important common effector for culture shock, DNA damage or oncogene induced senescence is reactive oxygen species (ROS) [47]. ROS levels increase in both replicative senescence and oncogene-induced senescence [52, 53]. Moreover, lowering oxygen tension inhibits oncogene-induced senescence of human diploid fibroblasts and culture shock induced senescence of mouse embryonic fibroblasts [45, 47]. ROS have been suggested to induce either p53 or p16INK4a-Rb pathway to trigger senescence response [54, 55].

Senescent cells display striking change in their gene expression profile. Most of the genes displaying change in their expression profile play roles in the cell cycle,

inflammation and DNA repair. The three cell cycle genes, which often get expressed at a higher level, are p21, p16INK4a and p14 Arf (Fig. 4) [43]. p53 exerts its senescence function through p21 resulting cell cycle arrest at G1/S phase. Rb is being activated by p16 INK4a that inhibits CDK4/6 to keep Rb in its active hypophosphorylated state. Rb stalls cell proliferation by forming repressor complex with E2F, a transcription factor that stimulates genes required for cell proliferation. p14 Arf (p19 Arf in murine) activates p53 by inhibiting MDM2 [56]. On the other hand, p21 inhibits CDKs to suppress phosphorylation and inactivation of Rb. Hence; there is a critical interplay between the p53 and the Rb pathways that induces senescence.

As a part of my thesis research, I have observed an important role of DDB2 also in inhibiting epithelial to mesenchymal transition (EMT) in colon carcinoma cells. Therefore, below, I have provided an introduction to EMT.

1.6 EPITHELIAL TO MESENCHYMAL TRANSITION

Epithelial to mesenchymal transition (EMT) is an evolutionary conserved developmental process that is usurped often by epithelial tumors during metastatic progression. EMT involves polarized epithelial cells to lose their apical-basal polarity, characteristic cell-cell contact, and numerous biochemical changes that result in a conversion of the epithelial cells to mesenchymal cells with invasive properties, allowing them to migrate through the extracellular matrix (Fig. 5) [57]. EMT is characterized by loss of markers for epithelial cells including E-cadherin,

beta-catenin, and gain of mesenchymal markers such as vimentin, fibronectin and smooth muscle actin (Fig. 5) [57]. Several oncogenic pathways activated by Src, Ras, Ets, Integrin, Wnt, Notch, hypoxia and TGF-β signaling have been shown to induce EMT [58, 59]. Moreover, a number of transcriptional regulators such as Snail1, Slug, Twist, Zeb1 and Zeb2, which are downstream of the aforementioned signaling pathways, have been shown to stimulate EMT [60-66]. These transcriptional regulators inhibit expression of E-cadherin, which is considered to be a key event in the EMT of epithelial cancer cells [64]. For example, the TGF-β effectors Smads associate with the Zeb proteins to repress expression of E-cadherin [62, 67-70]. TGF-β and Wnt/β-catenin mediated EMT also involves activation of Snail1, which represses expression of E-cadherin [64, 70-72]. Likewise, the hypoxia activated transcription factor HIF-1 induces EMT by activating expression of Twist, Snail and VEGF-A [73-76]. Moreover, extracellular matrix (ECM) degrading matrix metalloproteinases (MMPs) also have been found to alter intracellular signaling pathway to initiate the EMT process. For instance, MMP3 has been shown to facilitate EMT of epithelial tumor cells in culture by increasing expression of Snail1 [77]. Thus, the pathways that lead to the activation of the EMT-inducing transcription factors (Snail1, Zeb1, Zeb2 and Twist) have been characterized, and they have been implicated in metastasis of epithelial tumors. However, except for some microRNA studies, the regulators that inhibit expression of these EMT-inducing transcription factors in the epithelial tumor cells and block mesenchymal transition remain poorly understood [78, 79].

Figure 5: Epithelial to mesenchymal transition.
EMT is a developmental process that is usurped by the tumor cells in order to undergo metastasis. Cuboidal shaped epithelial cells undergo change in morphology to become elongated mesenchymal cells. This process is accompanied by change in gene expression profile.

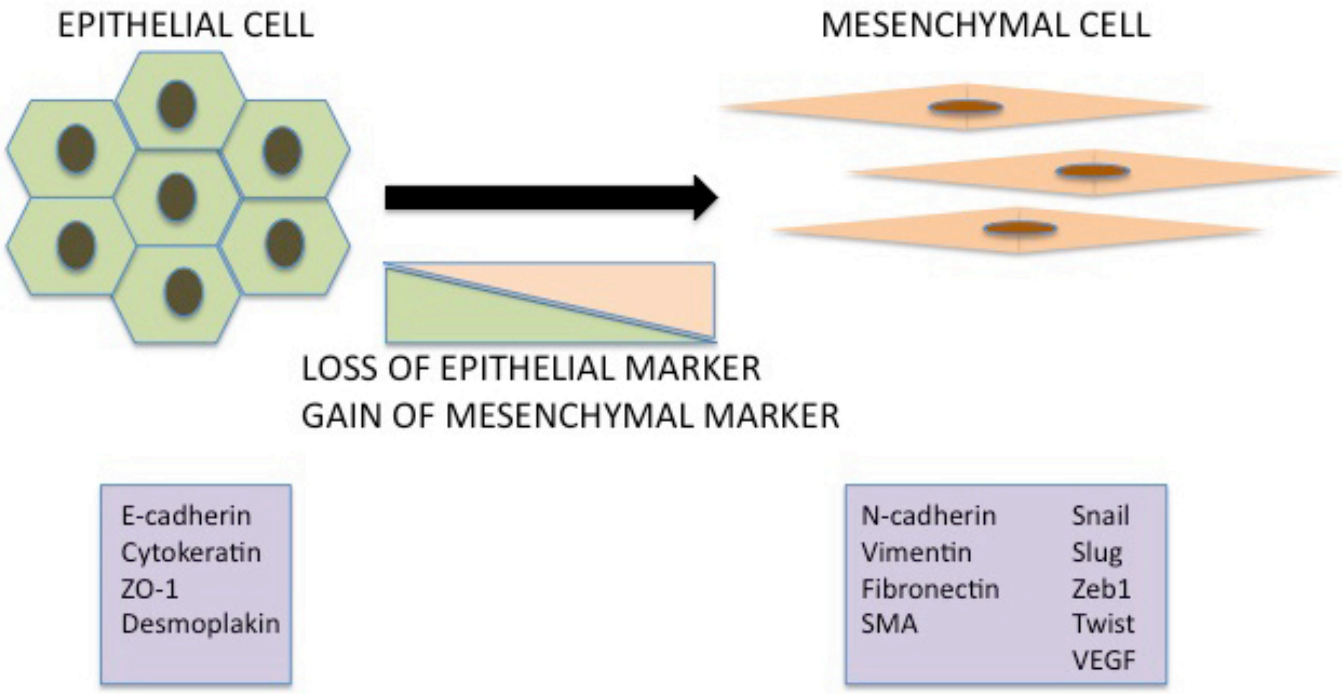
EPITHELIAL CELL
MESENCHYMAL CELL
LOSS OF EPITHELIAL MARKER
GAIN OF MESENCHYMAL MARKER
E-cadherin
Cytokeratin
ZO-1
Desmoplakin
N-cadherin
Vimentin
Fibronectin
SMA
Snail
Slug
Zeb1
Twist
VEGF

1.7 THESIS PROJECT

DDB2-/- cells accumulate p21 at a high level. p21 has been implicated to induce senescence. Hence, I was interested to see whether DDB2 mediated p21 regulation plays any part in senescence. Surprisingly, despite high-level accumulation of p21, the DDB2 deficient MEFs are deficient in replicative senescence. Moreover, DDB2 deficient MEFs or human carcinoma cells are refractory to DNA damage (UV, Cisplatin or Aclarubicin) induced or oncogene induced senescence. Further investigation revealed that DDB2 deficiency results impaired accumulation of ROS in the cell following DNA damage. I also provide evidence that DDB2 is a transcriptional repressor of SOD2 and catalase, two important anti-oxidant genes. In the absence of DDB2, high-level expression of SOD2 and catalase inhibits ROS accumulation and prevents the senescence response. My findings also show that ROS activates DDB2 expression. Thus, ROS augments DDB2 expression. DDB2 in turn, in a positive feedback loop, maintains the ROS level high by attenuating expression of SOD2/ catalase and induce senescence.

DDB2 mediated senescence plays an important role in its function as tumor suppressor. I provide evidence that DDB2-/- mice display increased hepatic fibrosis response following chronic liver damage, which is related to deficiency in senescence of hepatic stellate cells. Moreover, DDB2 mediated induction of premature senescence plays a major part in its role in suppressing UV induced skin carcinoma. My observations revealed that in the context of UV induced skin cancer

Figure 6: Role of DDB2 in EMT and senescence.
DDB2 acts as a transcriptional inhibitor of SOD2 and catalase and thus inducing senescence. DDB2 mediated inhibition of EMT is related to its role as a transcriptional inhibitor of VEGF, Snail and Zeb1.

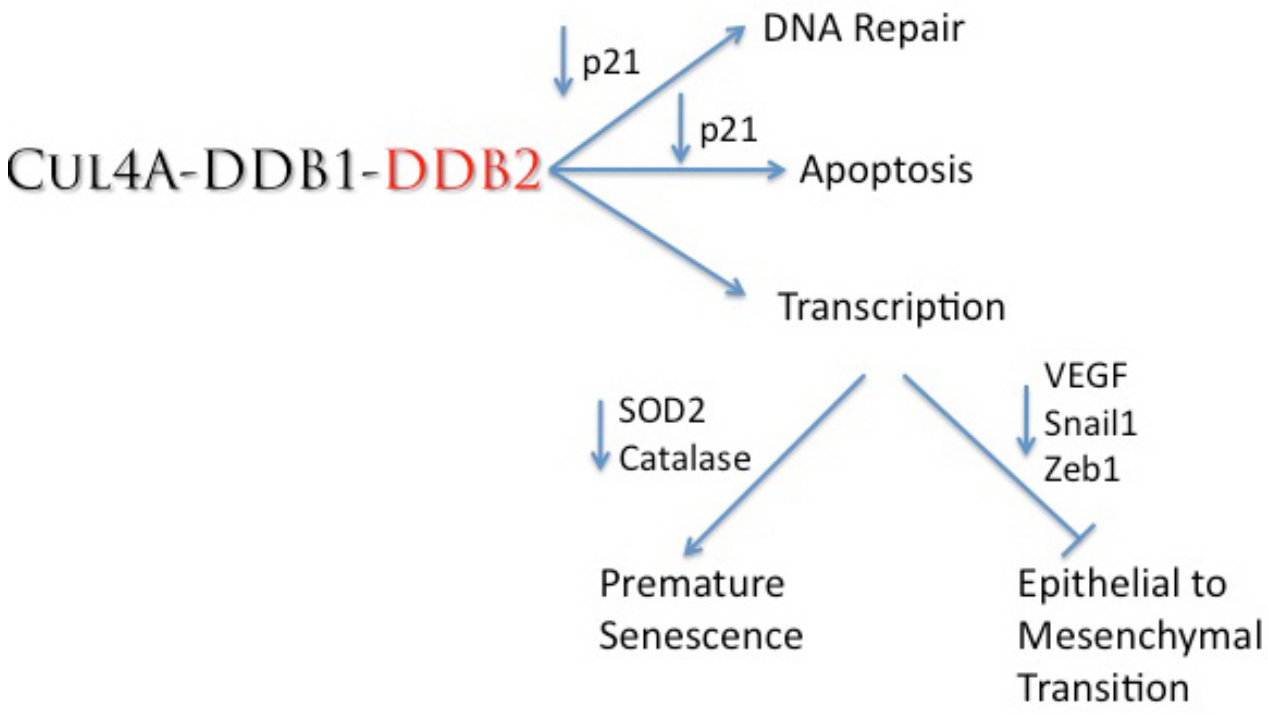
CUL4A-DDB1-DDB2
p21
DNA Repair
p21
Apoptosis
Transcription
SOD2
Catalase
VEGF
Snail1
Zeb1
Premature
Senescence
Epithelial to
Mesenchymal
Transition

development, DDB2 and p21 co-operate with each other to suppress tumorigenesis by inducing accumulation of ROS and thereby triggering senescence.

Several transcription factors have been shown to have opposing effects on senescence and epithelial to mesenchymal transition (EMT). For example, Twist/ Zeb1 induces EMT but inhibits cellular senescence. Conversely, p53/ p21 induces senescence but inhibits EMT. Similarly, my observations revealed that DDB2, an inducer of premature senescence, inhibits EMT. I found that, loss of DDB2 expression in colon carcinoma cells results EMT. This is accompanied by increased motility, aggressiveness and tumorigenicity of these cells both in vitro and in vivo. Moreover, DDB2 deficient cells are also resistant to anoikis that makes these cells proficient to metastasize to lung and liver. Further examination revealed that DDB2 inhibits EMT by attenuation of VEGF, Snail and Zeb1 transcription. I also examined DDB2 status in colon carcinoma patient samples. My observation revealed that low DDB2 expression is poor prognosis for colon carcinoma patients, which is likely related to increased metastatic potential of primary cells.

My observations suggest that activation of DDB2 would be potentially significant in therapy. Augmenting DDB2 expression will induce senescence and inhibit EMT. Hence, it will stop the proliferation of primary tumor cells and inhibit their dissemination to a distant organ. Towards that, I have used PEITC (Phenethyl Isothiocyanate), a naturally occurring compound to induce DDB2 expression. PEITC is currently in clinical trial. I show that PEITC mediated apoptosis and senescence

requires expression of DDB2. Moreover, PEITC mediated tumor regression in vivo involves DDB2. Taken together, I provide genetic basis and molecular mechanism deciphering new roles of DDB2 as a tumor suppressor (Fig. 6). I also provide evidence that DDB2 can be targeted therapeutically to inhibit tumorigenesis.

2.MATERIALS AND METHODS

2.1 MICE

$Ddb2^{-/-}$ mice were generated in our laboratory. $p21^{+/-}$ mice were crossed with $Ddb2^{+/-}$ mice to produce $Ddb2^{+/-}p21^{+/-}$progeny, which were crossed further to obtain the $Ddb2^{+/-}$ $p21^{-/-}$ mice. The$Ddb2^{+/-}$ $p21^{-/-}$ were crossed with $Ddb2^{+/-}$ $p21^{-/-}$ to obtain $p21^{-/-}$ and $Ddb2^{-/-}$ $p21^{-/-}$ mice. $Ddb2^{+/-}$ mice were crossed with $Ddb2^{+/-}$ mice to obtain $Ddb2^{-/-}$ and wild type mice.

2.2 ISOLATION OF MEF

MEFs were obtained from 13.5-day WT or $DDB2^{-/-}$ sibling embryos and were grown in Dulbecco's modified Eagle's medium (DMEM) containing 10% fetal bovine serum (FBS).

2.3 DRUG TREATMENTS AND UV IRRADIATION

UV irradiation (50 J/m^2) of cells was carried out with a Stratalinker (Fisher Scientific) adjusted to UV-C irradiation. The cells were washed with phosphate-buffered saline (PBS) before irradiation in the absence of any medium. Following irradiation, cells were supplemented with culture medium. Cisplatin (Sigma; P4394) was used at a final concentration of 30 μM, and aclarubicin (Sigma; A8959) was used at a final concentration of 0.5 μM. Cells were treated with the drugs for 8 h followed by washing with PBS and supplementation with culture medium.

PEITC was used at a final concentration of 10uM for indicated time points for DDB2 expression analysis. For TUNEL assay, cells were treated at a final concentration of 50uM for 8 hrs. For SA-beta-gal assay, cells were treated at a final concentration of 20uM for 6 hrs.

p38MAPK inhibitor (SB 203580) and JNK inhibitor (SP600125) were purchased from calbiochem. They were used at a final concentration of 20uM and 50 uM respectively as described previously [80].

2.4 WESTERN BLOT ANALYSIS

Cells were harvested following washing with PBS. Cells were lysed by suspension in 2 volumes of buffer containing 0.02 M HEPES (pH 7.9), 0.4 M NaCl, 0.1% NP-40, 10% (vol/vol) glycerol, 1 mM NaF, 1 mM sodium orthovanadate, and a protease inhibitor cocktail. Extracts were subjected to sodium dodecyl sulfate (SDS)-polyacrylamide gel electrophoresis, followed by blotting to nitrocellulose. The blots were probed with antibodies to p19Arf (Abcam), Cdk2 (Santa Cruz), human DDB2 (Santa Cruz/ Cell signaling), mouse DDB2 (Cell signaling), H-Ras (Santa Cruz), T7 monoclonal antibody (Novagen), catalase (Calbiochem), manganese superoxide dismutase (MnSOD) (Stressgen), FoxM1 (Santa Cruz), p21 Waf1/ Cip1 (BD Biosciences), E-cadherin (BD Biosciences), Vimentin (Sigma), P-ERK (Cell signaling), p-AKT (Cell signaling), total ERK (Cell signaling), total AKT (Cell signaling), cleaved caspase 3 (Santa cruz), Actin (Sigma), Tubulin (Sigma), HIF-1 (Abcam), Zeb1 (Santa cruz), Snail (Santa cruz).

2.5 SENESCENCE ASSOCIATED β GAL ASSAY

MEFs (WT or DDB2$^{-/-}$) and HCT116 cells (with short hairpin RNA [shRNA] targeting LacZ or DDB2) were plated at low density. Cells were washed twice with ice-cold PBS and fixed in 2% formaldehyde and 0.2% glutaraldehyde solution in PBS. Cells were incubated overnight at 37°C in staining solution containing 1 mg/ml X-Gal (5-bromo-4-chloro-3-indolyl-β-D-galactopyranoside), 40 mM citric acid-sodium phosphate (pH 6.0), 5 mM potassium ferrocyanide, 5 mM potassium ferricyanide, 150 mM NaCl, and 2 mM $MgCl_2$. They were photographed thereafter and scored by assessing 15 random fields/plate in triplicate.

Frozen skin sections were fixed in 3% formaldehyde in 1× PBS for 5 min at room temperature. Sections were washed two times with 1× PBS, pH 7.2, with 1 mM$MgCl_2$ and further incubated with X-gal staining solution overnight at 37 °C. Nuclei were counterstained with Nuclear Fast Red. Pictures of random fields were taken with Nikon microscope at ×10. SA-β-galactosidase-positive cells per field were counted.

2.6 POPULATION DOUBLING ASSAY

MEFs (WT or DDB2$^{-/-}$) were grown for 3 days (1 × 10^6 cells/60-mm plate). The MEFs were split every 3 days and replated at the same density. This 3T3 cultivation was repeated for 9 passages for WT MEFs and 20 passages for DDB2$^{-/-}$ MEFs. Population doublings were calculated according to the formula log(final cell number/plated cell number)/$\log_2$.

2.7 SEMI-QUANTITATIVE REVERSE TRANSCRIPTION PCR

Total RNA was extracted from the cells with Trizol. One microgram of total RNA was then subjected to DNase I treatment using RQ1 RNase-free DNase I (Invitrogen). The DNase I-treated RNA was reverse transcribed using an iScript cDNA synthesis kit (Bio-Rad) according to the manufacturer's protocol. PCR amplification was carried out with the following primers:

Mouse MnSOD

Forward: 5′-ATTAACGCGCAGATCATGCA-3′

Reverse: 5′-TGTCCCCCACCATTGAACTT-3′

Mouse catalase

Forward: 5′-CCGACCAGGGCATCAAAA-3′

Reverse: 5′-GAGGCCATAATCCGGATCTTC-3′

Mouse glyceraldehyde-3-phosphate dehydrogenase (GAPDH)

Forward: 5′-AACTTTGGCATTGTGGAAGG-3′

Reverse: 5′-CCATCCACAGTCTTCTGGGT-3′

Mouse DDB2

Forward: 5′-GCTCCAAAGGGGGAGATATT-3′

Reverse: 5′-CTTCTTGTGCATTCGGAGGT-3

p19Arf

Forward: 5′-CCCACTCCAAGAGAGGGTTT-3′

Reverse: 5′-TCTGCACCGTAGTTGAGCAG-3′

Human MnSOD

Forward: 5′-GGCTTGGTTTCAATAAGGAACGG-3′

Reverse: 5′-ATCCCCAGCAGTGGAATAAGG-3′

Human catalase

Forward: 5′-TGATTACACTCCAGCGTGGTGAG-3′

Reverse: 5′-CATAGATGCCCTCTGAGACTCTGC-3′

Human cyclophilin

Forward: 5′-GCAGACAAGGTCCCAAAGACAG-3′

Reverse: 5′-CACCCTGACACATAAACCCTGG-3′

Human DDB2

Forward: 5′-CCAACCAGTTTTACGCCTCCTC-3′

Reverse: 5′-TGTCTCCTGTGACCACCATTCG-3′

p14Arf

Forward: 5′-GAACATGGTGCGCAGGTTCT-3′

Reverse: 5′-CCTCAGCCAGGTCCACGGG-3′

E-cadherin

Forward: 5’- GTCATCCAACGGGAATGCA-3’

Reverse: 5’- TGATCGGTTACCGTGATCAAAA -3’

Cytokeratin 18

Forward: 5’- TGGTCACCACACAGTCTGCT -3’

Reverse: 5’- CCAAGGCATCACCAAGATTA - 3’

Cytokeratin 19

Forward: 5’- AGGTGGATTCCGCTCCGGGCA -3’

Reverse: 5’- ATCTTCCTGTCCCTCGAGCA -3’

Vimentin

Forward: 5’- GACACTATTGGCCGCCTGCAGGATGAG -3’

Reverse: 5’- ACTGCAGAAAGGCACTTGAAAGC -3’

N-cadherin

Forward: 5’- CACCCAACATGTTTACAATCAACAATGAGAC -3’

Reverse: 5’- CTGCAGCAACAGTAAGGACAAACATCCTATT -3’

Snail

Forward: 5’- TTCAACTGCAAATACTGCAACAAG -3’

Reverse: 5’- CGTGTGGCTTCGGATGTG -3’

Twist

Forward: 5’- CGGACAAGCTGAGCAAGATT -3’

Reverse: 5’- CCTTCTCTGGAAACAATGAC -3’

Zeb1

Forward: 5’- AACGCTTTTCCCATTCTGGC -3’

Reverse: 5’- GAGATGTCTTGAGTCCTGTTCTTGG -3’

MMP3

Forward: 5’- ATTCCATGGAGCCAGGCTTTC -3’

Reverse: 5’- CATTTGGGTCAAACTCCAACTGTG -3’

VEGF

Forward: 5’- CTACCTCCACCATGCCAAGT -3’

Reverse: 5’- GCAGTAGCTGCGCTGATAGA -3’

Hif-1

Forward: 5’- CTCAAAGTCGGACAGCCTCA -3’

Reverse: 5’- CCCTGCAGTAGGTTTCTGCT -3’

Pinch1

Forward: 5'- CCGCTGAGAAGATCGTGAAC -3'

Reverse: 5'- GGGCAAAGAGCATCTGAAAG -3'

Each PCR mix contained 5 µl 5× PCR mix, 0.5 µl deoxynucleoside triphosphate (dNTP), 1.5 µl $MgCl_2$, 0.125 µl Taq polymerase (Promega), 2 µl cDNA, 13.875 µl water, and 1 µl (each) forward and reverse primer.

2.8 CHROMATIN IP ASSAY

Cells were either left untreated or infected with LacZ/DDB2-T7-expressing adenovirus. Infected cells were processed after 18 h for chromatin immunoprecipitation (ChIP) assay. Cells were first cross-linked by addition of 37% formaldehyde (Fisher) to a final concentration of 1% and incubated for 10 min with gentle swirling at room temperature. Cross-linking was stopped by addition of 2.5 M glycine at a final concentration of 0.125 M glycine for 5 min with gentle swirling. Cells were washed twice with ice-cold sterile PBS and then collected by adding 1 ml of ice-cold sterile PBS containing 1 mM phenylmethylsulfonyl fluoride (PMSF) and protease inhibitors (Roche). Cells were scraped, transferred into an Eppendorf tube, and centrifuged at 2,000 rpm for 5 min. The cell pellet was then resuspended in a 2× pellet volume of sodium dodecyl sulfate (SDS) lysis buffer (1% SDS, 10 mM EDTA, 50 mM Tris, pH 8.1) and placed on ice for 10 min. The resulting extract was sonicated and precleared, and immunoprecipitation was carried out with 2 µg of antibody (DDB2, Santa Cruz; T7, Novagen; H3K9Me3, Upstate; Suv39h, Upstate; immunoglobulin G [IgG], Santa Cruz; XPC, Santa Cruz; Cul4a, DDB1). Cross-links

were reversed on all samples, including input, by addition of 100 µl Tris-EDTA (TE) containing 200 mM NaCl and 0.1 mg proteinase K/ml, and then samples were incubated overnight. DNA was extracted from the digested samples using a PCR purification kit (Qiagen). Extracted DNA was amplified by PCR alongside 0.1% of the input chromatin used to carry out the immunoprecipitation. PCR primers used to carry out PCR are as follows.

Human MnSOD promoter-specific primers

Forward: 5′-GGCAGGAATCTGAGAATTGG

Reverse: 5′-TTCTGACTGTGAAGGGACCA-3′

Human catalase-specific primers

Forward: 5′-CATTTTTCCCATCACAAGGG-3′

Reverse: 5′-TTTGCAACCAAAGGATGGAT-3′

Human VEGF promoter specific primers I

Forward: 5’-AGACCTTGTCCCTGCTGCT-3’

Reverse: 5’-GCTGGTTTCTGACCTGGCTA-3’

Human VEGF promoter specific primers II

Forward: 5’-AAGGTGAGGCCCTCCAAG-3’;

Reverse: 5’-TGTACTCTTAAGGACTCAGCCAGTG-3’

Human Snail specific primers

Forward: 5’-AGGAACGAGGGTACAATGAA-3’

Reverse-5’-CTCCCTGTCTGTCCTCAAGC-3’

Human Zeb1 specific primers

Forward: 5’-GCAAATAGGTGCAAAAGGGTTT-3’

Reverse: 5'- CAAATCAAACGGTAGGGGATA- 3'

Human DDB2 specific Primer I (-431 site)

Forward: 5'- CCTGTAGGGACCAGCCAAT-3'

Reverse: 5'-GCCCGGCTAATTTCTCTCTC-3'

Human DDB2 specific Primer II (-1581 site)

Forward: CACGCCTATAATCCCAGCAT

Reverse: CAGCCTCCTCACTGCTTTTT

Human RARβ Primer

Forward: TGGTGATGTCAGACTAGTTGGGTC

Reverse: GCTCACTTCCTACTACTTCTGTCAC

The PCR products were separated on agarose gels and visualized by ethidium bromide staining. For re-ChIP analysis, complexes from the primary ChIP were eluted with 10 mmol/liter of dithiothreitol (DTT) for 30 min at 37°C, diluted 10 times with ChIP dilution buffer (0.01% SDS, 1.1% Triton X-100, 1.2 mM EDTA, 16.7 mM Tris, pH 8.0, 167 mM NaCl) followed by reimmunoprecipitation with the indicated second antibodies, and subjected to the ChIP procedure.

2.9 ROS MEASUREMENT

Cells were incubated with 5 mM dichlorodihydrofluorescein diacetate (DCFDA; Molecular Probes) for 30 min. Cells were then washed with PBS and immediately mounted on slides with mounting medium containing DAPI (4',6-diamidino-2-phenylindole; Vector Laboratories) and viewed with a Nikon microscope.

Harvested skin sections were embedded and frozen in OCT compound, and frozen sections were prepared. Sections were stained with 10 μM 5-(6)-chloromethyl-2-dichlorodihydrofluorescein diacetate (CM-H_2DCFDA) (Invitrogen) for 45 min at 37 °C. Images were taken using a fluorescent microscope at ×20 magnification. Three to five randomly selected areas were photographed with the same exposure time. The images were processed using the same fixed threshold in all samples by Photoshop software, and representative images are shown.

2.10 siRNA TRANSFECTION

A short interfering RNA (siRNA) duplex targeting the human DDB2 gene (5′-GAGCGAGAUCCGAGUUUAC-3′) was synthesized (Dharmacon Research). This siRNA duplex (50 nM) was transfected using Lipofectamine 2000 reagent (Invitrogen) in serum-free medium following the manufacturer's protocol. Four hours after transfection, medium containing 10% FBS was added. Cells were split 1:3 next day and used for experiments thereafter.

2.11 CARBON TETRACHLORIDE INJECTION

WT or DDB2$^{-/-}$ mice, 6 to 8 weeks old, were treated once a week with intraperitoneal injections of 1 ml CCl_4/kg of body weight for 2 weeks to induce liver damage. Animals were sacrificed 72 h after the last injection, and their livers were used for SA-β-Gal assay. Briefly, liver tissues were snap-frozen and sections were made. Sections were fixed with 2% formaldehyde-0.2% glutaraldehyde in PBS for

15 min, washed with PBS, and stained as mentioned previously. Sections were counterstained with nuclear fast red.

For chronic damage, WT or DDB2$^{-/-}$ mice, 6 to 8 weeks old, were treated twice a week with intraperitoneal injections of 1 ml CCl_4/kg of body weight for 6 weeks to induce liver damage. Animals were sacrificed 5, 10 and 20 days time-point after the last injection, and their livers were used for further analysis [81].

2.12 IRRADIATION OF MICE

10 to 15 mice each genotype were subjected to UV-B irradiation. Irradiation was carried out with FB-UVXL1000 UV cross-linker (Fisher) with UV-B tubes. Mice were exposed to UV light for 42 weeks, starting with 2 kJ/m^2 twice a week. The dose of UV light was gradually increased to 6 kJ/m^2 five times per week. Mice were shaved once a week. The dorsal area of the mice was exposed to UV-B.

2.13 BrdU INCORPORATION ASSAY

Mice were injected intraperitoneally at 100 μg of BrdU/g of body weight 4 h prior sacrificing. Skin sections were fixed, and immunostaining was performed with BrdU monoclonal antibody.

MEFs were pulse-labeled with 3 μg/ml BrdU for 1 h and 30 min and fixed with ice-cold 70% ethanol. Cells were kept with Denaturing solution (2 M HCl, 0.5% Triton X-100) for 1 h followed by 10 min of incubation with Neutralization solution

(0.1 M sodium borate). Cells were incubated with BrdU monoclonal antibody (Dako; 1:500 dilution) overnight at 4 °C. After rinsing with PBS, cells were incubated with TRITC-conjugated polyclonal rabbit anti-mouse antibody for 2 h at room temperature and counterstained with DAPI.

2.14 IMMUNOHISTOCHEMISTRY

Tumor tissues were fixed in 10% buffer formalin and paraffin embedded. Serial sections of 5 um thicknesses were de-paraffinized in xylene, followed by re-hydration in 100%, 95% and 70% ethanol, respectively. Sections were further treated for antigen retrieval with citrate buffer pH 6.0 at 95^{O} C for 20 minutes. Blocking was performed using mouse on mouse blocking reagents following manufacturer's protocol (VectorLabs BMK-2202). The sections were incubated with the DDB2 (Abcam), PCNA (Santa Cruz), Ki67 (Santa Cruz), SMA (Sigma) or cleaved caspase 3 (Cell signaling) antibody 1:200 dilution overnight. Sections were washed three times with 1xPBS and incubated with anti-mouse/ rabbit AP (VectorLabs AP-2000) and further developed with Alkaline Phosphatase Substrate (VectorLabs SK-5300) following manufacturer protocol. Nuclei were counterstained with hematoxylin.

2.15 TISSUE MICROARRAY

Human tissue microarray of normal and basal cell carcinoma (BCC) samples were obtained from US Biomax (SK482 and SK484). Immunohistochemical assay was performed as described above with antibodies against p21 (BD Biosciences) or

against DDB2 (Abcam). Tissues were counterstained with hematoxylin. Intensity of staining was blind-scored from 0 (no staining) to 4 (highest intensity of staining). Graphs represent the average intensity of staining and paired t test of BCC versus NL scores of intensity of the staining.

Human tissue microarray of normal and colon carcinoma samples were obtained from US Biomax (CO811, CO801, CO482, CO701, BC050112, CO726, CO802 and CO805). Immunohistochemical assay was performed as described above with antibodies against DDB2 (Abcam). Tissues were counterstained with hematoxylin. Intensity of staining was blind scored from 0 (no staining) to 4 (highest intensity of staining). Graphs represent the average intensity of staining and paired T-test of colon carcinoma versus normal colon scores of intensity of the staining.

2.16 IMMUNOFLUOROSCENCE

Cells were grown on coverslip overnight. Next day, cells were fixed with 4% paraformaldehyde in PBS for 20 minutes at room temperature, washed once with PBS followed by permeabilization for 5 minutes with 0.1% Triton-X in PBS. Cells were then washed with PBS five times (five minutes each) and blocked with 5% goat serum for one hour at room temperature. Cells were incubated with E-cadherin (1:250), vimentin (1:200) or smooth muscle actin (1:200) antibody overnight. Next day, cells were washed for five times with PBS (five minutes each) followed by incubation with FITC/ TRITC tagged goat anti-mouse antibody (1:500) for one hour at room temperature. Cells were washed with PBS for five times (five minutes each).

Cell nuclei were labeled with DAPI in PBS for five minutes at room temperature. After a final wash with PBS, cells were mounted on slides with Vectashield (Vector Labs) mounting medium and photographed under microscope.

Skin/tumor tissues were fixed in 10% buffered formalin, and paraffin-embedded. Serial sections of 5 μm thickness were de-paraffinized in xylene, followed by re-hydration in 100, 95, and 70% ethanol. Sections were further treated for antigen retrieval with citrate buffer, pH 6.0, at 95 °C for 20 min. Blocking was performed using 5% goat serum in PBS for 1 h at room temperature. Sections were incubated overnight at 4 °C using the following primary antibodies: p19Arf (5C3 Mab) and p16INK4a (SC-1207) or mentioned as above. After washing with PBS, sections were incubated with anti-rat, mouse or rabbit immunoglobulin conjugated with FITC or TRITC. Coverslips were mounted in Vectashield (Vector Laboratories) containing DAPI to stain nuclei.

2.17 CELL CULTURE

Human colon carcinoma cell lines were cultured in DMEM (HCT 116) or RPMI 1640 (SW 480 and SW 620) medium supplemented with 10% FBS and Penicillin/ Streptomycin. Stable clones of HCT 116 cells expressing control shRNA or DDB2shRNA were selected using Puromycin. Stable clones of SW620 cells expressing empty vector or vector expressing DDB2 were selected using G418.

2.18 ANOIKIS, SOFT AGAR, INVASION AND MIGRATION ASSAYS

For anoikis assays, cells were trypsinized and $1x10^5$ cells were seeded into poly-HEMA (Sigma) coated six-well plates. At 24, 48 and 72 h time points, cells were harvested and western blot analysis was performed.

For soft agar assays, 25,000 cells were seeded into 0.4% low melting point agarose on top of 1% agarose layer. After 10 days, pictures were taken under phase contrast microscope. For quantification ten representative pictures were taken and the number of colonies was counted.

For matrigel invasion assay, experiment was performed according to the manufacturers protocol (BD Biosciences, Cat no: 354481).

For the scratch-healing assay, $1x10^5$ cells were seeded into 12-well plates and incubated overnight to achieve confluency. Next day, the cell layer in each well was scratched using a plastic pipette tip. The migration of the cells at the edge of the scratch was monitored at 0, 18 and 24 h later. Cells were visualized under microscope and photographed.

2.19 TUMORIGENECITY AND METASTASIS EXPERIMENT

8 weeks old male nude mice were subcutaneously injected with 2 million cells into both flanks. Mice were inspected thrice a week for tumor formation and tumor volume was measured with caliper. At the end point of the experiment, mice were

euthanized by CO_2 followed by cervical dislocation and tumor mass was measured. Tumors were examined by hematoxylin and eosin staining.

To study lung metastasis $1x10^6$ cells were injected into the tail vein of 8 weeks old male nude mice. Four weeks after the injection, mice were euthanized by CO_2 followed by cervical dislocation. Lung was removed and were fixed in 10% buffer formalin and paraffin embedded. Serial sections of lung tissue was made and examined by hematoxylin and eosin staining.

To study metastasis using an orthotopic model, $1x10^6$ cells were injected into the peritoneal cavity of immunocompromised SCID Beige mice. The cells were allowed to grow into a tumor over the course of two weeks. This allowed a tumor of roughly a centimeter to grow and be dissected. Tumor sections were then taken and implanted against the cecum of another SCID beige mouse and held in place using surgical glue. As the liver is the common first site of metastasis of colorectal cancer, the livers were examined after four weeks of implantation. Liver sections were stained with hematoxylin and eosin. Micro-metastases were then counted and statistically evaluated.

8 weeks old male nude mice were subcutaneously injected with 2 million cells (HCT116 cells expressing control shRNA or DDB2 shRNA) into both flanks. Mice were equally randomized into two groups for PEITC or vehicle treatment. When tumors reached volume of 10-15 mm3, mice were treated with PEITC (35mg/ kg of

body weight) for 5 days a week for 4 weeks by intraperitoneal injection as described previously . At the end point of the experiment, mice were euthanized by CO_2 followed by cervical dislocation and tumor mass was measured.

2.20 HYPOXIA AND TGF-β TREATMENT

For hypoxia experiment cells were grown in hypoxia chamber (1% CO2; 5% O2) for 24 hours.

For TGF-β experiment cells were incubated with TGF-β (5ng/ml; Peprotech) for 24-48 hrs.

2.21 TUNEL EXPERIMENT

Cells were grown on glass cover slips and treated with PEITC. Twenty-four hours after treatment cells were fixed in 1% paraformaldehyde pH 7.4. The ApopTag Red In situ Apoptosis Detection Kit (S7165) was used following manufacturer's protocol.

2.22 CLONOGENECITY ASSAY

Clonogenecity assay were performed as described previously [82]. Briefly, cells were treated with Cisplatin, Aclraubicin or PEITC. After being rinsed with PBS, fresh medium was added and they were allowed to grow for 12 days to form colonies. Colonies were stained with Crystal Violet (Sigma).

DDB2, an essential mediator of premature senescence

3.RESULTS:

3.1 ABSENCE OF DDB2 CAUSES DEFICIENCY IN SENESCENCE IN MEF

It has been shown previously that the DDB2$^{-/-}$MEFs are deficient in the proteolysis of p21 after DNA damage [16]. Because upregulation of p21 is associated with senescence, I compared the wild-type and DDB2$^{-/-}$ MEFs obtained from embryos from heterozygote mating for senescence in culture. Surprisingly, I observed that, unlike the MEFs from the wild-type littermates, the DDB2$^{-/-}$ MEFs continued to grow beyond passages 9/10 (Fig. 7A). Typically, the WT MEFs stopped proliferating at passages 6/7, and by passage 9, they exhibited all the morphological phenotypes of senescent cells (Fig. 7A). The DDB2$^{-/-}$ MEFs slowed down proliferation at passages 6/7, but the cells exhibited senescent phenotypes at a much lower frequency at passages 9/10. Moreover, I found that the DDB2$^{-/-}$ MEFs could be immortalized very easily (Fig. 7A). To further investigate the lack of senescence in the DDB2$^{-/-}$ MEFs, population-doubling studies were performed. The MEFs were divided every 3 days and counted for cell number. The population doublings were plotted against days in culture. As expected, the wild-type MEFs stopped proliferating after 15 or 18 days. The DDB2$^{-/-}$ MEFs also exhibited crisis, as did the wild-type MEFs, between passages 7 and 10, but they escaped the crisis at a very high frequency (Fig. 7B). A similar lack of senescence phenotype was found for the MEFs derived from the DDB2$^{-/-}$ p21$^{-/-}$ embryos, whereas the p21$^{-/-}$ MEFs senesced similarly to the wild-type MEFs. Next, I assayed for the senescence marker SA-β-Gal. MEFs (WT and DDB2-/-) at various passages were subjected to SA-β-Gal staining.

Figure 7: DDB2$^{-/-}$ MEFs are deficient in replicative senescence.
(A) Cells were grown following the 3T3 protocol as described in Materials and Methods. Representative phase-contrast images of early-passage and late-passage WT or DDB2$^{-/-}$ MEFs are shown. (B) For population doubling assay Cells were counted at each passage every 3 days, and the population doubling level (PDL) was calculated for WT and DDB2$^{-/-}$ MEFs. An average from three experiments is plotted with the bar representing the standard error. (C) WT or DDB2$^{-/-}$ MEFs were stained for SA-β-Gal at each passage from 2 to 7. (Top) Representative images of WT and DDB2$^{-/-}$ MEFs stained for SA-β-Gal at passage 5. (Bottom) SA-β-Gal-positive cells were counted in at least 10 fields from triplicate plates. A quantification of SA-β-Gal-positive WT or DDB2$^{-/-}$ MEFs is shown for each passage.

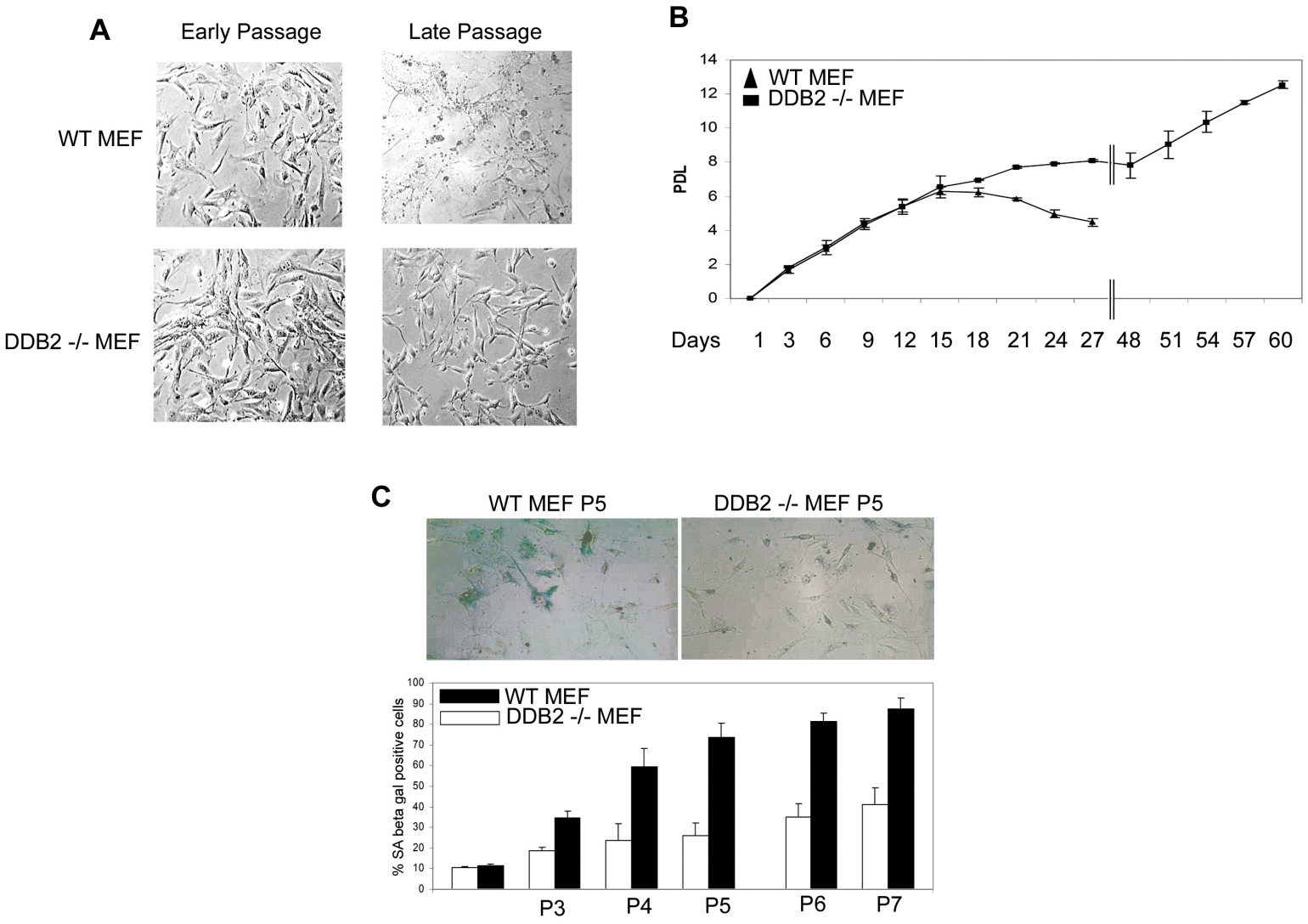
A
Early Passage
Late Passage
WT MEF
DDB2 -/- MEF
B
WT MEF
DDB2 -/- MEF
PDL
Days
1 3 6 9 12 15 18 21 24 27 48 51 54 57 60
C
WT MEF P5
DDB2 -/- MEF P5
WT MEF
DDB2 -/- MEF
% SA beta gal positive cells
P3
P4
P5
P6
P7

Figure 8: Increased DDB2 expression with passage number in WT MEFs.
WT MEFs were maintained in the culture medium up to passage 7. Total RNA for each passage was analyzed by semi-quantitative PCR for the level of DDB2. Western blot analysis of DDB2 for each passage was done using protein lysate of WT MEFs from passages 2 to 7.

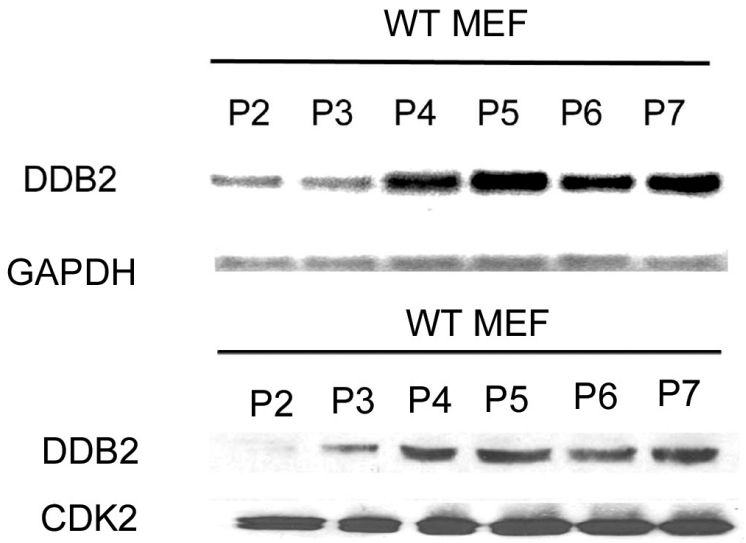
WT MEF
P2
P3
P4
P5
P6
P7
DDB2
GAPDH
WT MEF
P2
P3
P4
P5
P6
P7
DDB2
CDK2

DDB2$^{-/-}$ MEFs expressed the senescence marker at lower frequencies than did the WT MEFs (Fig. 7C). Also, the positive cells in the DDB2$^{-/-}$ MEFs had less intense staining of SA-β-Gal.

Interestingly, I observed that the expression of DDB2 in the wild-type MEFs increased with passage numbers (Fig. 8). The increased expression of DDB2 coincided with the increase in senescence, as judged by SA-β-Gal expression. WT and DDB2$^{-/-}$ MEFs at various passages were compared for the levels of p19Arf, which is critical for senescence in the MEFs. I consistently found a decrease in the levels of p19Arf mRNA in the DDB2$^{-/-}$ MEFs (Fig. 9A). A detailed analysis of the levels of p19Arf was carried out. The mRNA level of p19Arf increased in the DDB2$^{-/-}$ MEFs, as in the WT-MEFs, in passages 5 and 6, but the DDB2$^{-/-}$ MEFs failed to maintain expression in the late passages. (The plating efficiency of the WT MEFs decreases significantly beyond passage 7; therefore, they were not analyzed beyond passage 7.) (Fig. 9A). The deficiency in senescence did not involve inactivation of p53 or deletion of p16Ink4a (Fig. 9C). On the other hand, expression of p19Arf restored senescence in the DDB2$^{-/-}$ MEFs (Fig. 9B), indicating that the deficiency in senescence is related to a lack of p19Arf expression.

3.2 DDB2 DEFICIENT CELLS ARE RESISTANT TO OXIDATIVE STRESS INDUCED SENESCENCE

It was shown that the senescence of the MEFs in culture is linked to reactive oxygen species (ROS) and oxidative stress [45]. Therefore, I investigated whether there is

Figure 9: Late-passage DDB2$^{-/-}$ MEFs are deficient in p19Arf expression.
(A) WT MEFs were maintained in the culture medium up to passage 7, and DDB2$^{-/-}$ MEFs were maintained up to passage 12. Total RNA for each passage was analyzed by semiquantitative PCR for the level of p19Arf. (B) Immortalized DDB2$^{-/-}$ MEFs were infected with retrovirus expressing empty pBabe Puro vector or vector expressing p19Arf. Cells were selected with puromycin and assayed for SA-β-Gal activity. (Left) Representative images of SA-β-Gal-positive immortalized DDB2$^{-/-}$ MEFs infected with empty vector or vector with p19Arf. (Right) Total cell extracts from the MEFs infected with empty vector or vector expressing p19Arf were subjected to Western blot assay with p19Arf antibody. (C) Immortalized DDB2$^{-/-}$ MEFs were treated with UV as mentioned in Materials and Methods. Total cell extracts were subjected to Western blot assay with p53, p21, DDB1, p16INK4a, or beta-actin antibody.

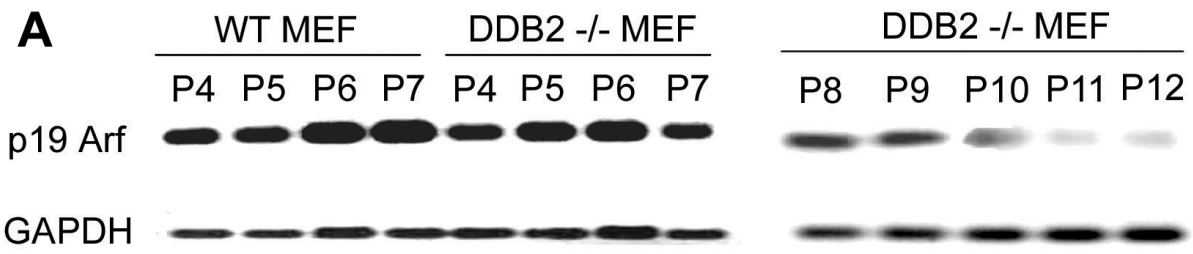
A
WT MEF
DDB2 -/- MEF
DDB2 -/- MEF
P4 P5 P6 P7 P4 P5 P6 P7
P8 P9 P10 P11 P12
p19 Arf
GAPDH

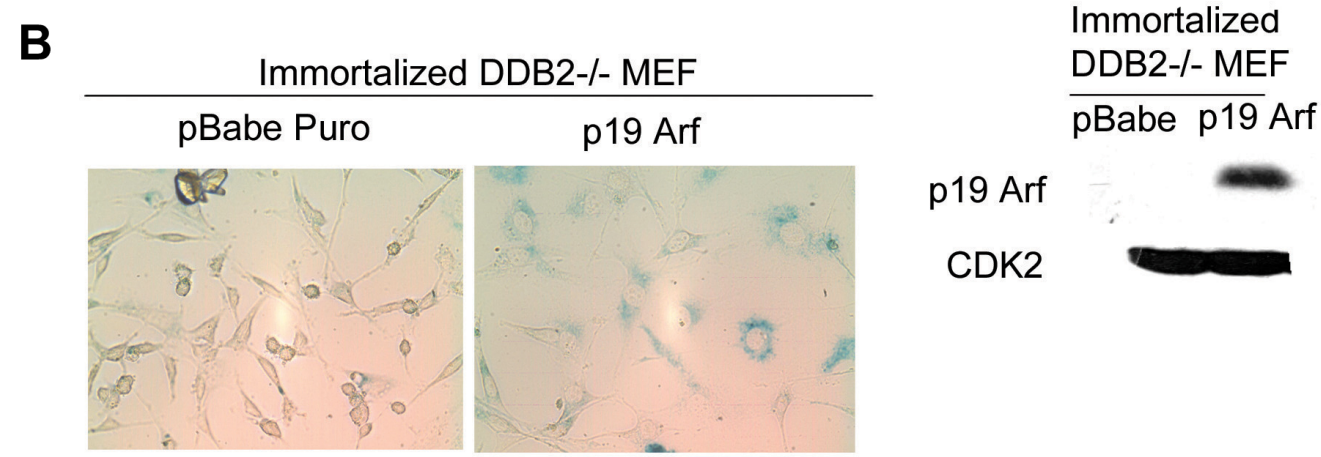
B
Immortalized DDB2-/- MEF
pBabe Puro
p19 Arf
Immortalized
DDB2-/- MEF
pBabe p19 Arf
p19 Arf
CDK2

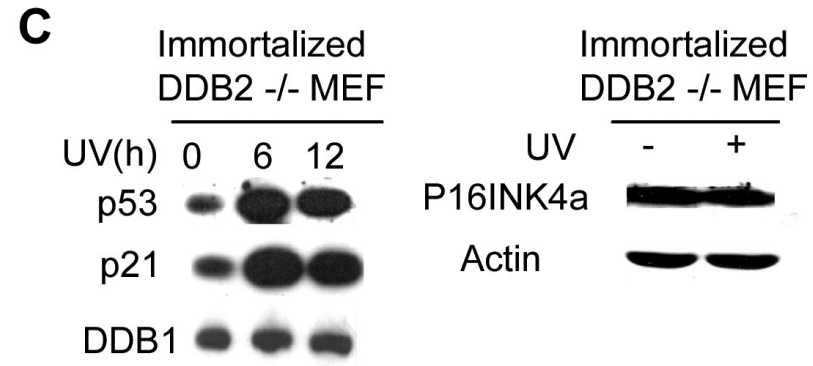
C
Immortalized
DDB2 -/- MEF
UV(h) 0 6 12
p53
p21
DDB1
Immortalized
DDB2 -/- MEF
UV - +
P16INK4a
Actin

Figure 10: DDB2-deficient cells are resistant to oxidative stress-induced senescence.
(A) WT or DDB2$^{-/-}$ MEFs were treated with 150 μM hydrogen peroxide for 4 h. After 3 days, cells were analyzed for the SA-β-Gal activity. (Top) Representative images of WT and DDB2$^{-/-}$ MEFs stained for SA-β-Gal after hydrogen peroxide treatment. (Bottom) SA-β-Gal-positive cells were counted from at least 10 fields of triplicate plates. (B) HCT116 cells expressing LacZ shRNA or DDB2 shRNA were treated with 150 μM hydrogen peroxide for 4 h. After 3 days, cells were analyzed for SA-β-Gal activity. (Top) Representative images of HCT116 cells expressing LacZ shRNA or DDB2 shRNA stained for SA-β-Gal after hydrogen peroxide treatment. (Bottom) SA-β-Gal-positive cells were counted from at least 10 fields of triplicate plates. (C) HCT116 cells expressing LacZ shRNA or DDB2 shRNA were analyzed for the level of DDB2 expression.

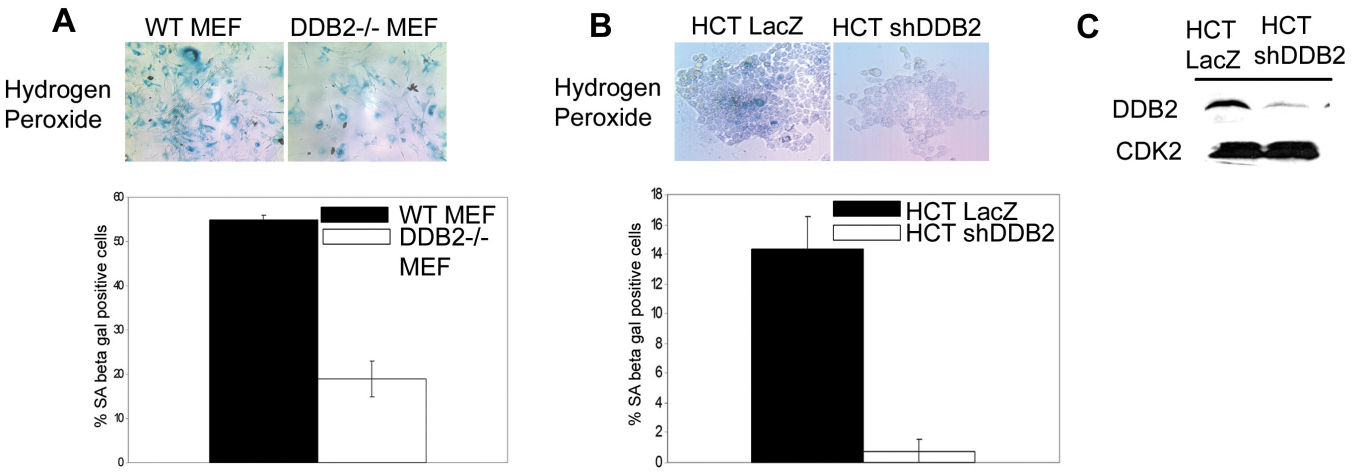
A
WT MEF
DDB2-/- MEF
Hydrogen Peroxide
% SA beta gal positive cells
WT MEF
DDB2-/- MEF
B
HCT LacZ
HCT shDDB2
Hydrogen Peroxide
% SA beta gal positive cells
HCT LacZ
HCT shDDB2
C
HCT LacZ
HCT shDDB2
DDB2
CDK2

Figure 11: Oxidative stress increases DDB2 expression.
(A and B) WT MEFs or HCT116 cells were treated with 150 μM hydrogen peroxide for 4 h or the indicated time points. (Top) Extract of the cells was analyzed for the level of DDB2 by Western blotting. (Bottom) Total RNA was analyzed by semiquantitative PCR for the level of DDB2. (C) $ARF^{-/-}$ MEFs were treated with 150 μM hydrogen peroxide for 4 h. (Top) Extract of the cells was analyzed for the level of DDB2 by Western blotting. (Bottom) Total RNA was analyzed by semiquantitative PCR for the level of DDB2. GAPDH was used as a loading control. (D) WT MEFs were maintained in the culture medium either in 3% oxygen or in 20% oxygen up to passage 5. Total RNA for each passage was analyzed by semiquantitative PCR for the level of DDB2.

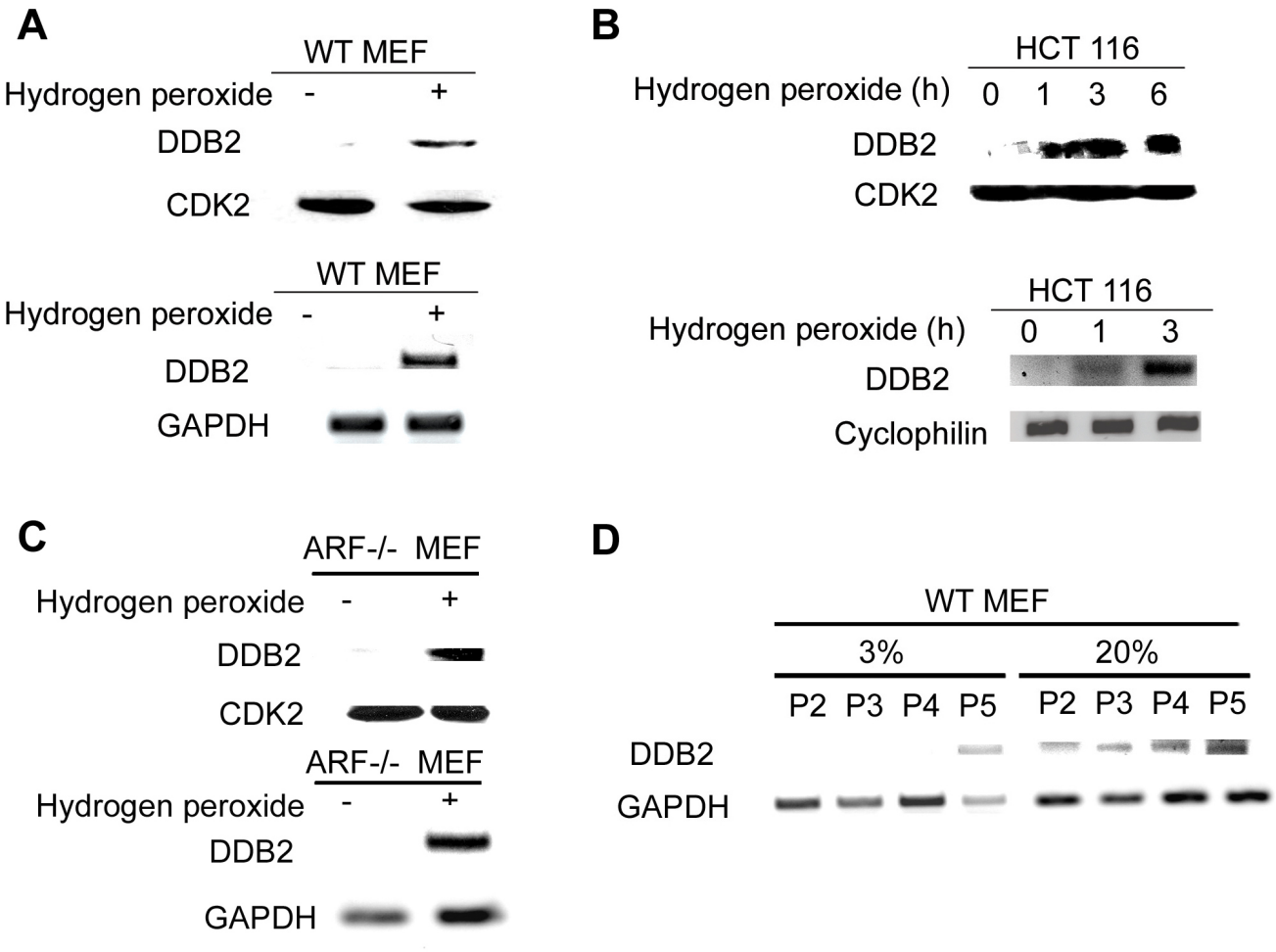
A
WT MEF
Hydrogen peroxide - +
DDB2
CDK2
WT MEF
Hydrogen peroxide - +
DDB2
GAPDH
B
HCT 116
Hydrogen peroxide (h) 0 1 3 6
DDB2
CDK2
HCT 116
Hydrogen peroxide (h) 0 1 3
DDB2
Cyclophilin
C
ARF-/- MEF
Hydrogen peroxide - +
DDB2
CDK2
ARF-/- MEF
Hydrogen peroxide - +
DDB2
GAPDH
D
WT MEF
3%
20%
P2 P3 P4 P5 P2 P3 P4 P5
DDB2
GAPDH

Figure 12: Overexpression of DDB2 sensitizes the cell to senescence.
HCT116 cells were transfected with DDB2. On the next day, transfected or nontransfected cells were treated with 50 μM hydrogen peroxide for 4 h followed by change of medium. After 36 h cells were stained for SA-β-Gal expression.

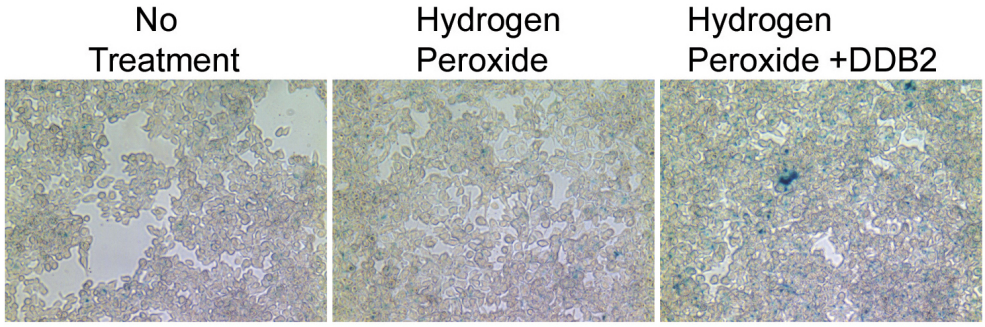
No Treatment
Hydrogen Peroxide
Hydrogen Peroxide +DDB2

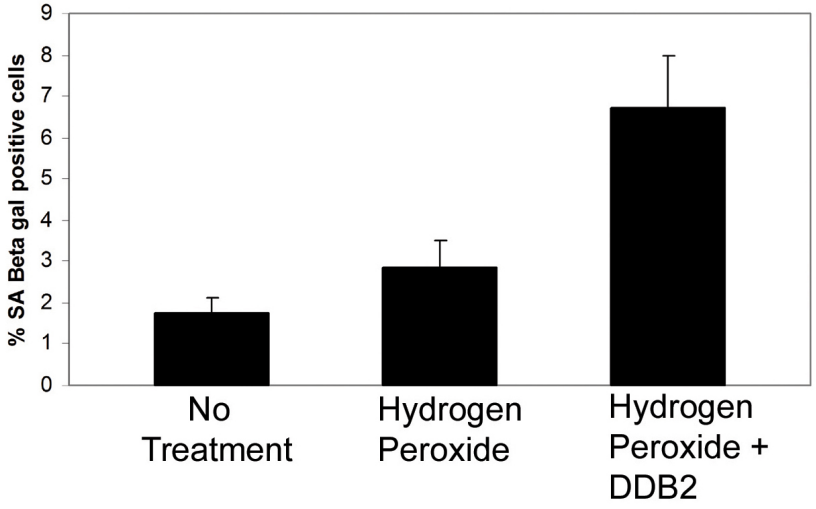
% SA Beta gal positive cells
0
1
2
3
4
5
6
7
8
9
No Treatment
Hydrogen Peroxide
Hydrogen Peroxide + DDB2

any deficiency in ROS-induced senescence in the DDB2$^{-/-}$MEFs. Passage 1 WT and DDB2$^{-/-}$ MEFs, obtained from heterozygote mating, were treated with hydrogen peroxide (150 μM) for 4 h and then maintained in culture for 3 days. To measure oxidative stress-induced premature senescence, the cells were assayed for SA-β-Gal. Clearly, there was a significantly lower expression of SA-β-Gal in the DDB2$^{-/-}$ MEFs (Fig. 10A). To extend the observations in human cells, I used HCT116 cells and generated cell lines stably expressing DDB2 shRNA. The HCT116 cells expressing the lacZ shRNA were compared with the DDB2 shRNA-expressing clones for response to oxidative stress, as in the previous experiment. Consistent with the observations in the MEFs, the HCT116 cells expressing DDB2 shRNA exhibited a similar deficiency in the expression of senescence marker following treatments with hydrogen peroxide (Fig. 10 B). The knockdown of DDB2 in the DDB2 shRNA-expressing cells was confirmed by Western blotting (Fig. 10 C). Interestingly, expression of DDB2 in the WT MEFs and in the HCT116 cells was found to be increased by the oxidative stress, suggesting that DDB2 expression is activated by ROS (Fig. 11A and B). The induction was observed at the level of mRNA expression within 1 h of treatment with hydrogen peroxide, suggesting that it is an early effect of oxidative stress. Furthermore, the induction of DDB2 expression was observed in alternative reading frame -null cells that fail to senesce, supporting the notion that the induction is not a consequence of initiation of the senescence program (Fig. 11 C). Because senescence of MEFs in culture is believed to be a result of oxidative stress caused by culturing cells in 20% oxygen, I compared expression of DDB2 in MEFs grown at 3% oxygen and in 20% oxygen. Clearly, cells grown in 3% oxygen

expressed much lower levels of DDB2 in all passages examined (Fig. 11D). Furthermore, expression of DDB2 in the HCT116 cells increased the level of senescence, as judged by the expression of SA-β-Gal (Fig. 12).

3.3 ROS MEDIATED UP-REGULATION OF DDB2 IS MEDIATED BY P38MAPK AND JNK

Next, I investigated the mechanism of ROS- mediated DDB2 induction. ROS increases expression of DDB2 both at the RNA and protein level, suggesting that ROS mediated DDB2 up-regulation is at the transcriptional level. DDB2 is a p53-regulated gene in human[32]. To examine whether ROS mediated DDB2 induction is p53 mediated, HCT p53-/- cells were treated with hydrogen peroxide for four hours and looked for expression of DDB2 at the RNA level. There was a clear accumulation of DDB2 in the hydrogen peroxide treated cells suggesting that ROS induced DDB2 expression is independent of p53 (Fig.13 A). ROS can induce DDB2 expression in mouse embryonic fibroblasts where DDB2 is not under p53 regulation suggesting p53 independent mechanism for ROS mediated DDB2 up-regulation. A major downstream effector pathway of ROS is JNK and stress activated protein kinase [83]. Therefore, I investigated whether the ROS activated MAPK pathway causes DDB2 up-regulation. Towards that, HCT116 cells were treated with hydrogen peroxide with or without p38MAPK inhibitor (SB 203580) or JNK inhibitor (SP 600125). In the absence of the inhibitor, hydrogen peroxide was able to up-regulate expression of DDB2, whereas in the presence of either of these inhibitors, hydrogen peroxide was not able to up-regulate DDB2 expression, suggesting that ROS mediated

Figure 13: ROS mediated DDB2 induction is p38MAPK/JNK dependent.
(A) HCT116 p53-/- cells were treated with 150 uM Hydrogen Peroxide for 4 hrs. Total RNA was analyzed by Semi-quantitative PCR for the level of DDB2. Cyclophlin was used as a loading control. (B) HCT116 cells were treated with 150 uM Hydrogen Peroxide for 4 hrs with or without p38MAPK inhibitor SB 203580. Total RNA was analyzed by Semi-quantitative PCR for the level of DDB2. Cyclophlin was used as a loading control. (C) HCT116 cells were treated with 150 uM Hydrogen Peroxide for 4 hrs with or without JNK inhibitor SP 600125. Total RNA was analyzed by Semi-quantitative PCR for the level of DDB2. Cyclophlin was used as a loading control. (D) HCT116 cells were treated with 150 uM Hydrogen Peroxide for 4 hrs with or without all-trans Retinoic Acid. Total RNA was analyzed by Semi-quantitative PCR for the level of DDB2. Cyclophlin was used as a loading control. (E) HCT116 cells were treated with 150 uM Hydrogen Peroxide for 4 hrs. Next, cells were subjected to ChIP assay, as described in Materials and Methods. Antibody against AP-1 or IgG was used for Immunoprecipitation. Filled boxes indicate the binding region of primers used to detect interaction of AP-1 with DDB2 promoter.

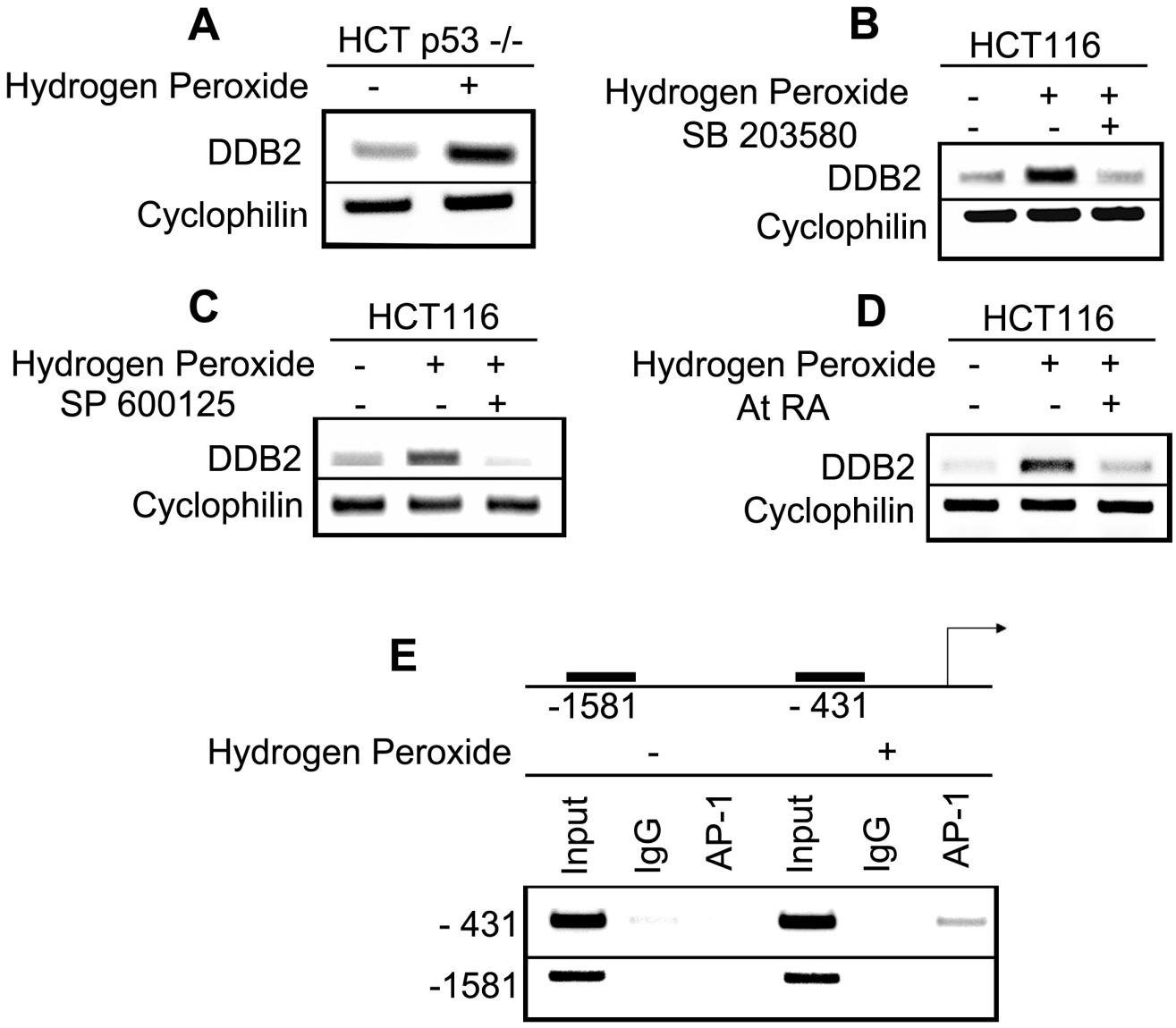
A
HCT p53 -/-
Hydrogen Peroxide - +
DDB2
Cyclophilin
B
HCT116
Hydrogen Peroxide - + +
SB 203580 - - +
DDB2
Cyclophilin
C
HCT116
Hydrogen Peroxide - + +
SP 600125 - - +
DDB2
Cyclophilin
D
HCT116
Hydrogen Peroxide - + +
At RA - - +
DDB2
Cyclophilin
E
-1581
- 431
Hydrogen Peroxide - +
Input
IgG
AP-1
Input
IgG
AP-1
- 431
-1581

activation of the MAPK pathway causes induction of DDB2 (Fig.13 B and C). AP-1 is a heterodimeric transcription factor downstream of the MAPK pathway [83]. Therefore, I examined whether AP-1 transcriptionaly activates DDB2 following ROS treatment. All-trans-Retinoic Acid (AtRA) is a specific inhibitor of AP-1 transcription factor [84, 85]. To examine the involvement of AP-1 in the ROS mediated up-regulation of DDB2, HCT116 cells were treated with hydrogen peroxide with or without AtRA. In the presence of AtRA, hydrogen peroxide did not result accumulation of DDB2, suggesting AP-1 transcriptionaly activates DDB2 after ROS accumulation (Fig.13 D). Bioinformatics analyses revealed two potential AP-1 binding sites in the DDB2 promoter, one at -431 and the other at -1581 from the start site. Both of these sites have consensus TPA response element. I performed chromatin IP to determine binding of AP-1 to these sites following hydrogen peroxide treatment. In the absence of hydrogen peroxide, there was no binding of AP-1. However, there was evidence of increased AP-1 accumulation in the -431 site following hydrogen peroxide treatment (Fig.13 E). Thus, ROS activates p38MAPK/ JNK that in turn triggers AP-1 accumulation on the promoter of DDB2, leading to up-regulation of DDB2 expression.

3.4 DDB2 DEFICIENCY CONFERS RESISTANCE TO ONCOGENE INDUCED SENESCENCE

It has been shown that expression of oncogenic Ras or activated Akt induces premature senescence in primary cells [86, 87]. Therefore, I sought to investigate whether expression of an oncogenic form of Ras would induce premature

Figure 14: DDB2-deficient cells are resistant to oncogene-induced premature senescence.
(A and B) IMR90 cells were infected with RasV12-ER. Following selection with puromycin, cells were further transfected with control siRNA or DDB2 siRNA. After 24 h, cells were treated with 4-hydroxytamoxifen to induce expression of Ras. Forty-eight hours following 4-hydroxytamoxifen induction, total cell extracts were analyzed for expression of Ras and depletion of DDB2. (C) Cells were stained for SA-β-Gal activity 48 h after tamoxifen induction. (Left) Representative images of Ras-expressing IMR90 cells transfected with control siRNA or DDB2 siRNA. (Right) SA-β-Gal-positive cells were counted from at least 10 fields of triplicate plates.

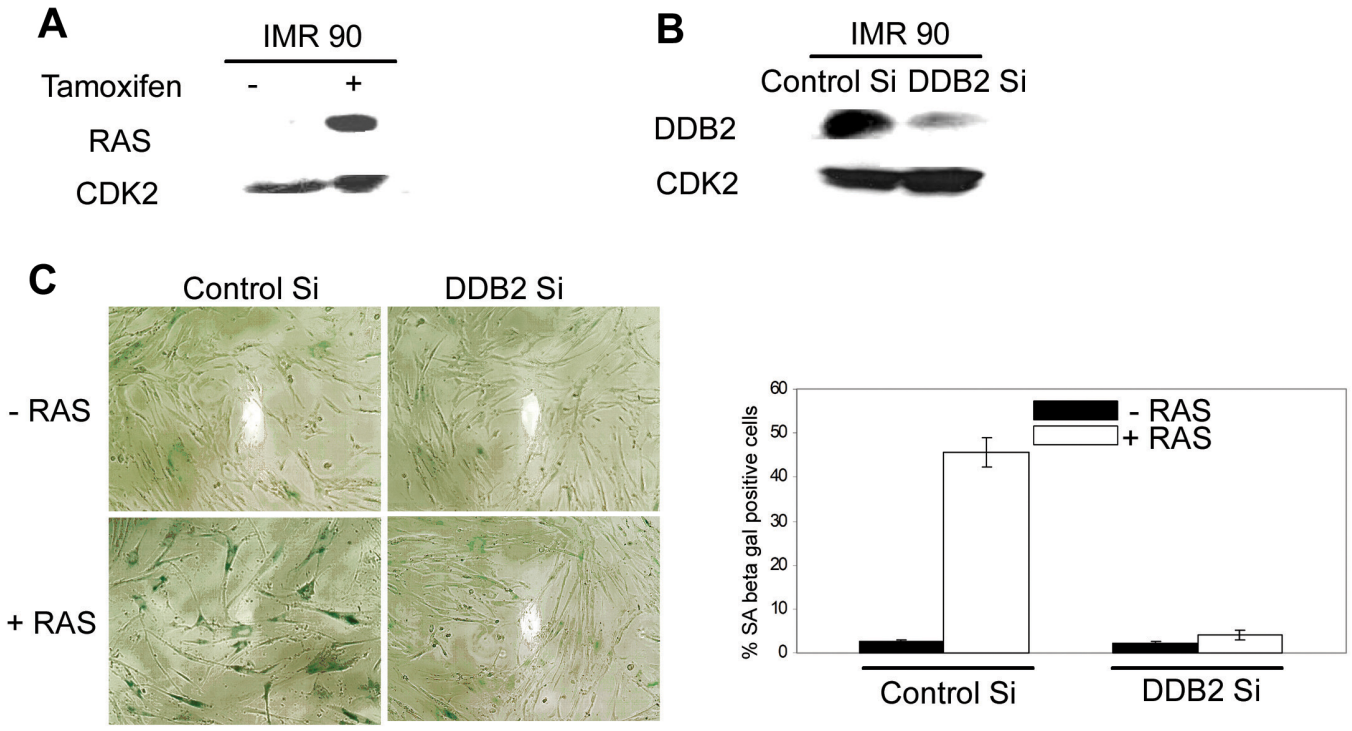
A
IMR 90
Tamoxifen
-
+
RAS
CDK2
B
IMR 90
Control Si
DDB2 Si
DDB2
CDK2
C
Control Si
DDB2 Si
- RAS
+ RAS
% SA beta gal positive cells
60
50
40
30
20
10
0
- RAS
+ RAS
Control Si
DDB2 Si

senescence in the DDB2-deficient cells. Because of the short life span of the MEFs, it was difficult to design a good experiment to compare the wild-type and the DDB2$^{-/-}$ MEFs. Therefore, I employed the primary human cell line IMR90. The IMR90 cells could be efficiently transfected with siRNA to knock down expression (Fig.14 A) [88]. First, I infected the cells with a retroviral vector expressing a 4-hydroxytamoxifen-inducible RasV12-ER fusion protein. Addition of tamoxifen stabilized the RasV12-ER protein (Fig.14 B). The RasV12-ER-expressing cells were then transfected with siRNA against DDB2 or control siRNA. The knockdown of DDB2 expression was confirmed by Western blot assays. Twenty-four hours after siRNA transfection, the cells were treated with 4-hydroxytamoxifen to activate RasV12-ER [89, 90]. Forty-eight hours after the induction, the cells were subjected to SA-β-Gal expression assays. As expected, in the control siRNA-transfected cells, induction of RasV12 caused senescence in a high percentage of cells, as judged by the senescence marker SA-β-Gal. The DDB2 siRNA-transfected cells, on the other hand, did not exhibit any significant increase in premature senescence (Fig.14 C). These results are consistent with the notion that DDB2 is required also for premature senescence induced by oncogenes.

3.4 DDB2 IS REQUIRED FOR DNA DAMAGE INDUCED SENESCENCE

DNA-damaging agents have been shown to induce premature senescence in tumor and normal cells [46]. Therefore, I investigated whether the DNA-damaging agents could induce premature senescence in the DDB2-deficient cells. The MEFs (WT or DDB2$^{-/-}$) were treated with cisplatin (30 μM for 8 h), aclarubicin (0.5 μM for 8 h), or

Figure 15: DDB2-/- MEFs do not senesce after DNA damage.
(A) WT or DDB2$^{-/-}$ MEFs were treated with UV (50 J/m^2), cisplatin (30 μm), or aclarubicin (0.5 μM) for 8 h. Seventy-two hours after the treatment, the cells were subjected to SA-β-Gal assay. (Left) Representative images of UV-, aclarubicin-, or cisplatin-treated WT or DDB2$^{-/-}$ MEFs stained for SA-β-Gal. (Right) SA-β-Gal-positive cells were counted from at least 10 fields of triplicate plates. A quantification of SA-β-Gal-positive WT or DDB2$^{-/-}$ MEFs with different treatments is shown. (B) WT and DDB2$^{-/-}$ MEFs were treated with UV (50 J/m^2), cisplatin (30 μm), or aclarubicin (0.5 μM) for 8 h. Cells were counted from next day onwards up to 7 days. An average count from three experiments is plotted.

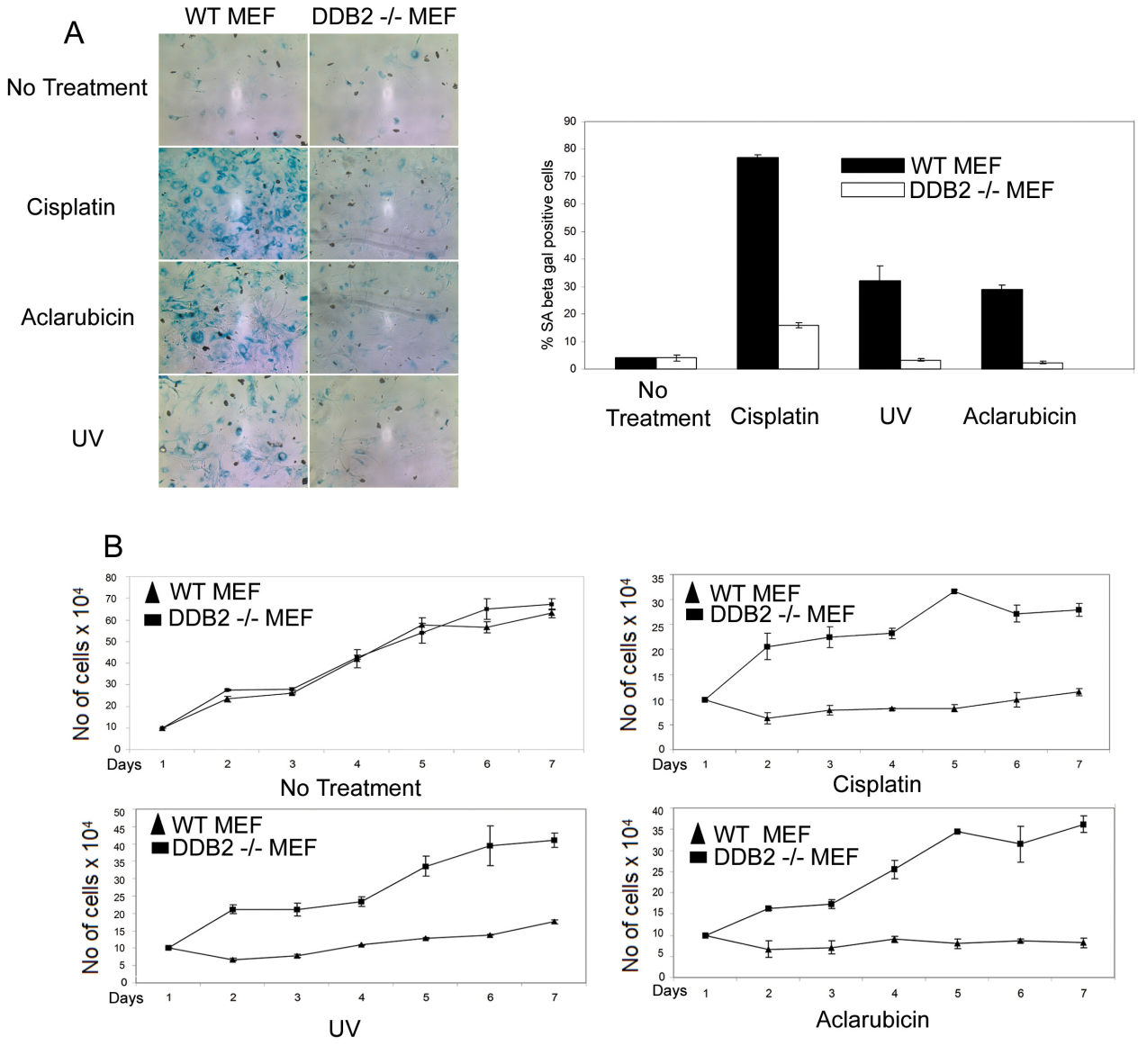
A
WT MEF
DDB2 -/- MEF
No Treatment
Cisplatin
Aclarubicin
UV
% SA beta gal positive cells
WT MEF
DDB2 -/- MEF
No Treatment
Cisplatin
UV
Aclarubicin
B
No of cells x 10⁴
Days
WT MEF
DDB2 -/- MEF
No Treatment
Cisplatin
UV
Aclarubicin

Figure 16: DDB2-deficient HCT116 cells do not senesce after DNA damage.
HCT116 control or HCT11shDDB2 cells were treated with UV (50 J/m^2), cisplatin (30 μm), or aclarubicin (0.5 μM) for 8 h. Seventy-two hours after the treatment, the cells were subjected to SA-β-Gal assay. (Left) Representative images of UV-, aclarubicin-, or cisplatin-treated HCT116 control or HCT116shDDB2 cells stained for SA-β-Gal. (Right) SA-β-Gal-positive cells were counted from at least 10 fields of triplicate plates. A quantification of SA-β-Gal-positive HCT116 control or HCT116shDDB2 cells with different treatments is shown.

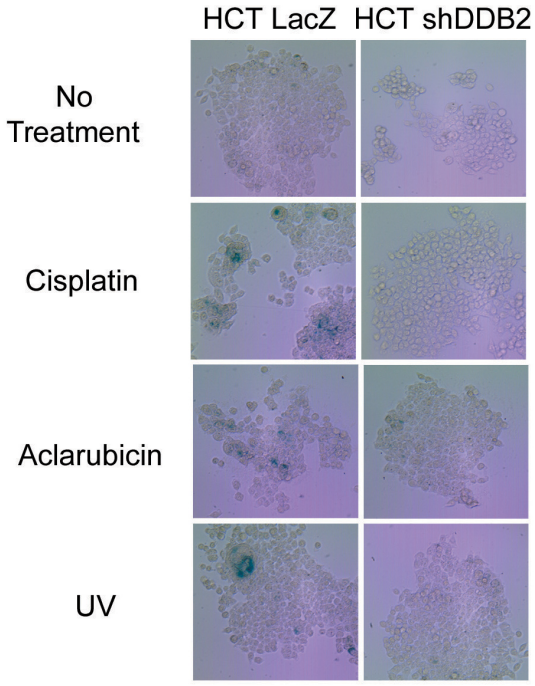
HCT LacZ
HCT shDDB2
No Treatment
Cisplatin
Aclarubicin
UV

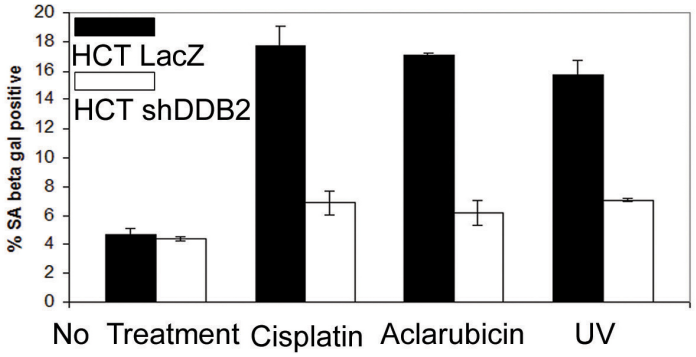
% SA beta gal positive
20
18
16
14
12
10
8
6
4
2
0
HCT LacZ
HCT shDDB2
No Treatment
Cisplatin
Aclarubicin
UV

Figure 17: DDB2 does not play role in DNA damage induced checkpoint activation.
HCT116 shLacZ or HCT116 shDDB2 expressing cells were treated with Cisplatin. Following the treatment, cells were subjected to immunofluoroscence staining with H2AX or DAPI. Representative images of untreated or treated control /DDB2 deficient cells are being shown.

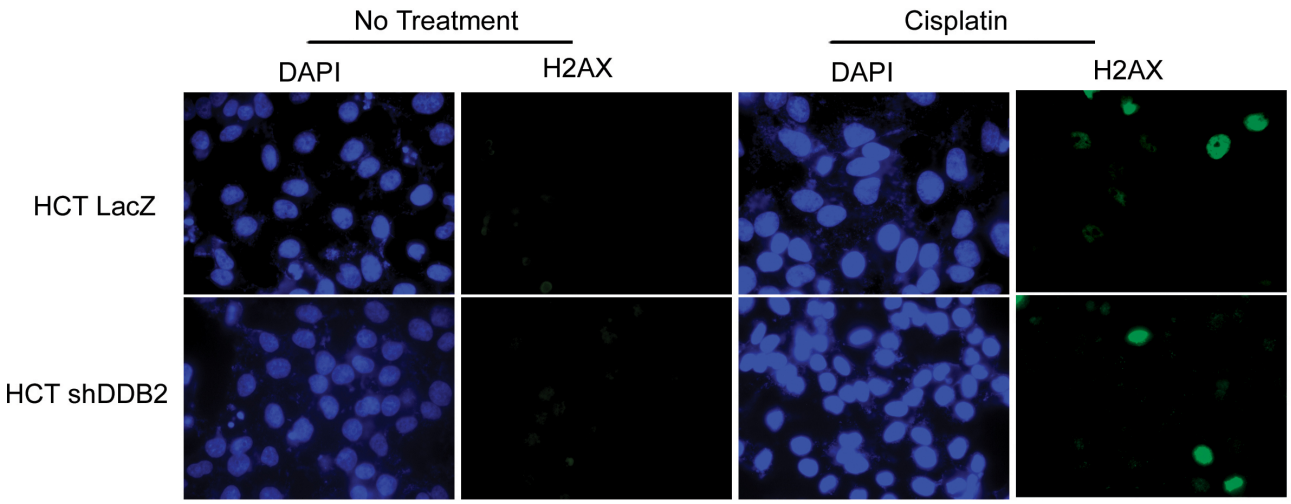
No Treatment
Cisplatin
DAPI
H2AX
DAPI
H2AX
HCT LacZ
HCT shDDB2

UV irradiation (50 J/m^2). Treatment of the wild-type MEFs for 18 h with cisplatin or aclarubicin induces apoptosis. That is why I used a shorter treatment time. The dosage of UV irradiation used in our experiments also induces apoptosis in the wild-type MEFs. However, I was able to detect senescence in the surviving population. Two days after treatment, the cells were assayed for SA-β-Gal expression. The wild-type MEFs exhibited a significant increase in SA-β-Gal-positive cells in comparison to the DDB2$^{-/-}$ MEFs (Fig.15 A). Also, I performed proliferation assays after treatment with the DNA-damaging agents. As expected, the wild-type MEFs exhibited a dramatic decrease in proliferation rate, whereas the DDB2$^{-/-}$ MEFs continued to proliferate (Fig.15 B). Consistent with the observations with the MEFs, the HCT116 cells expressing the DDB2 shRNA did not exhibit any significant increase in SA-β-Gal-positive cells after treatment with the DNA-damaging agents (Fig.16). The lack of DNA damage-induced senescence is not related to a lack of checkpoint activation, as we detected efficient H2AX focus formation in the HCT116 cells expressing DDB2 shRNA after cisplatin treatment (Fig.17).

3.6 DDB2 DEFICIENT CELLS ARE IMPAIRED IN ROS ACCUMULATION FOLLOWING DNA DAMAGE

DNA-damaging agents also increase the levels of reactive oxygen species and oxidative stress, which leads to premature senescence [91, 92]. Therefore, I sought to compare the levels of ROS production between the wild-type MEFs and the DDB2$^{-/-}$ MEFs, as well as the HCT116 cells with or without DDB2 knockdown. As in the previous experiments, the cells were treated with UV irradiation, cisplatin, or

Figure 18: DDB2-deficient cells are impaired in accumulation of ROS following DNA damage.

(A) WT or DDB2$^{-/-}$ MEFs were treated with UV (50 J/m^2), cisplatin (30 μm), or aclarubicin (0.5 μM) for 8 h. After the treatments, cells were stained with DCFDA and DAPI. (Top) Representative images of DCFDA- or DAPI-stained WT or DDB2$^{-/-}$ MEFs following treatments. (Bottom) A quantification of treated or untreated WT and DDB2$^{-/-}$ MEFs positive for DCFDA staining is shown. (B) HCT116 cells expressing LacZ shRNA or DDB2 shRNA were treated with UV (50 J/m^2), cisplatin (30 μm), or aclarubicin (0.5 μM) for 8 h. After the treatments, cells were stained with DCFDA or DAPI. (Top) Representative images of DCFDA- or DAPI-stained HCT116 cells following treatments. (Bottom) A quantification of treated or untreated HCT116 cells expressing LacZ shRNA or DDB2 shRNA positive for DCFDA staining is shown.

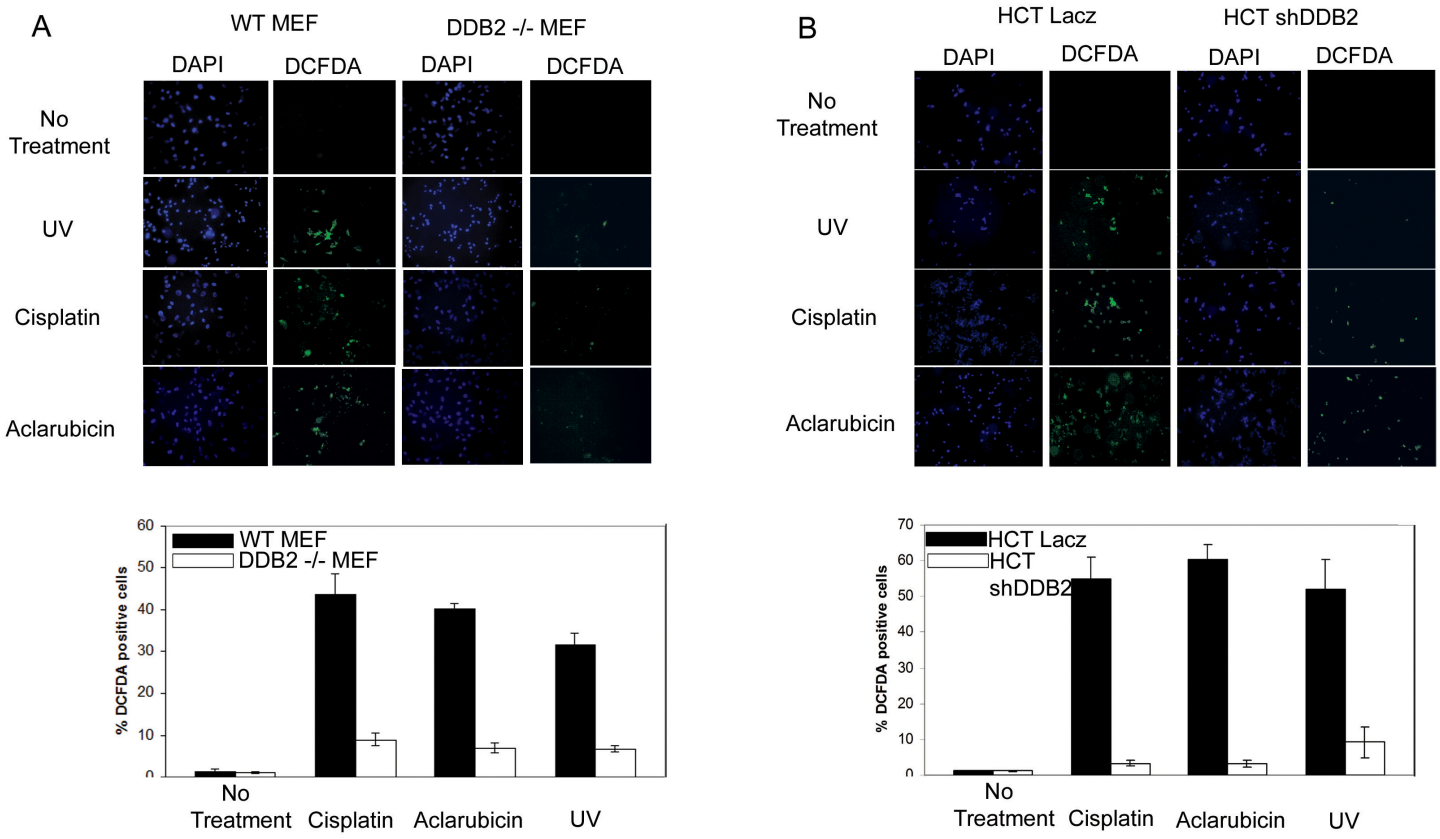
A
WT MEF
DDB2 -/- MEF
DAPI
DCFDA
DAPI
DCFDA
No Treatment
UV
Cisplatin
Aclarubicin
B
HCT Lacz
HCT shDDB2
DAPI
DCFDA
DAPI
DCFDA
No Treatment
UV
Cisplatin
Aclarubicin
% DCFDA positive cells
WT MEF
DDB2 -/- MEF
No Treatment
Cisplatin
Aclarubicin
UV
% DCFDA positive cells
HCT Lacz
HCT shDDB2
No Treatment
Cisplatin
Aclarubicin
UV

aclarubicin. Eight hours following the treatments, the cells were treated with 2,7-dicholorofluorescein diacetate (DCFDA) to measure the levels of peroxide. Following a treatment with DCFDA for 30 min, the cells were stained also with DAPI. Peroxides convert DCFDA to a fluorescent compound. The fluorescence-positive cells were visualized and quantified by direct counting. The average percentages of fluorescence-positive cells with respect to DAPI signals from at least 10 different fields were plotted. In the MEFs as well as in the HCT116 cells, DDB2 deficiency clearly inhibited the accumulation of ROS following DNA damage (Fig.18). Together, these results suggest that the deficiency in premature senescence is related to a deficiency in ROS accumulation in the absence of DDB2.

3.7 DDB2 IS A REPRESSOR OF THE ANTI-OXIDANT GENES SOD2 AND CATALASE

Coincidentally, a recent study indicated that DDB2 could bind to the promoter of MnSOD and inhibits its expression [93]. Inhibition of the antioxidant genes could potentially explain my observations. Because I detected a loss of accumulation of peroxides, I assayed for both MnSOD and catalase expression in the presence and absence of DDB2. MnSOD and catalase mRNA levels were measured by RT-PCR assays. In the absence of DDB2, both the MEFs and the HCT116 cells exhibited a much greater expression of MnSOD and catalase (Fig. 19 A). The protein expression of MnSOD and catalase was also significantly higher in the DDB2-deficient cells (Fig.19 B). In reciprocal experiments, expression of DDB2 in the $DDB2^{-/-}$ MEFs caused a severe inhibition of MnSOD and catalase expression (Fig.19 C and D). Thus, DDB2 regulates the level of ROS by inhibiting expression of the antioxidant genes.

Figure 19: DDB2 is a repressor of MnSOD and catalase.
(A) Total RNA from WT or DDB2$^{-/-}$ MEFs was analyzed by semiquantitative PCR for the levels of MnSOD and catalase. GAPDH was used as a loading control. Total RNA from HCT116 cells expressing LacZ shRNA or DDB2 shRNA was analyzed by semiquantitative PCR for the levels of MnSOD and catalase. Cyclophilin was used as a loading control. (B) Total cell extracts from HCT116 cells expressing LacZ shRNA or DDB2 shRNA were subjected to Western blot assay with MnSOD or catalase antibody. CDK2 was used as a loading control. (C) Immortalized DDB2$^{-/-}$ MEFs were infected with adenovirus expressing T7-tagged DDB2 or adenovirus expressing LacZ. Total cell extracts were subjected to Western blot assay with T7 or p19Arf antibody. CDK2 was used as a loading control. (D) Immortalized DDB2$^{-/-}$ MEFs were infected with adenovirus expressing T7-tagged DDB2 or adenovirus expressing LacZ. Total RNA was analyzed by semiquantitative PCR for the levels of p19Arf, MnSOD, and catalase. GAPDH was used as a loading control.

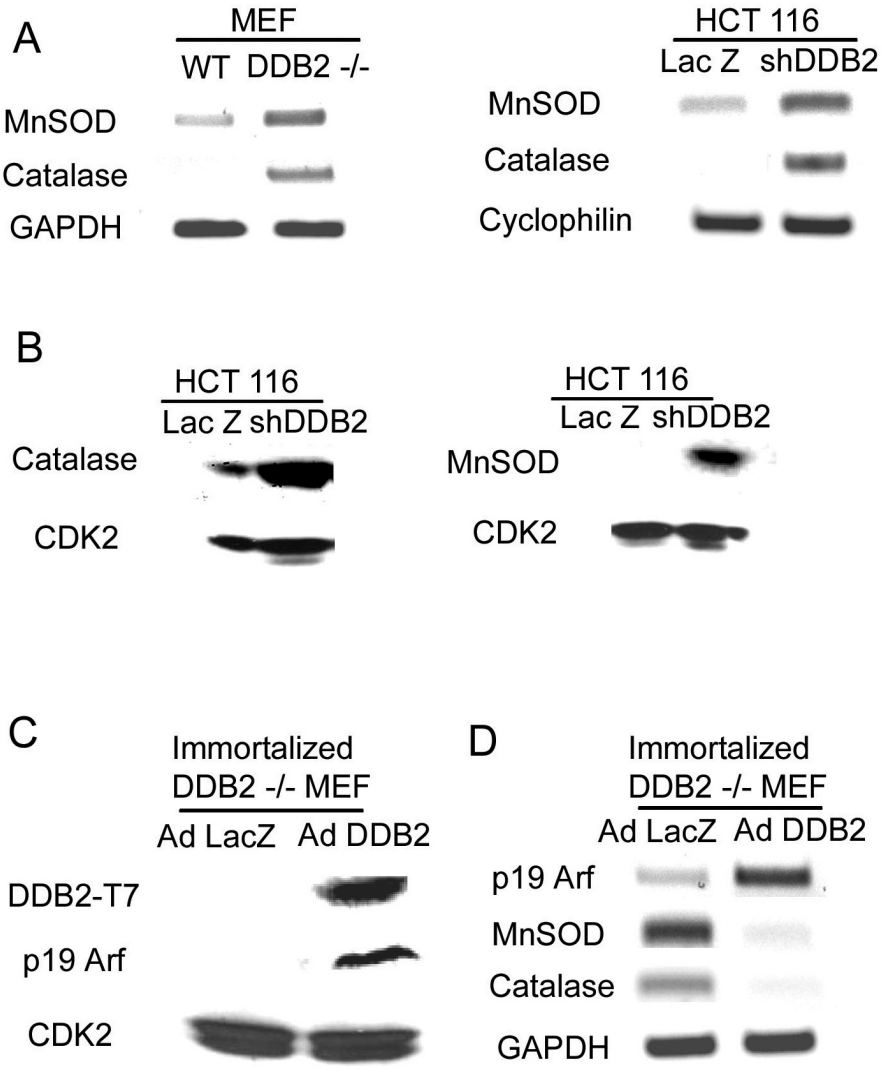
A
MEF
WT DDB2 -/-
MnSOD
Catalase
GAPDH
HCT 116
Lac Z shDDB2
MnSOD
Catalase
Cyclophilin
B
HCT 116
Lac Z shDDB2
Catalase
CDK2
HCT 116
Lac Z shDDB2
MnSOD
CDK2
C
Immortalized
DDB2 -/- MEF
Ad LacZ Ad DDB2
DDB2-T7
p19 Arf
CDK2
D
Immortalized
DDB2 -/- MEF
Ad LacZ Ad DDB2
p19 Arf
MnSOD
Catalase
GAPDH

Figure 20: DDB2 mediated up-regulation of p14Arf is p38MAPK dependent.
(A) WT or DDB2$^{-/-}$ MEFs were treated with UV, cisplatin (Cis) or aclarubicin (Acla) as previously mentioned. Total cell extracts were subjected to Western blot assay with phospho-p38MAPK or total p38MAPK antibody. NT, no treatment. (B) HCT116 cells expressing DDB2 shRNA were infected with adenovirus expressing T7-tagged DDB2 or LacZ. One set of cells was treated with p38MAPK inhibitor SB203580, and the other set was left untreated. Total RNA was analyzed by semiquantitative PCR for the level of p14Arf. Cyclophilin was used as a loading control.

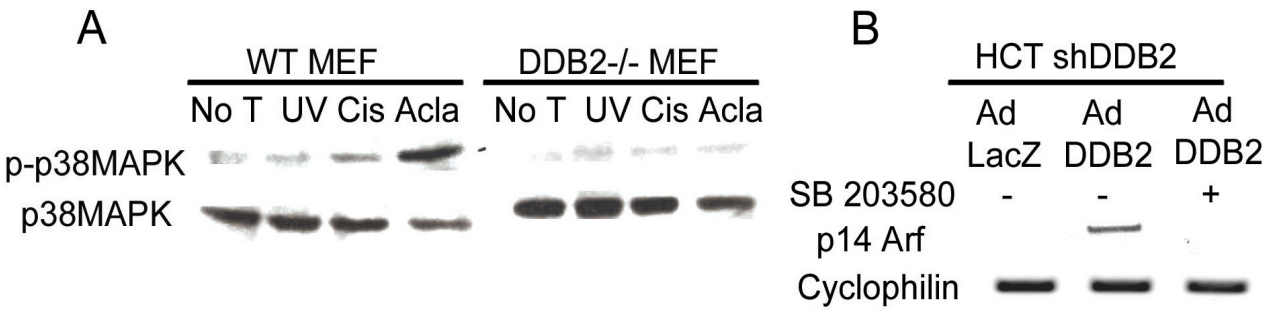
A
WT MEF
DDB2-/- MEF
No T UV Cis Acla
No T UV Cis Acla
p-p38MAPK
p38MAPK
B
HCT shDDB2
Ad LacZ
Ad DDB2
Ad DDB2
SB 203580 - - +
p14 Arf
Cyclophilin

ROS accumulation increases the activity of p38MAPK, which increases expression of ARF. Consistent with that, the DDB2-mediated increase in p14Arf expression was inhibited by an inhibitor of p38MAPK (Fig.20 B). Moreover, activation of p38MAPK in response to DNA-damaging agents, which increase ROS, is impaired in the DDB2-deficient cells (Fig.20 A). Thus, it appears that DDB2 activates p19/p14Arf expression by increasing the level of ROS, which causes activation of p38MAPK.

3.8 DDB2 RECRUITS SUV39H ON THE PROMOTER OF SOD2 AND CATALASE AND RESULTS HETEROCHROMATINIZATION

To investigate a direct inhibition of expression of the MnSOD and catalase genes by DDB2, I performed ChIP experiments using different sets of primers covering 1 kb of the promoter-proximal region of both the genes. In addition, I scanned the 1.6-kb promoter region of p14Arf. The ChIP experiments were carried out with HCT116 cells. Fewer amplicons for the MnSOD promoter were used because of the previous work that identified a binding site for DDB2 in the MnSOD promoter. I observed evidence for a physical interaction of DDB2 with promoters of both MnSOD and catalase, but no interaction could be detected within the 1.6-kb region of the p14Arf promoter (Fig.21). The DDB2-associated protein Cul4 was shown to associate with the histone H3K9 methyltransferase Clr4 to induce heterochromatin formation in fission yeast [94]. Moreover, a recent study indicated that Cul4 could recruit H3K4 methyltransferase MLL1 to activate expression of p16Ink4a expression [95]. Since I observed an inhibition of the MnSOD and catalase expression by DDB2, we considered the possibility that DDB2 might recruit Clr4 homolog Suv39h through its

Figure 21: DDB2 binds to the promoter region of MnSOD and catalase.
(A and B) HCT116 cells were subjected to ChIP assay, as described in Materials and Methods. Antibody against DDB2 or IgG was used for immunoprecipitation. The primers used to detect interaction of DDB2 with MnSOD promoter, catalase promoter, Arf promoter, and negative controls are indicated by arrows.

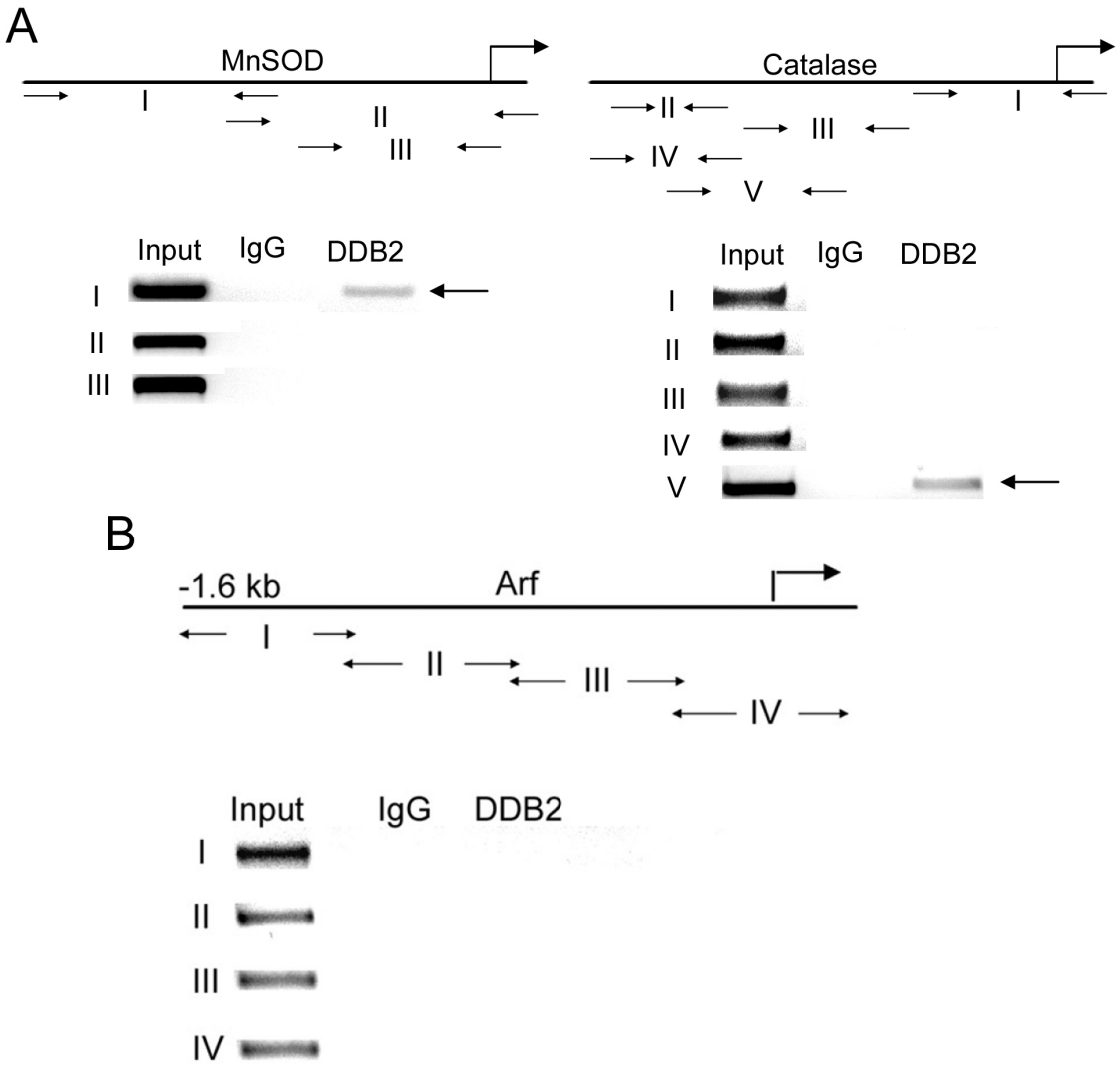
A
MnSOD
I
II
III
Input
IgG
DDB2
I
II
III
Catalase
II
III
I
IV
V
Input
IgG
DDB2
I
II
III
IV
V
B
-1.6 kb
Arf
I
II
III
IV
Input
IgG
DDB2
I
II
III
IV

Figure 22: DDB2 is an epigenetic regulator of SOD2 and catalase.
(A) DDB2 recruits Suv39h to induce H3K9 trimethylation at MnSOD and catalase promoters. HCT116 cells expressing LacZ shRNA or DDB2 shRNA were subjected to ChIP assay, as described in Materials and Methods. Antibody against H3K9Me3, Suv39h, Cul4a, or IgG was used for immunoprecipitation. The MnSOD and catalase promoter fragments in the immunoprecipitated chromatins were quantified by semiquantitative PCR with the primer pairs I for MnSOD and V for catalase in panel A. (B) HCT116 cells were infected with adenovirus expressing T7-tagged DDB2 or adenovirus expressing LacZ. Following 18 h of incubation with adenovirus, they were subjected to ChIP assay. Antibody against H3K9Me3, Suv39h, or IgG was used for immunoprecipitation. The MnSOD and catalase promoter fragments in the immunoprecipitated chromatins were quantified by semiquantitative PCR with the primer pairs I for MnSOD and V for catalase in panel A. (C) ChIP-reChIP analysis of HCT116 cells. Soluble chromatin was prepared from HCT116 cells and divided into two chromatin aliquots which were immunoprecipitated with antibodies to DDB2 and Suv39h, respectively. Immunocomplexes were eluted with DTT, and soluble chromatin fractions were reimmunoprecipitated with reciprocal antibodies against Suv39h and DDB2, respectively. (D) Cell extracts from HCT116 cells (3 mg) were subjected to immunoprecipitation (IP) with Suv39h antibody or with isotype-matched immunoglobulin G (IgG). The immunoprecipitates were analyzed for the presence of DDB2 by Western blot assay. Total extracts (0.45 mg) were also analyzed for the level of DDB2.

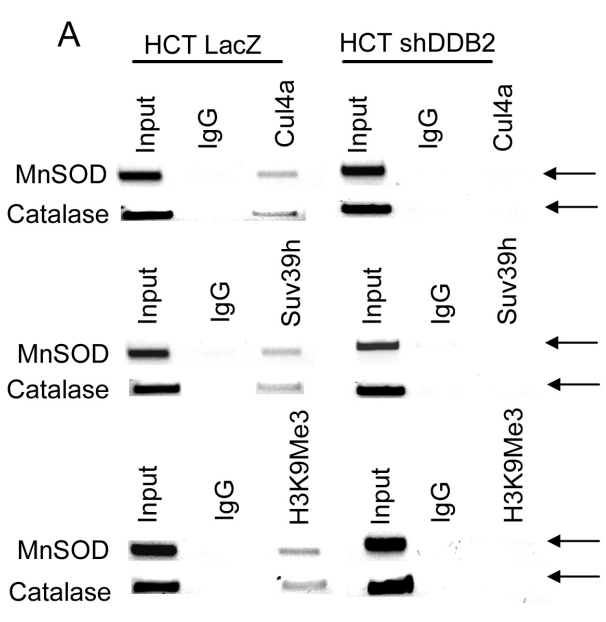
A
HCT LacZ
HCT shDDB2
Input
IgG
Cul4a
Suv39h
H3K9Me3
MnSOD
Catalase

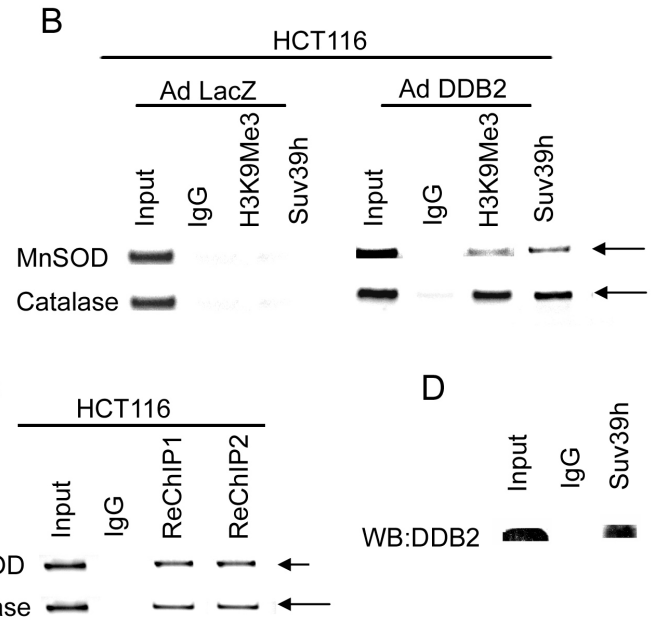
B
HCT116
Ad LacZ
Ad DDB2
Input
IgG
H3K9Me3
Suv39h
MnSOD
Catalase
C
HCT116
ReChIP1
ReChIP2
D
WB:DDB2

interaction with Cul4 to induce inhibitory methylation. First, I investigated whether Cul4A and Suv39h associate with the MnSOD and catalase gene promoters. We compared the HCT116 cells expressing LacZ shRNA and those expressing DDB2 shRNA in ChIP experiments. Both Cul4A and Suv39h interaction could be easily detected in the HCT116 cells expressing LacZ shRNA (Fig.22 A). However, the DDB2 shRNA-expressing cells did not exhibit any significant interaction of Cul4A and Suv39h with the MnSOD and catalase promoter. Next, I assayed for H3K9 trimethylation using ChIP experiments. I could detect the presence of trimethylated histone H3K9 in the promoter regions of MnSOD and catalase in the HCT116 cells expressing LacZ shRNA but not in those expressing DDB2 shRNA (Fig. 22 A). Moreover, expression of DDB2 in the HCT116 cells caused a significant increase in the recruitment of Suv39h and H3K9 trimethylation (Fig. 22 B). Furthermore, ChIP/re-ChIP experiments confirmed that DDB2 and Suv39h interacted with the promoters simultaneously (Fig.22 C). Also, coimmunoprecipitation experiments provided evidence for a physical interaction between DDB2 and Suv39h (Fig.22 D). Together, these results suggest that DDB2 recruits Suv39h onto the promoters of MnSOD and catalase to repress expression of these antioxidant genes by increasing histone H3K9 trimethylation.

3.9 IN VIVO EVIDENCE FOR A ROLE OF DDB2 IN SENESCENCE

To investigate the role of DDB2 in the regulation of MnSOD and catalase in vivo, RNAs from various tissues harvested from adult WT or DDB2$^{-/-}$ mice were analyzed for the levels of MnSOD and catalase. Clearly, brain, thymus, lung, and liver from the

Figure 23: DDB2-deficient mice are impaired in senescence following CCl_4 treatment.
(A) Total RNA isolated from different tissues of WT and $DDB2^{-/-}$ mice was analyzed by semiquantitative PCR for the levels of MnSOD and catalase. GAPDH was used as a loading control. (B) $DDB2^{-/-}$ mice do not initiate senescence following carbon tetrachloride treatment. WT and $DDB2^{-/-}$ mice were treated with carbon tetrachloride (1 ml/kg CCl_4) for 2 weeks. Animals were sacrificed 72 h after the last injection, and their livers were used for further analysis. Detection of SA-β-Gal activity was performed as described in Materials and Methods. (Left) Representative images of tissue sections stained for SA-β-Gal. (Right) SA-β-Gal-positive cells were counted from at least 10 fields of triplicate sections. A quantification of SA-β-Gal-positive cells is shown.

A

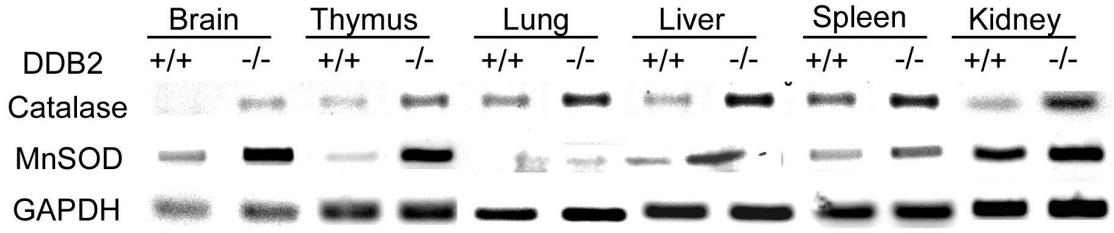

B

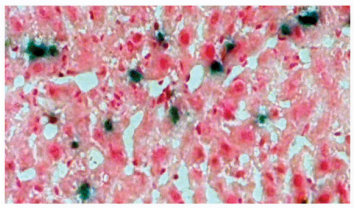

WT Liver

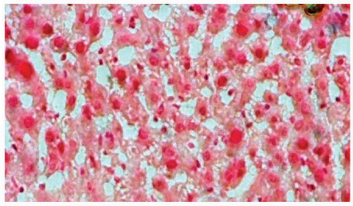

DDB2 -/- Liver

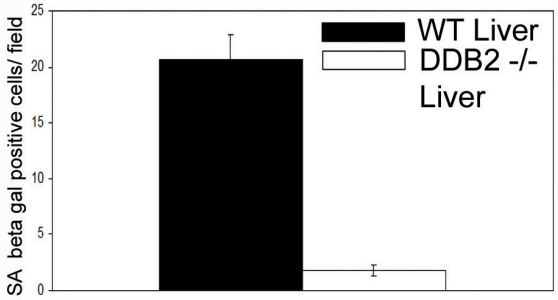

DDB2$^{-/-}$ mice exhibited significantly higher expression of MnSOD and catalase than did those tissues from the WT mice, indicating that DDB2 is a key regulator of MnSOD and catalase expression in these tissues (Fig.23 A).

To investigate the consequences of high-level antioxidant gene expression in an in vivo set up, WT and DDB2$^{-/-}$ mice were subjected to CCl4-induced liver damage, which is known to increase the levels of ROS and senescence of the hepatic stellate cells [81]. Hepatic stellate cells contribute to fibrotic response in the liver following chronic liver damage. Upon withdrawal of chronic damage, hepatic stellate cells undergo premature senescence or apoptosis and get removed from the system leading to regression of liver fibrosis. Deficiency of hepatic stellate cell senescence keeps these cells functionally active, causing an impaired fibrotic response. For example, p53-/- or p53-/- INK4a/ARF-/- mice are deficient in restricting fibrotic regression following withdrawal of chronic damage owed to their deficient senescence response [81]. Similarly, DDB2-/- mice were found to be deficient in senescence of liver cells following withdrawal of chronic liver damage, suggesting that DDB2 might play a critical role in controlling liver fibrosis. The liver sections were assayed for expression of the senescence marker SA-β-Gal. As expected, the liver sections from the DDB2$^{-/-}$ mice exhibited greatly reduced expression of SA-β-Gal compared to the sections from the WT mice (Fig.23 B), confirming the notion that DDB2 plays an important regulatory role in the expression of the antioxidant MnSOD and catalase genes that is significant for premature senescence of cells in vivo. Next, I did a time course experiment where WT and DDB2-/- female mice were

Figure 24: DDB2 -/- mice exhibit augmented hepatic fibrosis following chronic damage.
WT and DDB2$^{-/-}$ female mice were treated with carbon tetrachloride (1 ml/kg CCl_4) twice a week for 6 weeks. Animals were sacrificed at indicated time-points after the last injection, and their livers were used for further analysis. Liver sections were fixed in 10% Formalin, processed and embedded with paraffin for sectioning. Prepared skin section slides were then subjected H & E staining. Representative pictures are shown.

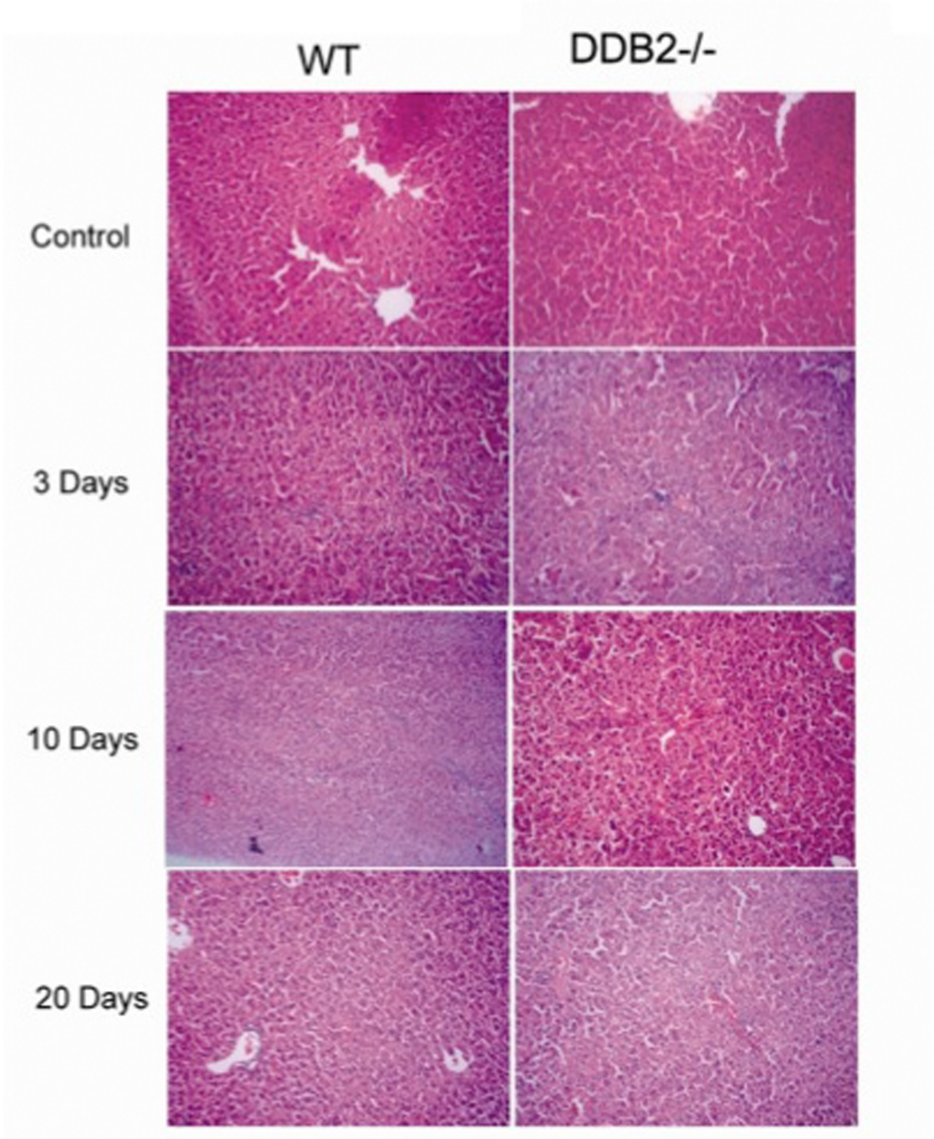
WT
DDB2-/-
Control
3 Days
10 Days
20 Days

Figure 25: DDB2-/- mice exhibit elevated fibrosis response.
WT and DDB2$^{-/-}$ female mice were treated with carbon tetrachloride (1 ml/kg CCl_4) twice a week for 6 weeks. Animals were sacrificed at indicated time-points after the last injection, and their livers were used for further analysis. Liver sections were fixed in 10% Formalin, processed and embedded with paraffin for sectioning. Prepared skin section slides were then subjected Sirius Red staining. (Top) Representative pictures are shown. (Bottom) Sirius Red positive area was quantified by ImageJ. 10 random fields were chosen.

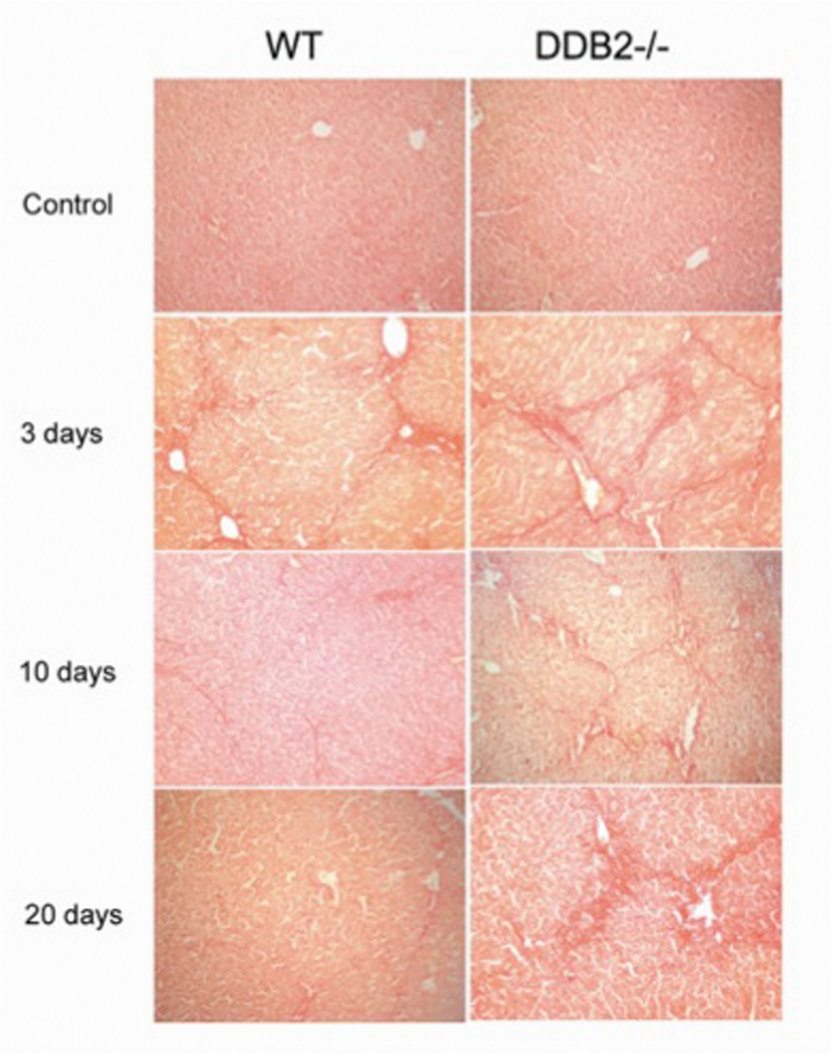
WT
DDB2-/-
Control
3 days
10 days
20 days

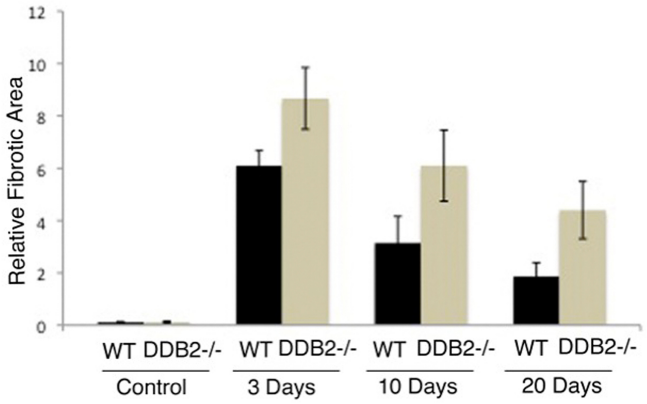
Relative Fibrotic Area
12
10
8
6
4
2
0
WT DDB2-/-
Control
WT DDB2-/-
3 Days
WT DDB2-/-
10 Days
WT DDB2-/-
20 Days

Figure 26: DDB2-/- mice exhibit elevated extracellular matrix deposition.
(Top) WT and DDB2$^{-/-}$ female mice were treated with carbon tetrachloride (1 ml/kg CCl_4) twice a week for 6 weeks. Animals were sacrificed at indicated time-points after the last injection, and their livers were used for further analysis. Liver sections were fixed in 10% Formalin, processed and embedded with paraffin for sectioning. Prepared liver section slides were then subjected to immunohistochemical analysis using SMA antibody. Representative images (20X magnification) are shown. (Bottom) Protein extracts from the liver were subjected to Western blot assay with SMA or Tubulin antibody.

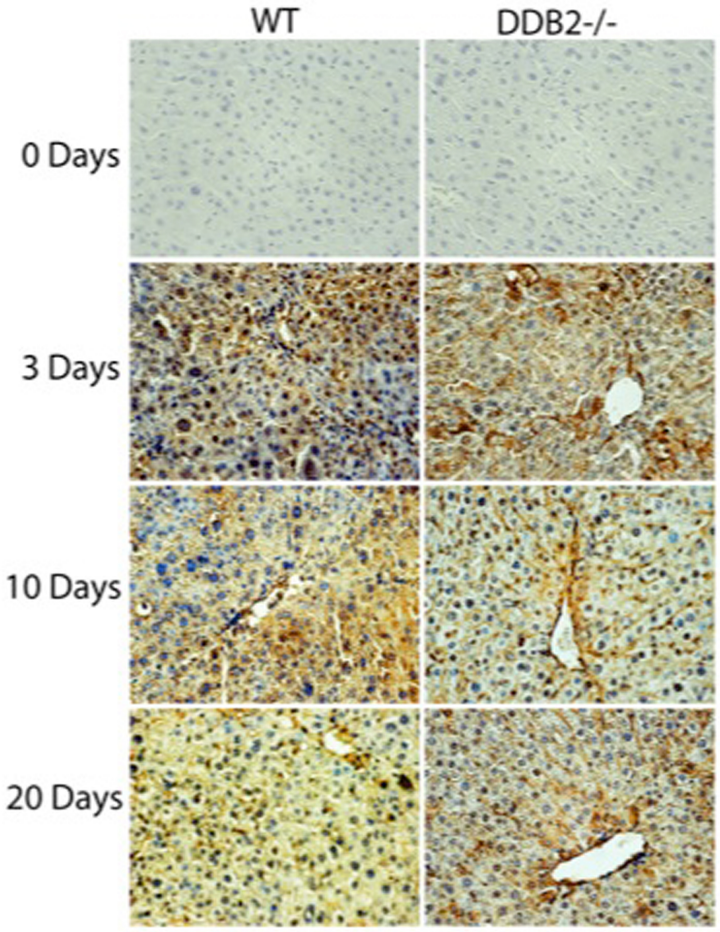
WT
DDB2-/-
0 Days
3 Days
10 Days
20 Days

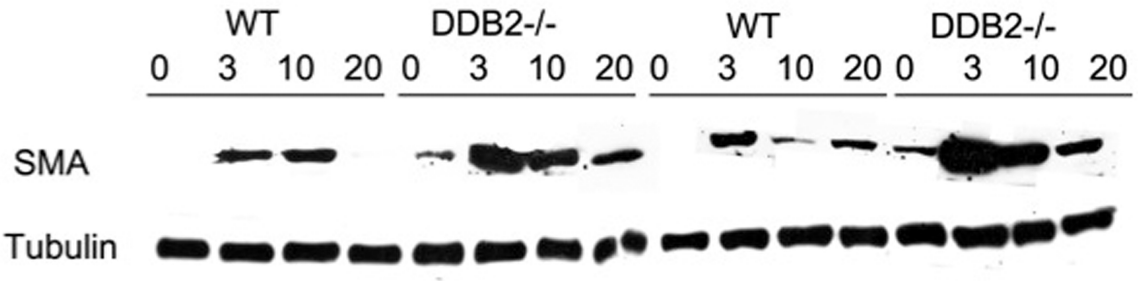
WT
DDB2-/-
WT
DDB2-/-
0 3 10 20 0 3 10 20 0 3 10 20 0 3 10 20
SMA
Tubulin

Figure 27: DDB2-/- mice are deficient in chronic damage induced apoptosis.
(Top) WT and DDB2$^{-/-}$ female mice were treated with carbon tetrachloride (1 ml/kg CCl_4) twice a week for 6 weeks. Animals were sacrificed at indicated time-points after the last injection, and their livers were used for further analysis. Liver sections were fixed in 10% Formalin, processed and embedded with paraffin for sectioning. Prepared liver section slides were then subjected to TUNEL assay. (Top) Representative pictures are shown. (Bottom) TUNEL positive cells were quantified by ImageJ. 10 random fields were chosen.

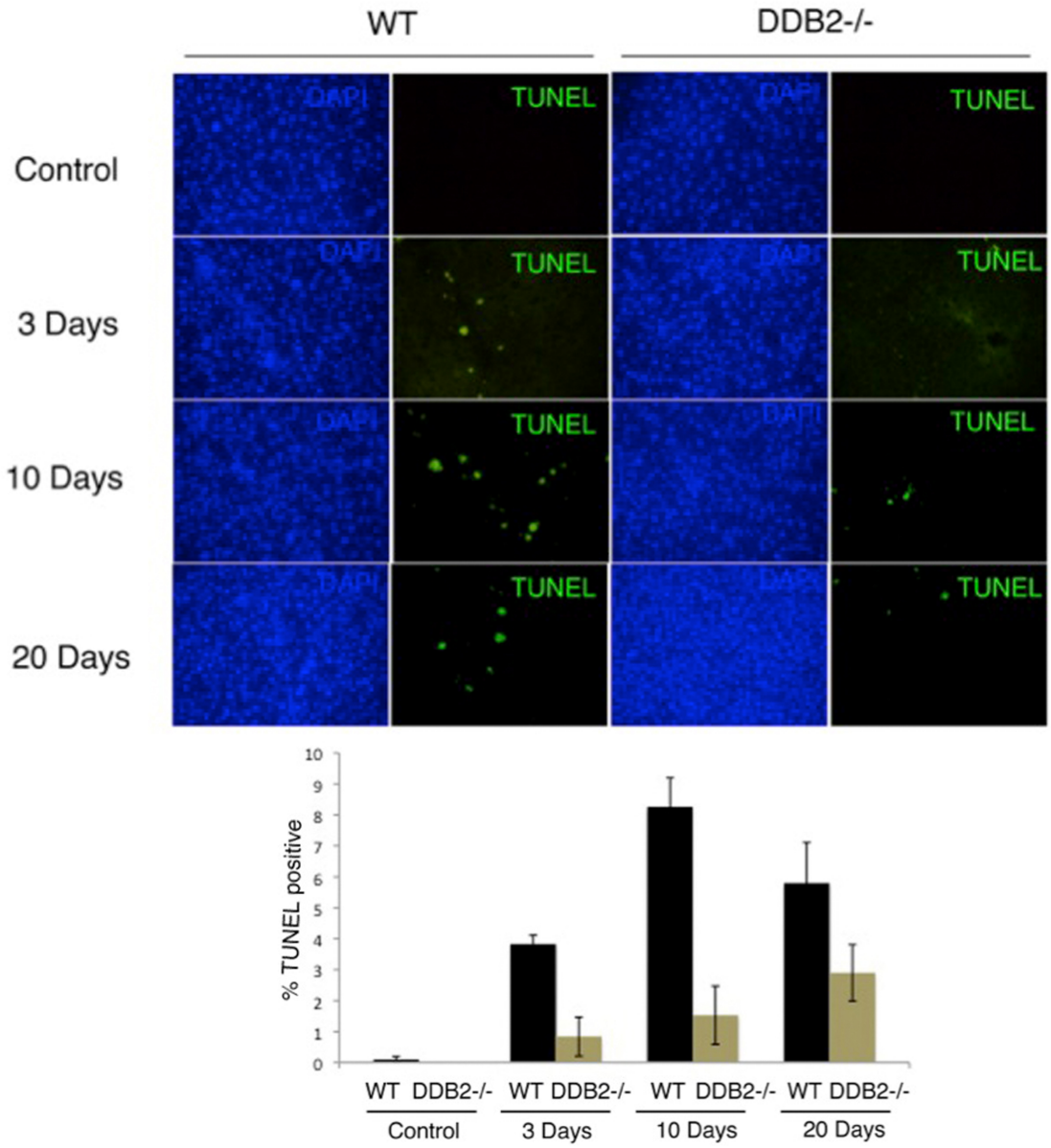
WT
DDB2-/-
Control
3 Days
10 Days
20 Days
DAPI
TUNEL
% TUNEL positive
0
1
2
3
4
5
6
7
8
9
10
WT DDB2-/-
Control
3 Days
10 Days
20 Days

Figure 28: DDB2-/- mice are deficient in chronic damage induced senescence. WT and DDB2$^{-/-}$ female mice were treated with carbon tetrachloride (1 ml/kg CCl_4) twice a week for 6 weeks. Animals were sacrificed at indicated time-points after the last injection, and their livers were used for further analysis. Protein extracts from the liver were subjected to Western blot assay with p19Arf or Actin antibody.

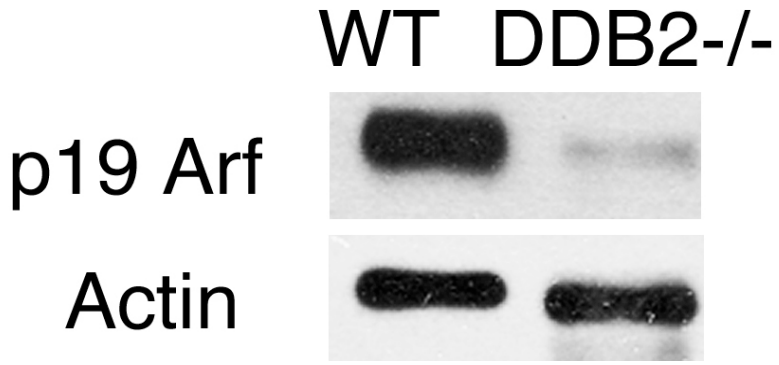
WT
DDB2-/-
p19 Arf
Actin

treated with carbon tetrachloride for 6 weeks, twice a week. Following withdrawal of the treatment, mice were sacrificed at 5, 10 and 20 days time point. At each time point, mice were sacrificed and fibrosis response was measured in the liver by immuno-histological analysis. In the WT mice, there was a high-level deposition of fibrotic tissues at 5 days time-point. However, with time, at 10 and 20 days time point, there was attenuation in the fibrosis in the WT mice as measured by H & E staining (Fig.24). In contrast, in the DDB2/- mice, at the early time point there was higher fibrosis response. Moreover, the rate of attenuation of fibrotic response was significantly slower than the WT mice reminiscent of p53-/- mice (Fig.24). To confirm the observation, I further stained the liver sections from WT and DDB2-/- mice at different time points with Sirius Red (Fig.25) and Smooth muscle actin (SMA) (Fig.26). Sirius Red stain measure the level of fibrotic scar in the tissue whereas, SMA measures the activated hepatic stellate cells. Both of these stains further confirmed the observation that livers from DDB2-/- mice are more fibrotic in nature following chronic damage. This is accompanied by lower level of p19 Arf, a positive regulator of senescence, in DDB2-/- mice (Fig.28). I also looked at apoptosis function by TUNEL assay in the liver sections as apoptosis is hepatic stellate cells also plays critical role in fibrotic scar resolution [96]. TUNEL staining revealed attenuated apoptosis response in the DDB2-/- mice (Fig.27). Therefore, collectively, both deficient apoptosis and senescence function of hepatic stellate cells in DDB2-/- mice seem to contribute to the increased fibrotic response with chronic liver damage.

p21 co-operates with DDB2 in suppression of UV induced skin malignancies

3.10 DDB2 MEDIATED SENESCENCE INHIBITS UV INDUCED CARCINOGENESIS

The Ddb2 gene is mutated in XP-E, and its expression is reduced in a variety of cancers [97]. One study reported DDB2 as one of the top 5% underexpressed genes in head and neck squamous cell carcinoma [98]. DDB2 participates in tumor suppression in at least three ways as follows: promoting NER, supporting apoptosis, and inducing premature senescence after DNA damage. It participates in NER and apoptosis by maintaining p21 at a low level that is optimum for efficient repair and apoptosis. The senescence function of DDB2 is related to its function as a transcriptional repressor of anti-oxidant genes SOD2 and catalase. I wanted to examine which function of DDB2 is dominant in its role as a tumor suppressor during UV induced skin carcinogenesis.

First I looked at expression of DDB2 and p21 between normal skin and skin sections from Basal cell carcinoma (BCC) patients. Using tissue microarrays, I observed a significant loss of the DDB2 protein expression in BCCs (Fig.29 A). Interestingly I also observed loss of p21 expression in these patient samples (Fig.29 B). The tissue microarray in our experiment contained 52 BCC samples of which 75% exhibited lower expression for DDB1 and p21. Ddb2 and p21 is p53-induced gene [30, 32]. It is possible that the reduced expression is related to p53 mutations; however, the p53 status in those BCC samples in the microarray, obtained from US Biomax, was not characterized. But it is noteworthy that previous reports suggested that p53 is mutated at a high frequency in basal cell carcinoma (BCC) patients [99, 100].

Figure 29: Reduced expression of DDB2 and p21 in basal cell carcinoma.
(A) DDB2 immunohistochemistry of human tissue microarray of normal skin (upper panel) and basal cell carcinoma (BCC) (bottom panel). Intensity of DDB2 staining was scored from 0 to 4. One representative of normal human skin section with score 4 (n= 11) (upper panel) and one representative of basal cell carcinoma with score 2 (n= 52) (bottom panel) are shown. Right graph represents the average intensity of DDB2 staining and t-test for BCC versus NL. (B) Upper panels present p21 immunohistochemistry of human TMA of normal skin (n=11) with score 4 and the bottom panels present basal cell carcinoma (BCC) (n=52) with score 0. Intensity of p21 staining was scored from 0 to 4. Right graph presents the average intensity of p21 staining and t-test for BCC versus NL. (C) Table presents percent basal cell carcinoma patients with lower p21 and DDB2 intensity of the staining in comparison to the average normal intensity of staining ($p21^{low}$ $DDB2^{low}$). $p21^{low}$ $DDB2^{hi}$ represents patients with lower than average normal p21 staining and equal to average normal DDB2 staining.

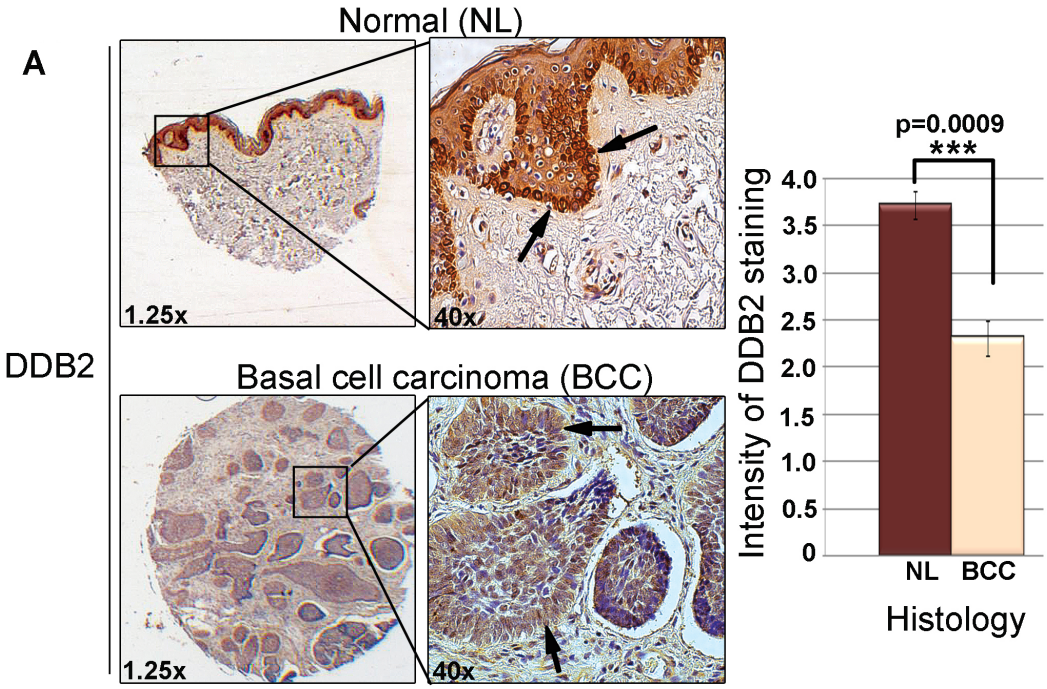

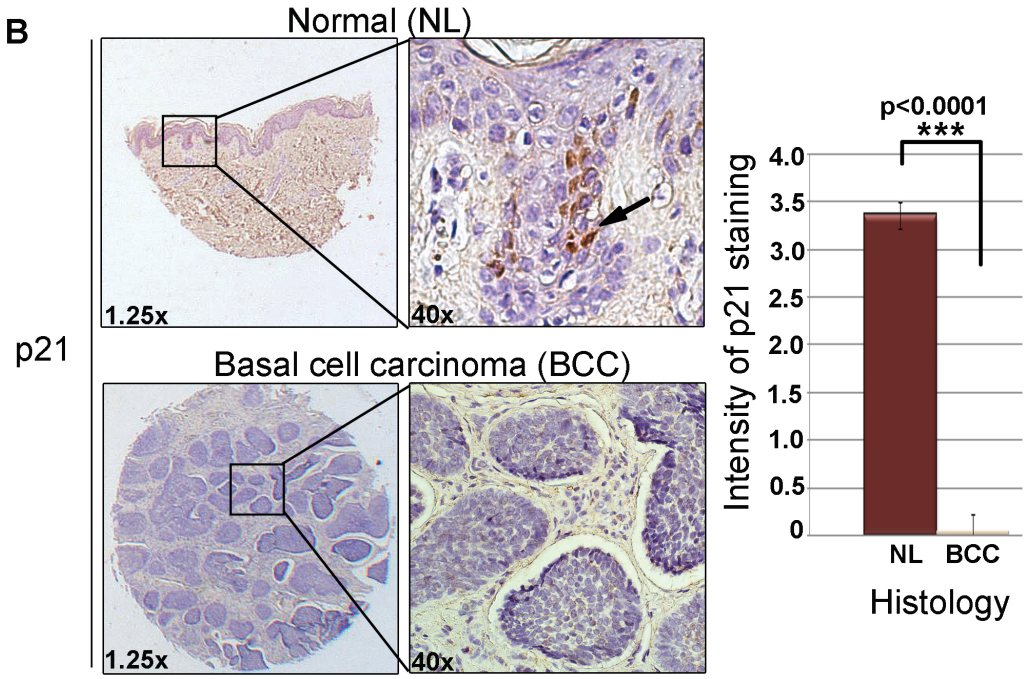

C

	$p21^{low}$ $DDB2^{low}$	$p21^{low}$ $DDB2^{hi}$
% BCC patients	75%	25%

n (BCC patients)=52

DDB2 participates in NER and apoptosis by maintaining p21 at a low level that is optimum for efficient repair synthesis and apoptosis. In agreement with that, DDB2-/- p21-/- mice exhibit efficient apoptosis and DNA repair function following UV irradiation. However, quite interestingly, despite efficient apoptosis and DNA repair function, DDB2-/- p21-/- mice developed tumor more aggressively than the DDB2-/- mice [101]. Wild type (n = 10), $Ddb2^{-/-}$ (n = 10), $p21^{-/-}$ (n = 8), and DKO ($Ddb2^{-/-}p21^{-/-}$) (n = 15) littermate mice were subjected to UV-B carcinogenesis protocol. The mice were shaved once a week and exposed to UV-B, initially 2 kJ/m2 twice a week for the first 8 weeks, followed by gradual increase of the frequency and dose of irradiation. The dose of UV-B used toward the end was 5 kJ/m2, five times per week. We observed that deletion of p21 in the $Ddb2^{-/-}$ background did not reverse the susceptibility to UV-induced skin carcinogenesis. On the contrary, loss of p21 in the $Ddb2^{-/-}$ background expedited the onset of tumor development [101]. The $Ddb2^{-/-}p21^{-/-}$ mice developed tumors as early as 18 weeks post-UV treatment, and by 33 weeks 50% of the animals developed tumors. The $Ddb2^{-/-}$ mice started exhibiting tumor phenotypes at week 28, reaching 50% at week 42. Only a few wild type mice exhibited papillary epithelioma beginning 41 weeks of treatment. The $p21^{-/-}$ mice exhibited increased susceptibility. All three genotypes ($p21^{-/-}$, $Ddb2^{-/-}$, and $p21^{-/-}Ddb2^{-/-}$) developed basal cell carcinoma, squamous epithelioma, and soft tissue sarcomas. Only Double knockout mice exhibited trichoblastoma.

Figure 30: DDB2-/-p21-/- mice are deficient in UV induced senescence.
Wild type, DDB2-/-, p21 -/- and DDB2-/- p21 -/- mice were irradiated with a single dose of UV (10kJ/m^2). Unfixed cryosections were prepared from the skin 24 hrs after UV. Frozen skin sections were subjected to SA-β-galactosidase. Arrows indicate SA-β-galactosidase positive cells. SA-β-galactosidase positive cells per 10x magnification field were counted. 10 random fields were chosen for quantification.

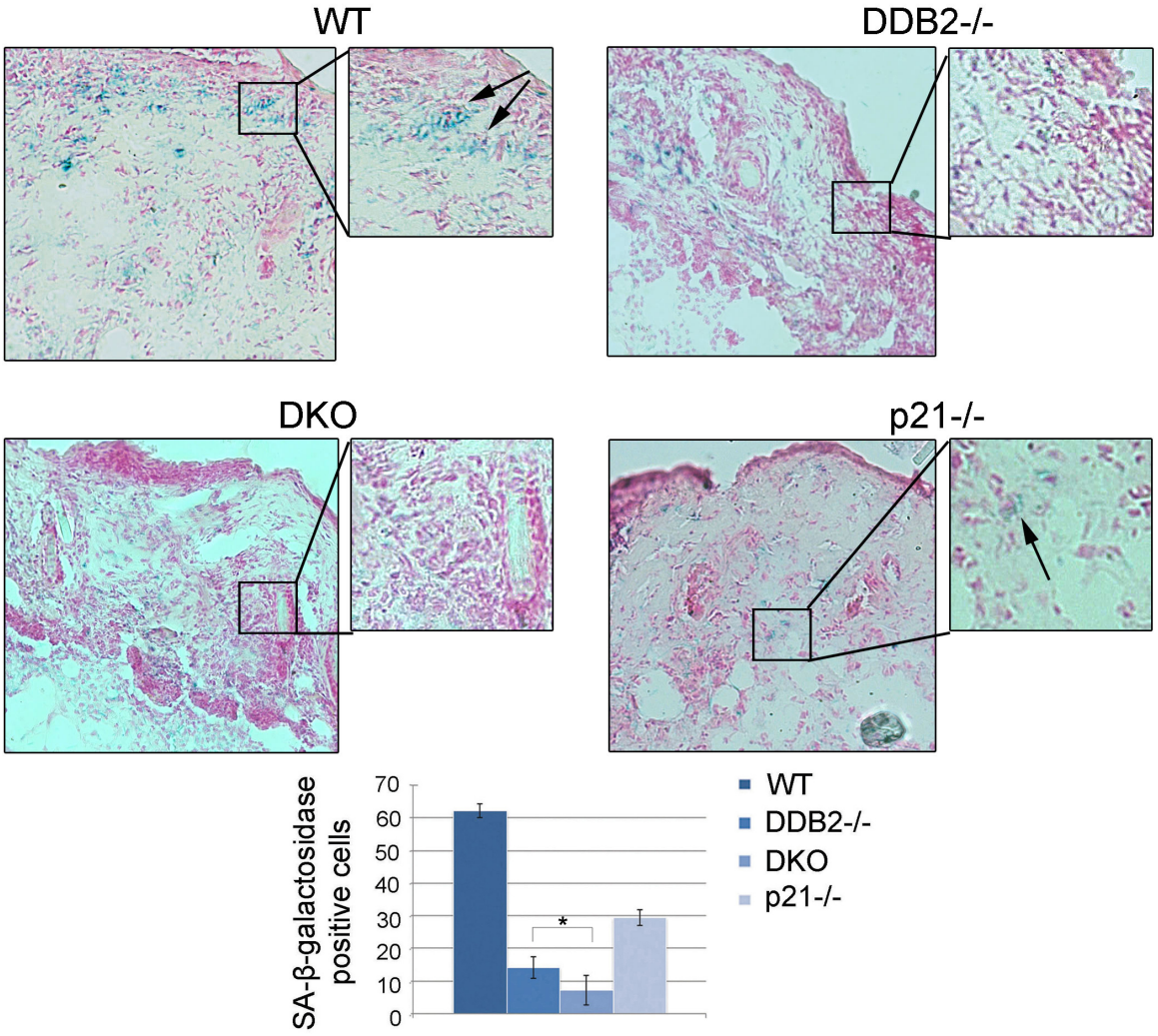
WT
DDB2-/-
DKO
p21-/-
SA-β-galactosidase positive cells
70
60
50
40
30
20
10
0
*
WT
DDB2-/-
DKO
p21-/-

Figure 31: DDB2-/-p21-/- mice are deficient in UV induced p16INK4a expression.
Wild type, DDB2-/-, p21 -/- and DDB2-/- p21 -/- mice were irradiated with a single dose of UV (10kJ/m^2). Mice were killed after 24 hrs and their skin were fixed in 10% Formalin, processed and embedded with paraffin for sectioning. Prepared skin section slides were then subjected to immunocytochemical analysis using p16INK4 and DAPI. P16INK4a positive staining identified senescent cells.

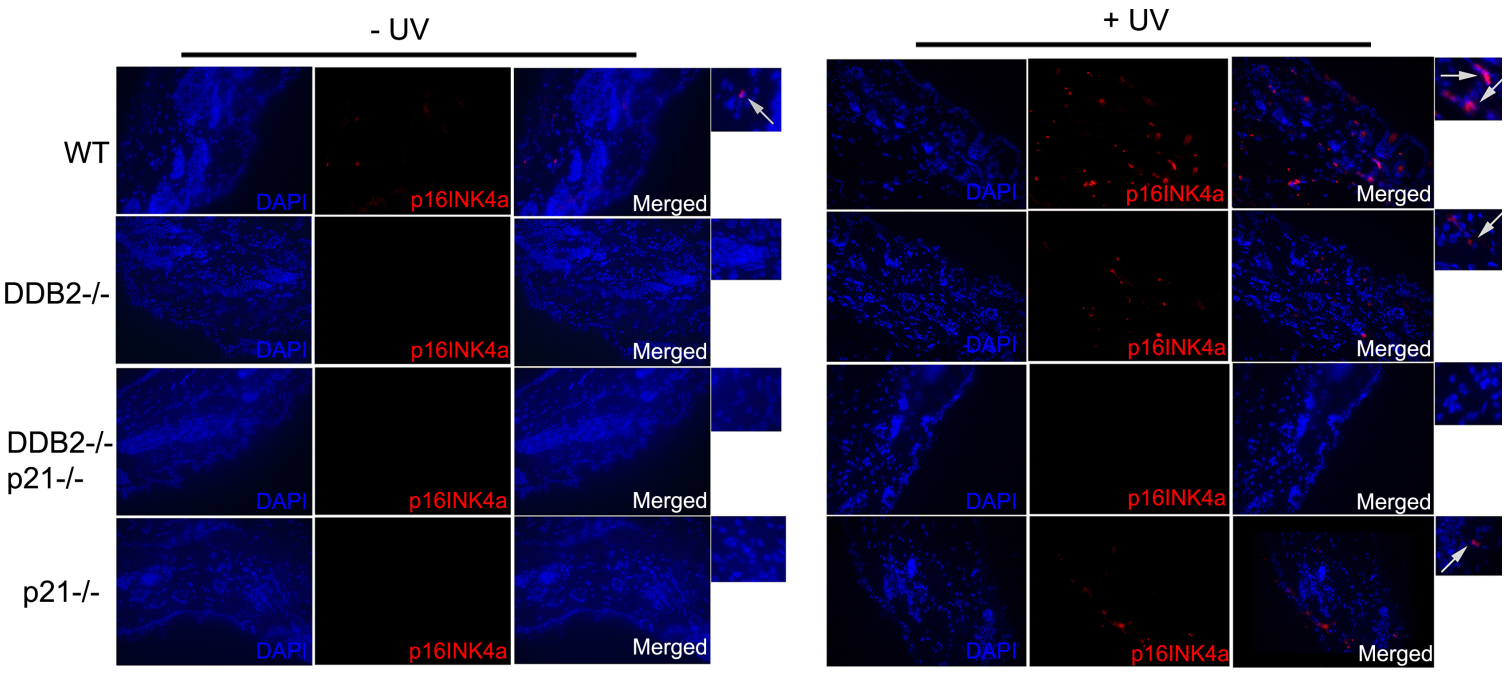
- UV
+ UV
WT
DDB2-/-
DDB2-/-
p21-/-
p21-/-
DAPI
p16INK4a
Merged

Figure 32: DDB2-/-p21-/- mice are deficient in UV induced p19Arf expression. Wild type, DDB2-/-, p21 -/- and DDB2-/- p21 -/- mice were irradiated with a single dose of UV (10kJ/m^2). Mice were killed after 24 hrs and their skin were fixed in 10% Formalin, processed and embedded with paraffin for sectioning. Prepared skin section slides were then subjected to immunocytochemical analysis using p19Arf antibody and DAPI. p19Arf positive staining identified senescent cells.

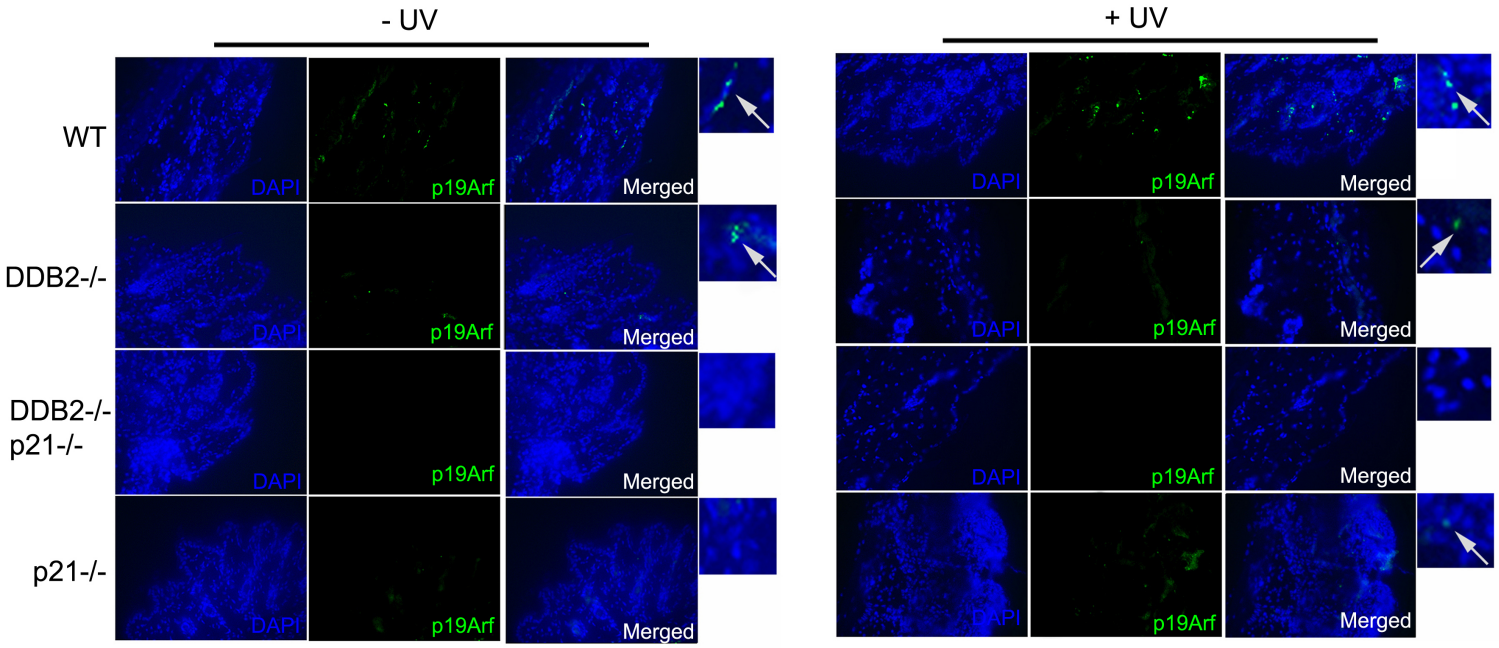
- UV
+ UV
WT
DDB2-/-
DDB2-/-
p21-/-
DAPI
p19Arf
Merged

Figure 33: Deficiency in p19Arf and p16INK4a expression in the absence of DDB2 and p21.
(A) p19Arf positive cells per 10X magnification field were counted. 10 random fields were chosen for quantification. (B) p16Ink4a positive cells per 10X magnification field were counted. 10 random fields were chosen for quantification.

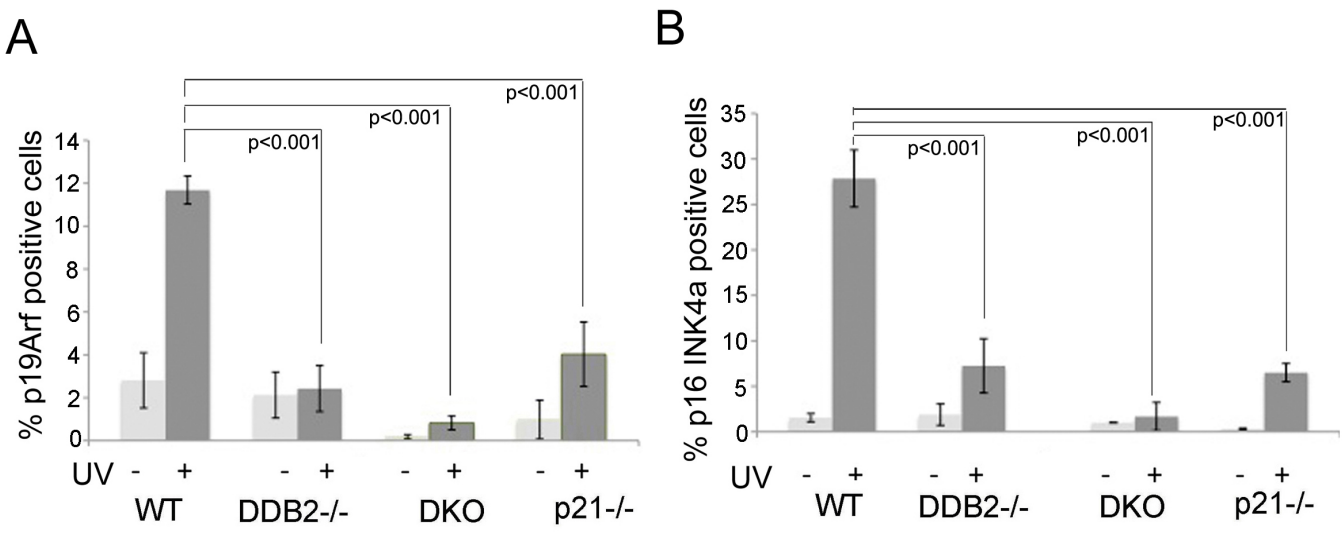
A
% p19Arf positive cells
14
12
10
8
6
4
2
0
p<0.001
p<0.001
p<0.001
UV - + - + - + - +
WT
DDB2-/-
DKO
p21-/-
B
% p16 INK4a positive cells
35
30
25
20
15
10
5
0
p<0.001
p<0.001
p<0.001
UV - + - + - + - +
WT
DDB2-/-
DKO
p21-/-

High-level p21 has been suggested to play an important role in triggering senescence [102-105]. Although Ddb2$^{-/-}$ cells have higher level of p21, these cells are deficient in premature senescence. I observed evidence that DDB2 and p21, in fact, have a synergistic effect in inducing premature senescence response following exposure to UV light. Mice of all four genotypes were exposed to acute UV-B followed by measurement of senescence response. I performed SA-β-galactosidase staining of skin sections from mice irradiated with UV-B using a procedure described previously. Both p21$^{-/-}$ and Ddb2$^{-/-}$ mice exhibited deficiencies in senescence response in comparison with WT mice after UV damage. Interestingly, the Ddb2$^{-/-}$p21$^{-/-}$ mice exhibited a more severe deficiency in senescence response compared with the Ddb2$^{-/-}$ or thep21$^{-/-}$ mice (Fig.30). I confirmed the observation by assessing the level of p16Ink4a (Fig.31) and p19Arf (Fig.32). Accumulation of p19Arf and p16Ink4a was observed in the WT mice and that was significantly reduced in the p21$^{-/-}$ and the Ddb2$^{-/-}$ mice (Fig.33). Moreover, consistent with the SA-β-galactosidase staining, there was a near complete loss of p19Arf and p16Ink4 expression in the Ddb2$^{-/-}$p21$^{-/-}$ mice (Fig.33), further confirming the notion that these mice are severely deficient in senescence, which might be the major contributing factor for the increased onset of tumorigenesis. Concordantly, DDB2-/-p21-/- mice exhibit a strong increase in proliferation following UV irradiation compared to the other three genotypes.

Figure 34: DDB2-/-p21-/- mice are deficient in UV induced ROS accumulation. Wild type, DDB2-/-, p21 -/- and DDB2-/- p21 -/- mice were irradiated with a single dose of UV (10kJ/m^2). Unfixed cryosections from treated and untreated mice were prepared from the skin 24 hrs after UV. Cryosections were incubated with 10 microM DCFDA for 45 minutes at 37 degree C to detect ROS (green). All images were photographed under 20X magnification. ROS positive cells per 20x magnification field were counted. Average of six different randomly chosen fields per mouse of each genotype is presented.

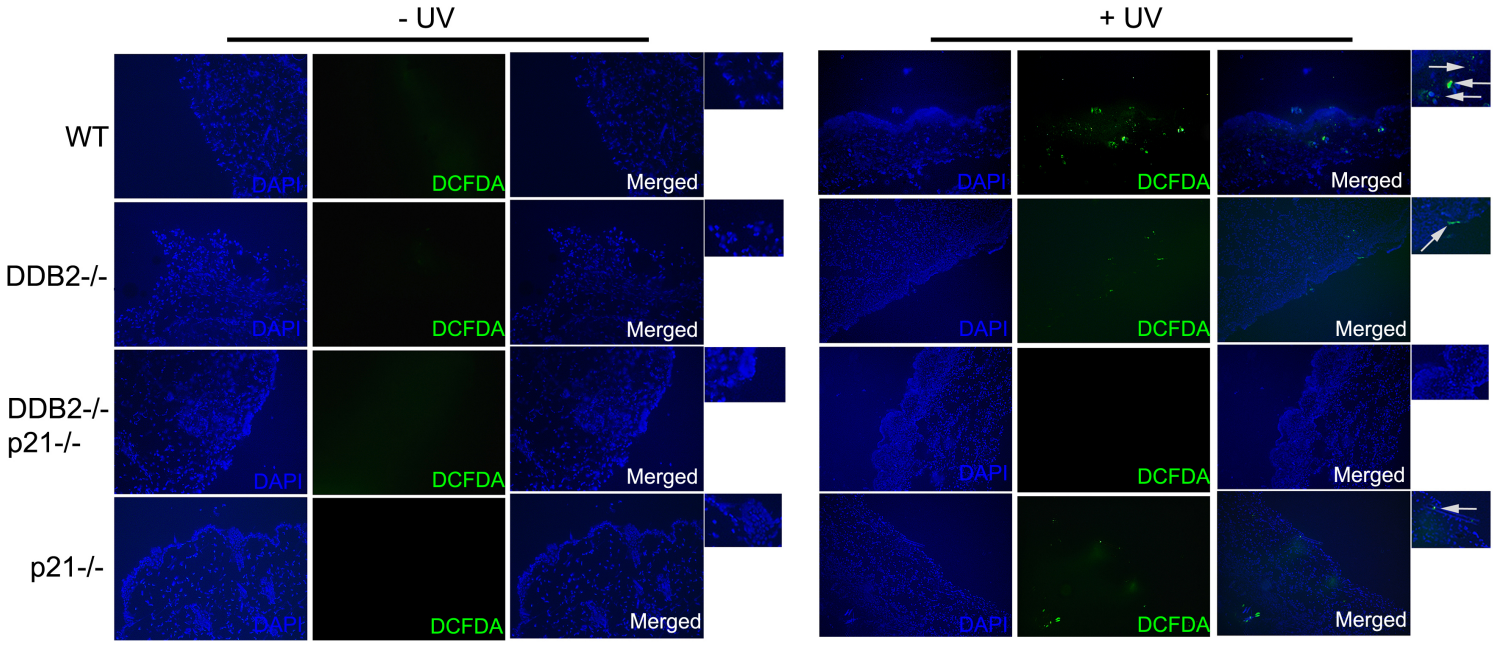
- UV
+ UV
WT
DDB2-/-
DDB2-/-
p21-/-
p21-/-
DAPI
DCFDA
Merged

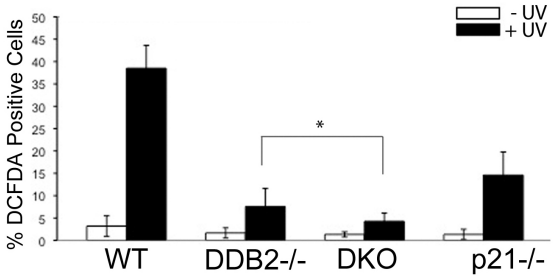
% DCFDA Positive Cells
- UV
+ UV
*
WT
DDB2-/-
DKO
p21-/-

Figure 35: DDB2-/-p21-/- mice exhibit increased catalase expression.
(A) and (B) Skin extracts from Wild type, DDB2-/-, p21 -/- and DDB2-/- p21 -/- mice were subjected to Western Blot analysis with Catalase and FoxM1 Antibody. Actin or GAPDH was used as loading control. Two different sets of mice have been shown for Catalase expression.

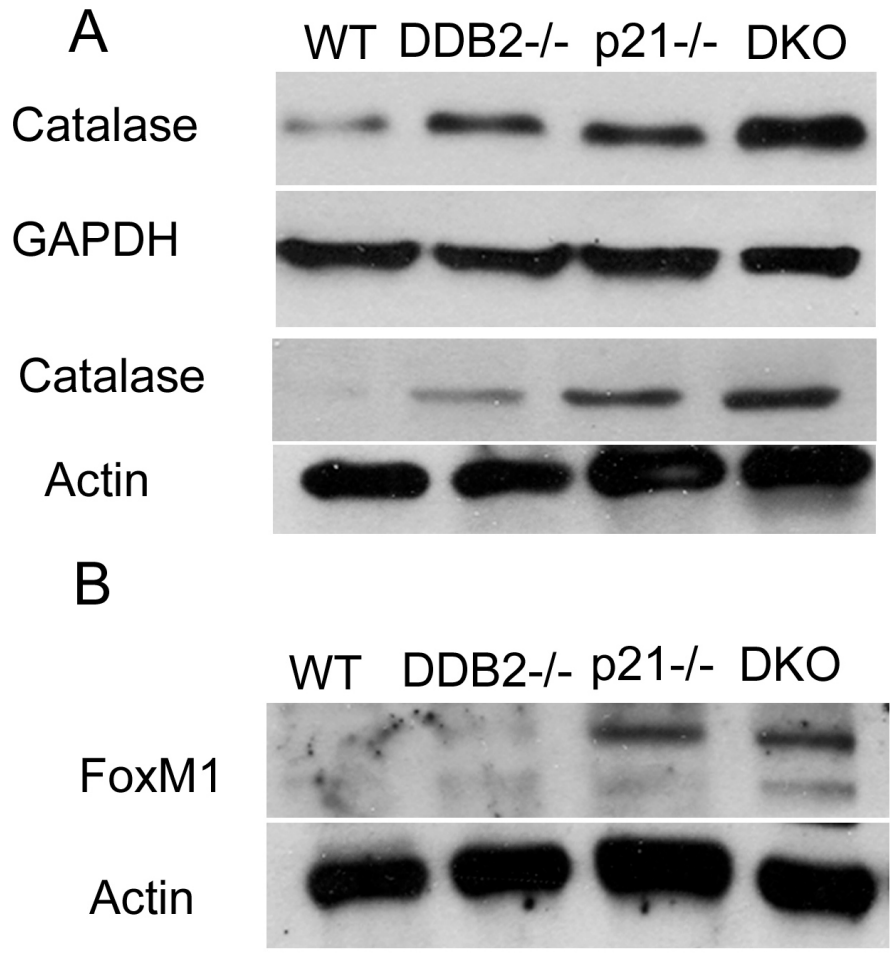
A
WT
DDB2-/-
p21-/-
DKO
Catalase
GAPDH
Catalase
Actin
B
WT
DDB2-/-
p21-/-
DKO
FoxM1
Actin

Figure 36: DDB2-/-p21-/- MEFs are deficient in UV induced senescence.
(A) WT, DDB2-/-, p21-/- and DDB2-/- p21-/- MEFs were plated at equal density (1 x 10^5). Next day cells were treated with UV (50 J/m^2). 48 hrs after UV treatment BrdU (3 ug/ ml) was added to the culture medium for 1 hour and 30 minutes. The cells were fixed in 70% ice cold Ethanol and subjected to immunostaining for BrdU using monoclonal BrdU antibody. The cells were also stained with DAPI. The percent BrdU positive cells from three experiments were plotted. (B) WT, DDB2-/-, p21-/- and DDB2-/- p21-/- MEFs were plated at equal density (1 x 10^5). Next day cells were treated with UV (50 J/m^2). 72 hrs after treatment cells were subjected to SA beta gal assay. SA beta gal positive cells were counted from at least 10 fields of triplicate plates. (C) WT MEFs were plated at equal density (1 x 10^5). Next day cells were treated with UV (50 J/m^2) and kept with or without NAC (20 mM NAC). 72 hrs after treatment cells were counted from at least 10 fields of triplicate plates. The asterisk in Panel indicates statistically significant differences, with the following P value calculated by Student's t-test: *P<0.05; **P<0.01; ***P<0.001; ns - not significant.

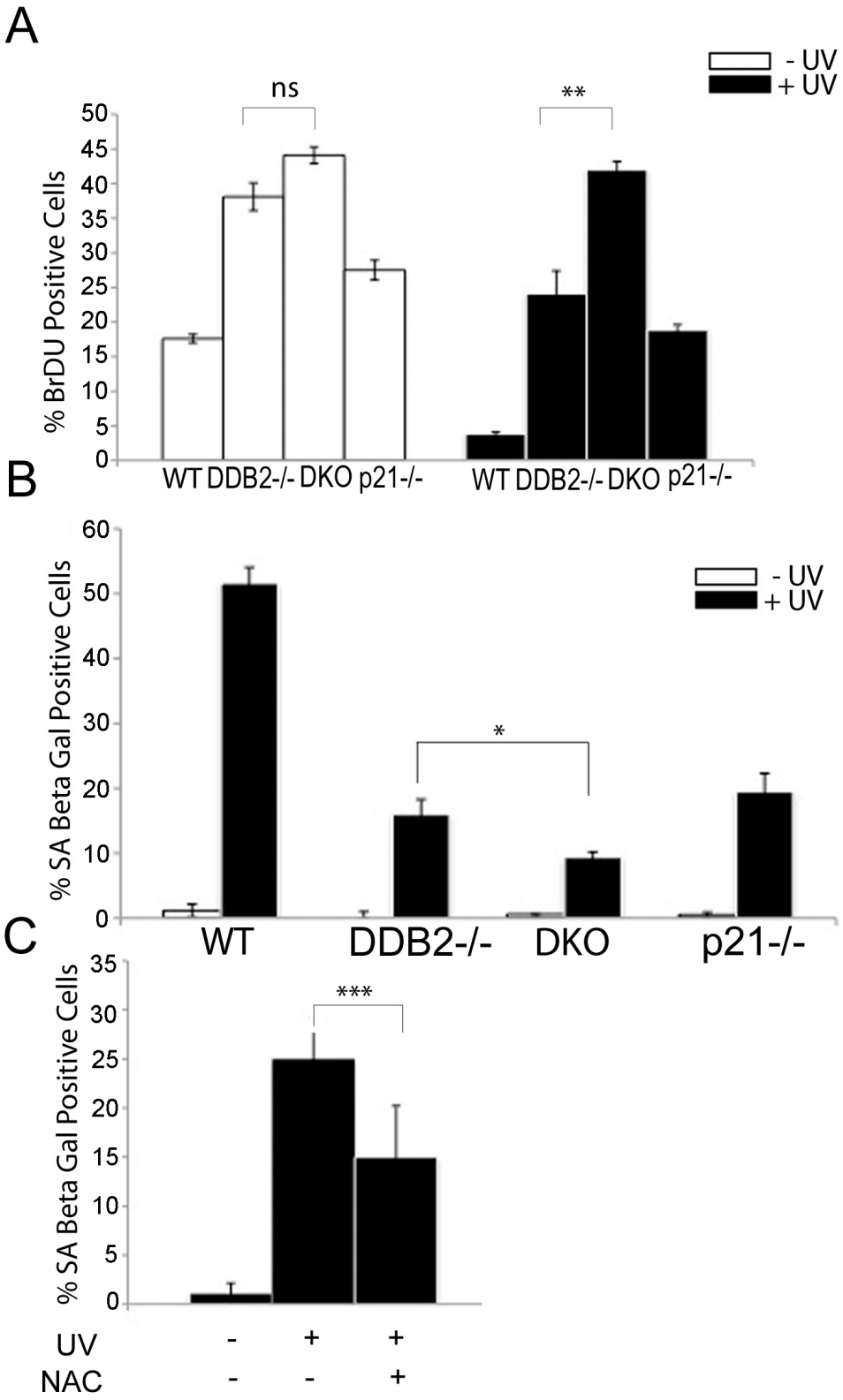
A
- UV
+ UV
ns
**
% BrDU Positive Cells
50
45
40
35
30
25
20
15
10
5
0
WT DDB2-/- DKO p21-/-
WT DDB2-/- DKO p21-/-
B
- UV
+ UV
*
% SA Beta Gal Positive Cells
60
50
40
30
20
10
0
WT
DDB2-/-
DKO
p21-/-
C
***
% SA Beta Gal Positive Cells
35
30
25
20
15
10
5
0
UV - + +
NAC - - +

3.11 INSTABILITY OF ROS AND INCREASED FOXM1 EXPRESSION IN THE DDB2-/- P21-/- MICE

Previously, I demonstrated that the senescence deficiency phenotype in Ddb2$^{-/-}$ mice is related to a deficiency in the accumulation of ROS. DDB2 supports ROS accumulation by repressing the antioxidant genes. ROS has been implicated also in the mechanism by which p21 participates in senescence [102]. I measured the levels of ROS using DCFDA staining (detects peroxides) in the skin of all four genotypes following subacute UV irradiation. Cryosections of skin from WT, Ddb2$^{-/-}$, p21$^{-/-}$, and Ddb2$^{-/-}$p21$^{-/-}$ mice were treated with 10 μM DCFDA for 45 min at 37 °C and visualized under microscope. Clearly, the Ddb2$^{-/-}$ and the p21$^{-/-}$ mice were deficient in peroxide accumulation compared with the WT mice. Moreover, the double knock-out skin sections also exhibited a stronger deficiency in peroxide accumulation (Fig.34). Extracts from the skin fragments of all four genotypes were compared by Western blot assays for catalase. The skin extracts from the double knock-out mice exhibited a much higher expression of catalase (Fig.35 A). p21 has been implicated in regulating expression of FoxM1 , a transcription factor that regulates oxidative stress-induced premature senescence and activates expression of proliferation genes, including genes involved in G_1 to S and G_2 to M progression [106-108]. Consistent with that, I observed a much higher expression of FoxM1 in the p21$^{-/-}$ background. Both p21$^{-/-}$ mice and the double knock-out mice expressed FoxM1 at much higher levels (Fig.35 B). The lack of senescence and increased expression of FoxM1 provide a clear explanation for the strong increase in proliferation in the p21$^{-/-}$Ddb2$^{-/-}$ mice. The higher rate of cell

proliferation and reduced senescence after UV irradiation in the $p21^{-/-}Ddb2^{-/-}$ background was confirmed also using MEFs (Fig.36A and B). It is noteworthy that the extent of increase in BrdU incorporation after UV irradiation in the double knock-out cells was somewhat less than what was seen in the in vivo experiment, which most likely reflects the differences in the in vitro and in vivo experimental set up. Finally, I observed that N-acetylcysteine, a ROS scavenger, inhibited UV-induced senescence (Fig.36 C), which is consistent with role of ROS in inducing premature senescence following UV irradiation.

DDB2 inhibits EMT of colon carcinoma cells

3.12 LOSS OF DDB2 RESULTS EMT OF COLON CARCINOMA CELLS

Increasing evidence suggests that senescence and EMT, two seemingly independent processes, are in fact intertwined. For example, the oncogene RasV12 induces premature senescence in human diploid fibroblast. However, in a co-operative fashion with TGF-β, RasV12 induces EMT in epithelial cells [109]. Similarly, ectopically expressed ErbB2 induces senescence. But, overexpression of Twist and ErbB2 induces EMT and bypass of senescence in both MEFs and human epithelial cells [110]. These studies suggest a possible link between EMT and cellular senescence. Moreover, there are several transcription factors that have opposing role in senescence and EMT. For example, Twist induces EMT by down-regulation of E-cadherin. However, Twist suppresses cellular senescence by attenuating expression of p14Arf [111]. Similarly, overexpression of Zeb1 results EMT and increased metastasis. Interestingly, Zeb1 mutant MEFs display diminished proliferative potential in culture leading to premature senescence response. This is accompanied by increased expression of p15Ink4b and p21 Waf1/Cip1. Thus, similar to Twist, Zeb1 induces EMT and inhibits the senescence process [111].

Since I found that loss of DDB2 results deficiency in senescence, I investigated whether this is related to the EMT regulation. Interestingly, I found that DDB2 inhibits epithelial to mesenchymal transition of the colon cancer cells. Analyses of the DDB2-knockdown colon carcinoma cells indicated a change in morphology of the cells. Unlike the epithelial cuboid appearance of the parental cells, the DDB2-deficient HCT116 cells exhibited elongated mesenchymal like morphology (Fig.37

A), a change that is observed during epithelial to mesenchymal transition (EMT). Also, there was a clear loss of surface expression of E-cadherin and increase in expression of the mesenchymal markers vimentin in the DDB2-deficient cells. Consistent with EMT-like changes, the DDB2 deficient cells were found to express significantly less E-cadherin and more Vimentin/Smooth Muscle Actin (Fig.37 A and B). p21 has been implicated to play an important role in EMT [112, 113]. Since DDB2 regulates p21, I explored the possibility whether induced EMT with loss of DDB2 expression is p21-dependent. However, siRNA mediated knockdown of DDB2 in HCT p21 null cells still resulted loss of E-cadherin and increased Vimentin expression (Fig.38), suggesting that DDB2 mediated inhibition of EMT is p21-independent. Also, I compared the human colon cancer lines SW480 and SW620. These lines were derived from the same patient. SW480 corresponds to an early stage, whereas SW620 corresponds to a later stage in which the tumor was metastatic [114]. The SW620 cells are mainly mesenchymal whereas SW480 cells are epithelial [115]. siRNA mediated knockdown of DDB2 in the SW480 cells resulted in EMT-like changes, as evidenced by reduced E-cadherin expression and increased Vimentin expression (Fig.39 A and D). The changes in morphology of these cells are reminiscent of the observations in HCT 116 cells. Interestingly, there was a decrease in the DDB2 expression during progression from SW480 to SW620 (Fig.39 C). Re-expression of DDB2 in the SW620 cells caused a significant increase in the epithelial phenotype, as measured by increased E-cadherin and reduced Vimentin expression (Fig.39 E and F). Together, these observations suggest that DDB2 is a regulator of EMT in colon cancer cells.

Figure 37: DDB2 inhibits epithelial to mesenchymal transition of colon cancer cells.

(A) Representative phase contrast images of HCT 116 cells expressing control shRNA or DDB2 shRNA. HCT 116 cells expressing control shRNA or DDB2 shRNA were subjected to immunocytochemical analysis using E-cadherin, Vimentin or Smooth Muscle Actin antibody. Representative pictures are shown in 20X magnification. (B) Protein extracts from HCT 116 cells expressing control shRNA or DDB2 shRNA were subjected to Western blot analysis with E-cadherin (20ug protein), Vimentin (50ug protein) and DDB2 (50ug protein) antibody. Tubulin was used as a loading control.

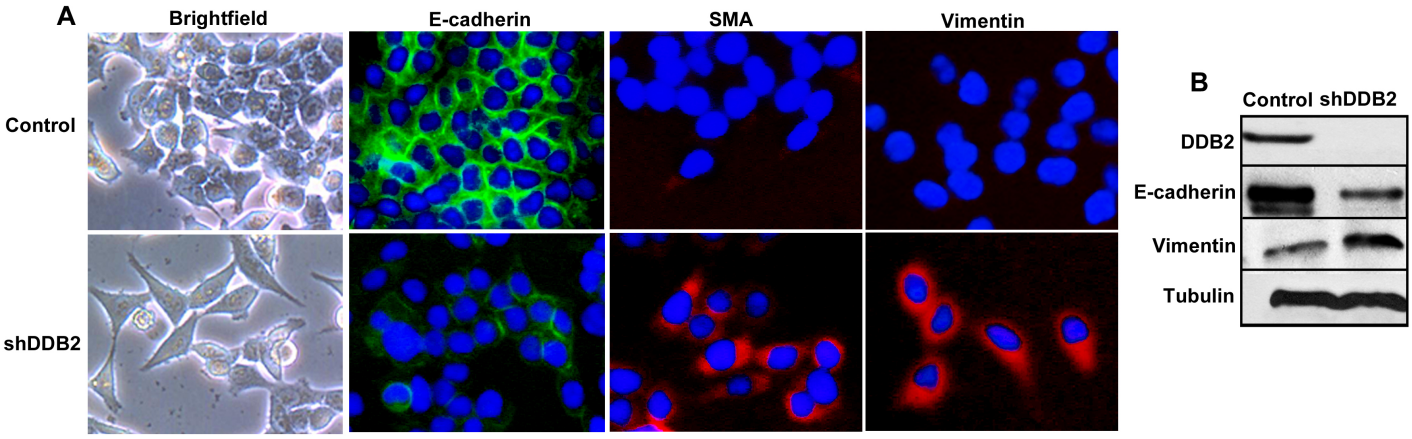
A
Brightfield
E-cadherin
SMA
Vimentin
Control
shDDB2
B
Control shDDB2
DDB2
E-cadherin
Vimentin
Tubulin

Figure 38: DDB2 mediated inhibition of EMT does not involve p21.
Protein extracts from HCT 116 p21 null cells expressing control siRNA or DDB2 siRNA were subjected to Western blot analysis with E-cadherin (20ug protein), Vimentin (50ug protein) and DDB2 (50ug protein) antibody. Tubulin was used as a loading control.

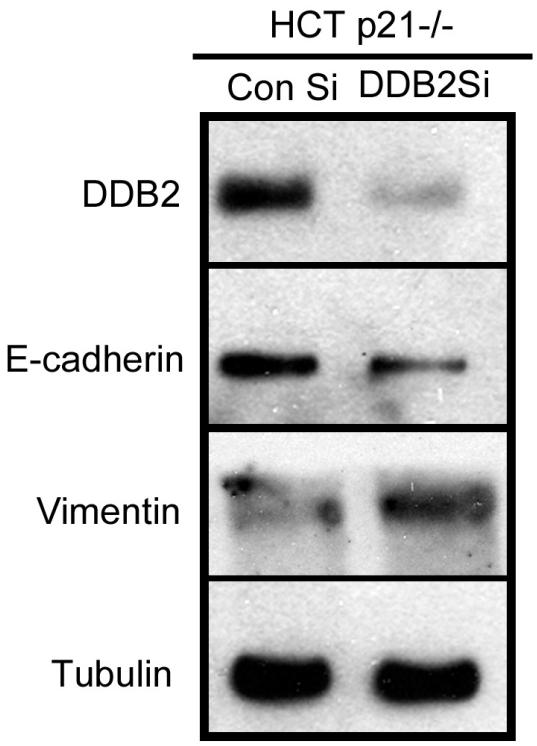
HCT p21-/-
Con Si
DDB2Si
DDB2
E-cadherin
Vimentin
Tubulin

Figure 39: Loss of DDB2 expression in mesenchymal colon cancer cells.
(A) Representative phase contrast images of SW480 cells expressing control siRNA or DDB2 siRNA. (B) Representative phase contrast images of SW620 cells expressing empty vector or vector expressing DDB2. (C) Protein extracts from SW480 and SW620 cells were subjected to western blot analysis using DDB2 (50ug protein), E-cadherin (20ug protein), Vimentin (50ug protein) antibody. Tubulin was used as a loading control. (D) Protein extracts from SW480 cells expressing control siRNA or DDB2 siRNA were subjected to Western blot analysis using E-cadherin (20ug protein), DDB2 (50ug protein) or Vimentin (50ug protein) antibody. Tubulin was used as a loading control. (E) Protein extracts from SW620 cells expressing empty vector or vector expressing DDB2 were subjected to Western blot analysis using E-cadherin (20ug protein), DDB2 (50ug protein) or Vimentin (50ug protein) antibody. Tubulin was used as a loading control. (F) SW620 cells expressing empty vector or vector expressing DDB2 were subjected to immunocytochemical analysis using E-cadherin, Vimentin or Smooth Muscle Actin antibody. Representative pictures are shown in 20X magnification.

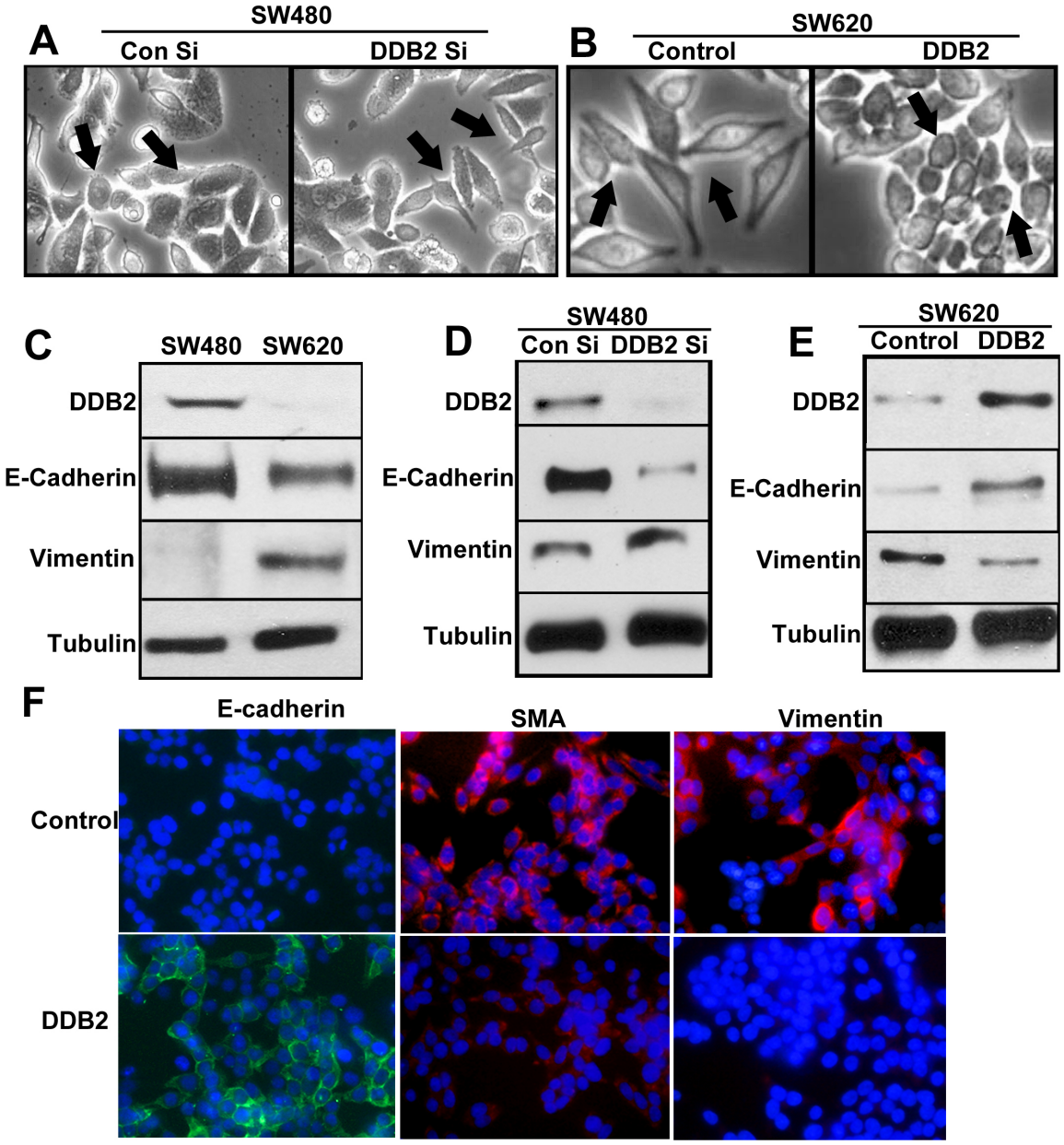
A
SW480
Con Si
DDB2 Si
B
SW620
Control
DDB2
C
SW480
SW620
DDB2
E-Cadherin
Vimentin
Tubulin
D
SW480
Con Si
DDB2 Si
DDB2
E-Cadherin
Vimentin
Tubulin
E
SW620
Control
DDB2
DDB2
E-Cadherin
Vimentin
Tubulin
F
E-cadherin
SMA
Vimentin
Control
DDB2

Figure 40: DDB2 inhibits TGF-β / hypoxia induced EMT.
(A) SW480 cells were transfected with empty vector or DDB2 expression vector. Next day, cells were divided into two plates and kept under normoxia or hypoxia. 24 hrs after the treatment, protein extracts were made and Western blot analysis was performed with DDB2 (50ug protein), E-cadherin (20ug protein), Vimentin (50ug protein), HIF-1 (100ug protein) antibody. Actin was used as a loading control. (B) SW480 cells were transfected with empty vector or DDB2 vector. Next day, cells were divided into two plates and treated with TGF-beta or left untreated. 48 hrs after the treatment, protein extracts were made and Western blot analysis was performed with DDB2 (50ug protein), E-cadherin (20ug protein), Vimentin (50ug protein) antibody. Actin was used as a loading control.

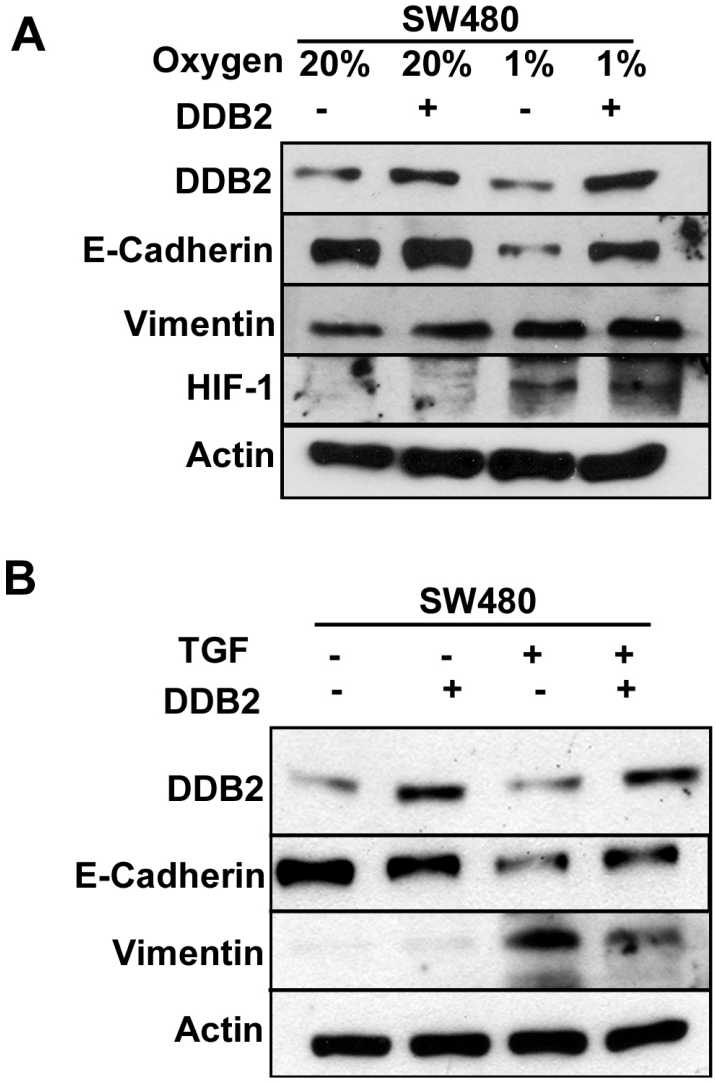
A
SW480
Oxygen 20% 20% 1% 1%
DDB2 - + - +
DDB2
E-Cadherin
Vimentin
HIF-1
Actin
B
SW480
TGF - - + +
DDB2 - + - +
DDB2
E-Cadherin
Vimentin
Actin

TGF-β and hypoxia are inducers of EMT [70, 116]. It was shown that treatment of the SW480 cells with TGF-β induces EMT [117]. To determine whether DDB2 inhibits EMT induced by TGF-β and hypoxia, I over-expressed DDB2 in SW480 cells. The cells were then subjected to treatments with TGF-β or hypoxia. Extracts of the treated cells were analyzed for expression of E-cadherin. As expected, treatments with TGF-β or hypoxia caused an inhibition in the levels of E-cadherin in SW480 cells, whereas the cells over-expressing of DDB2 exhibited attenuated inhibition of E-cadherin expression by TGF-β or hypoxia (Fig.40 A and B). Unlike the TGF-β treated cells, DDB2 expression did not inhibit the level of vimentin in the hypoxia treated cell. Nevertheless, the resistance of the DDB2-expressing cells to TGF-β and hypoxia mediated inhibition of E-cadherin, a driver for EMT-like changes, suggest that DDB2 is an inhibitor of the TGF-β and hypoxia pathways of EMT.

3.13 DDB2 DEFICIENCY RESULTS INCREASED AGGRESSIVENESS AND TUMORIGENECITY OF COLON CANCER CELLS

I next investigated the physiological relevance of DDB2 mediated inhibition of EMT. Database analyses indicated a reduced expression of Ddb2 in a variety of epithelial tumors. A closer look at the publicly available database revealed that the RNA-expression of Ddb2 is down regulated in majority of the colon carcinoma datasets. Out of 30 available datasets, 24 datasets showed significant down regulation of Ddb2-mRNA (Fig.41 A). I next performed a closer analysis on two datasets. In the first dataset, Ddb2 mRNA profile was compared between normal colon tissue and colon carcinoma patient samples. Ddb2 expression was significantly lower in the

colon carcinoma samples compared to normal colon (Fig.41 C). The other dataset consists of patients from different stages of colon carcinoma- grades I, II, III and IV. Colon carcinoma samples are graded from grades I to IV according to TNM grading system [118]. Grade IV tumors are least differentiated and most aggressive in nature. I looked at relative Ddb2 mRNA expression between these 4 groups of patient samples. Intriguingly, Ddb2 mRNA expression was lower in grade IV patient samples compared to grade I patient samples (Fig.41 B). This indicates that lower DDB2 expression might be indicative of poor prognosis of colon carcinoma patients. I confirmed these observations at the protein level. Analyses of DDB2 expression in matched normal colon and colon carcinoma tissues in tissue microarrays indicated significant down regulation of DDB2 in the colon carcinoma samples compared to the normal samples (Fig.43 D). I further analyzed tissue microarrays that contained samples of various grades of colon cancer- grades I, II, III and samples with metastatic dissemination in a different organ. These experiments revealed that the loss of DDB2 expression is strongly correlated with high-grade as well as metastatic colon cancers (Fig.42 and Fig.43 A). I further looked at E-cadherin and vimentin expression in the colon carcinoma samples. Earlier studies have indicated that loss of E-cadherin expression in colon carcinoma indicates aggressive form of the disease with a higher chance of metastatic dissemination. Consistent with that, I observed that there was a clear loss of E-cadherin expression in higher-grade colon cancers (Fig.42 and Fig.43 B). I did not observe any discernible change in the expression of vimentin (Fig.42 and Fig.43 C). This observation corroborates my earlier observation in HCT116 colon carcinoma cell line. Similar to the induction of

Figure 41: Loss of DDB2 mRNA expression in colon carcinoma patient samples. (A) Using the tools available in Oncomine, fold change in DDB2 expression was identified for pair wise comparison such as normal colon versus colorectal cancer. (B) and (C) Detailed analysis of two datasets from oncomine showing relative DDB2 mRNA expression in colon carcinoma samples.

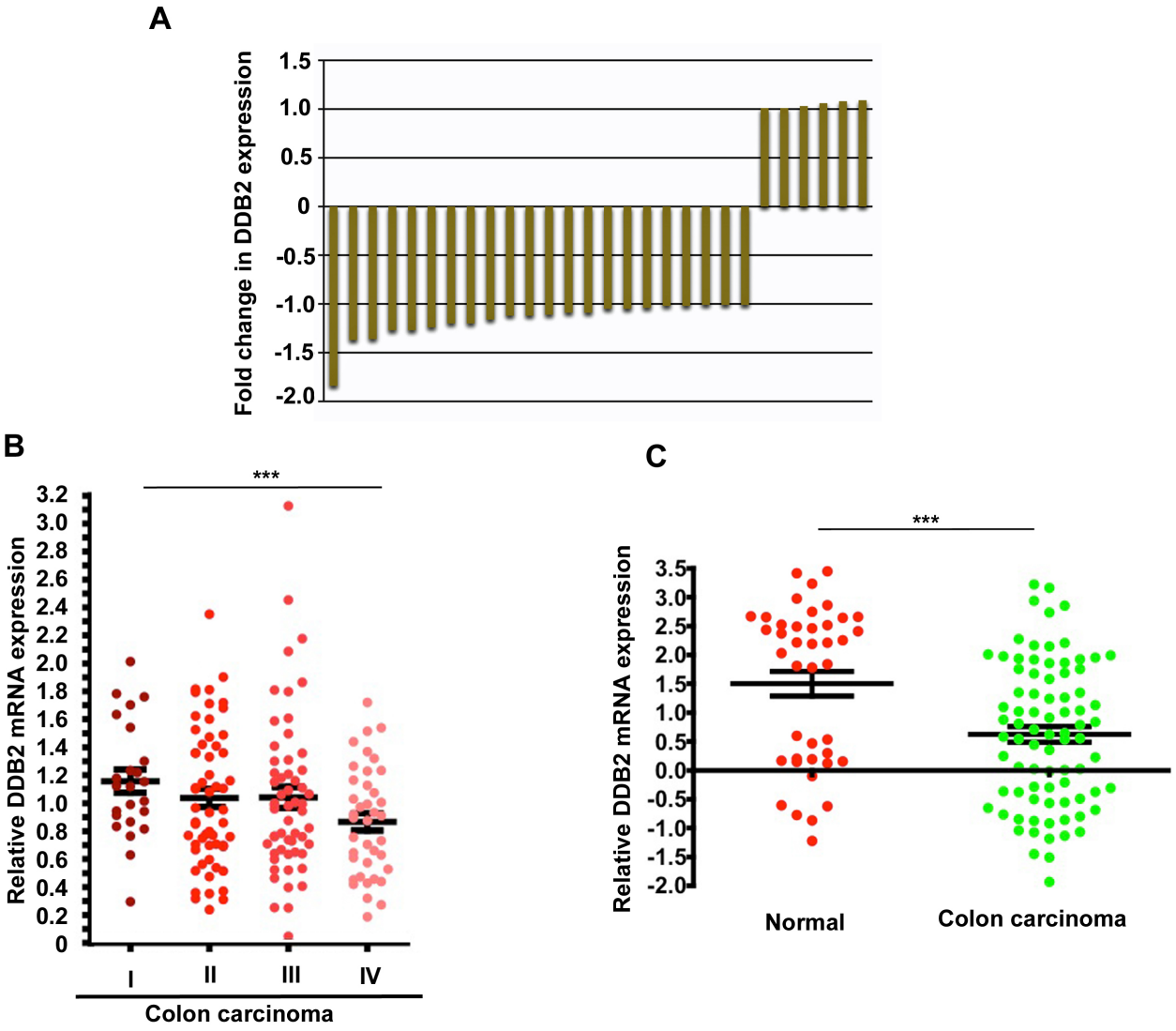
A
Fold change in DDB2 expression
1.5
1.0
0.5
0
-0.5
-1.0
-1.5
-2.0
B
***
Relative DDB2 mRNA expression
3.2
3.0
2.8
2.6
2.4
2.2
2.0
1.8
1.6
1.4
1.2
1.0
0.8
0.6
0.4
0.2
0
I
II
III
IV
Colon carcinoma
C
***
Relative DDB2 mRNA expression
3.5
3.0
2.5
2.0
1.5
1.0
0.5
0.0
-0.5
-1.0
-1.5
-2.0
Normal
Colon carcinoma

Figure 42: Loss of DDB2 expression in high - grade colon carcinoma.
DDB2, E-cadherin and Vimentin immunohistochemistry of human tissue microarray of normal colon (n=41) and colon carcinoma grade I (n=59), II (n=96) and III (n=51) and metastatic colon carcinoma (n=70).

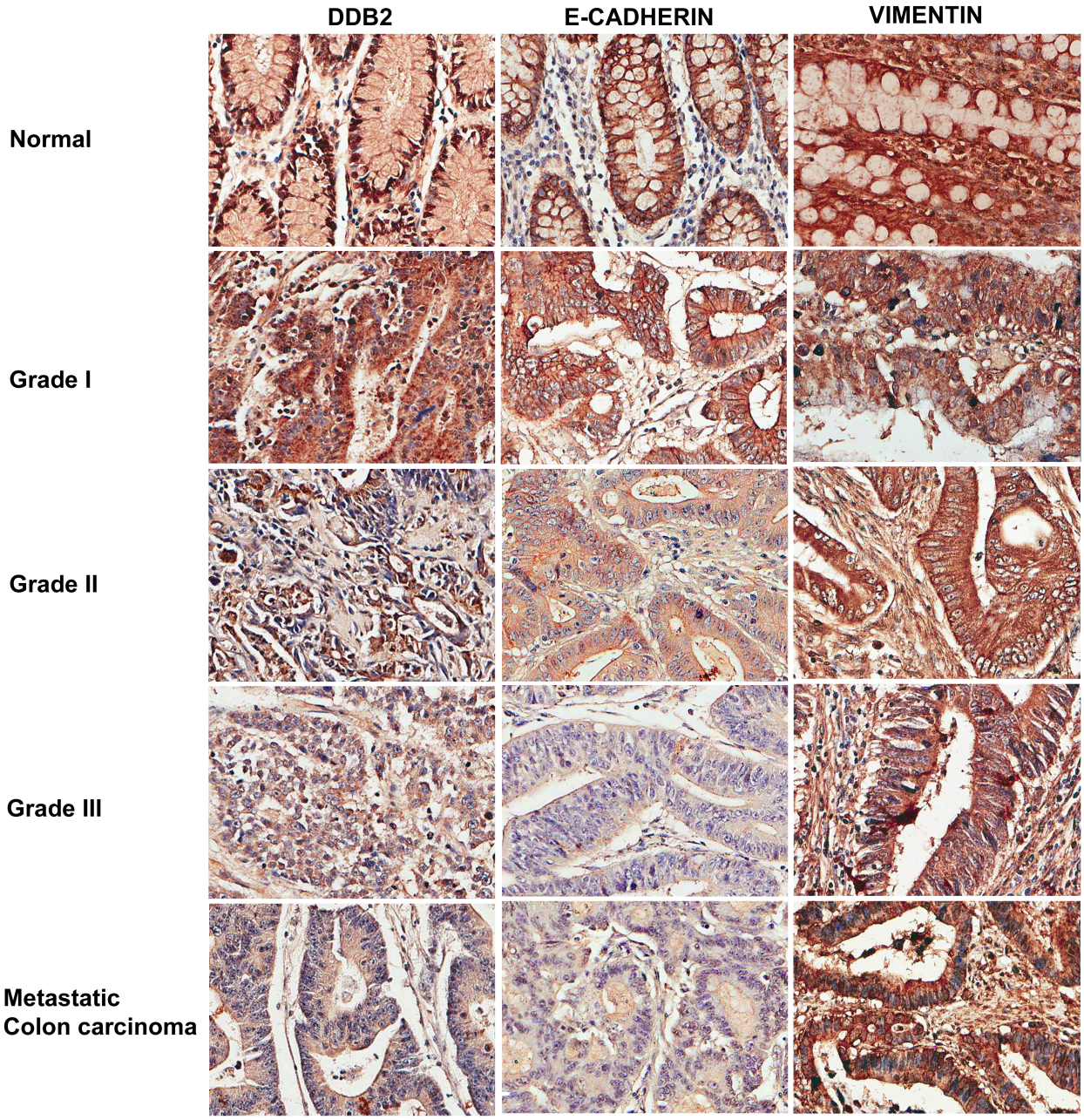
DDB2
E-CADHERIN
VIMENTIN
Normal
Grade I
Grade II
Grade III
Metastatic
Colon carcinoma

Figure 43: Loss of DDB2 expression in colon carcinoma.
DDB2, E-cadherin and Vimentin immunohistochemistry of human tissue microarray of normal colon (n=41) and colon carcinoma grade I (n=59), II (n=96) and III (n=51). Intensity of staining was scored from 0 to 4. Graph representing the average intensity of (A) DDB2, (B) E-cadherin and (C) Vimentin staining for the tissue microarrays. (D) DDB2 immunohistochemistry of human tissue microarray of matched normal colon and colon carcinoma (n=40). Intensity of DDB2 staining was scored from 0 to 4. Graph representing the average intensity of DDB2 staining for matched normal colon versus colon carcinoma.

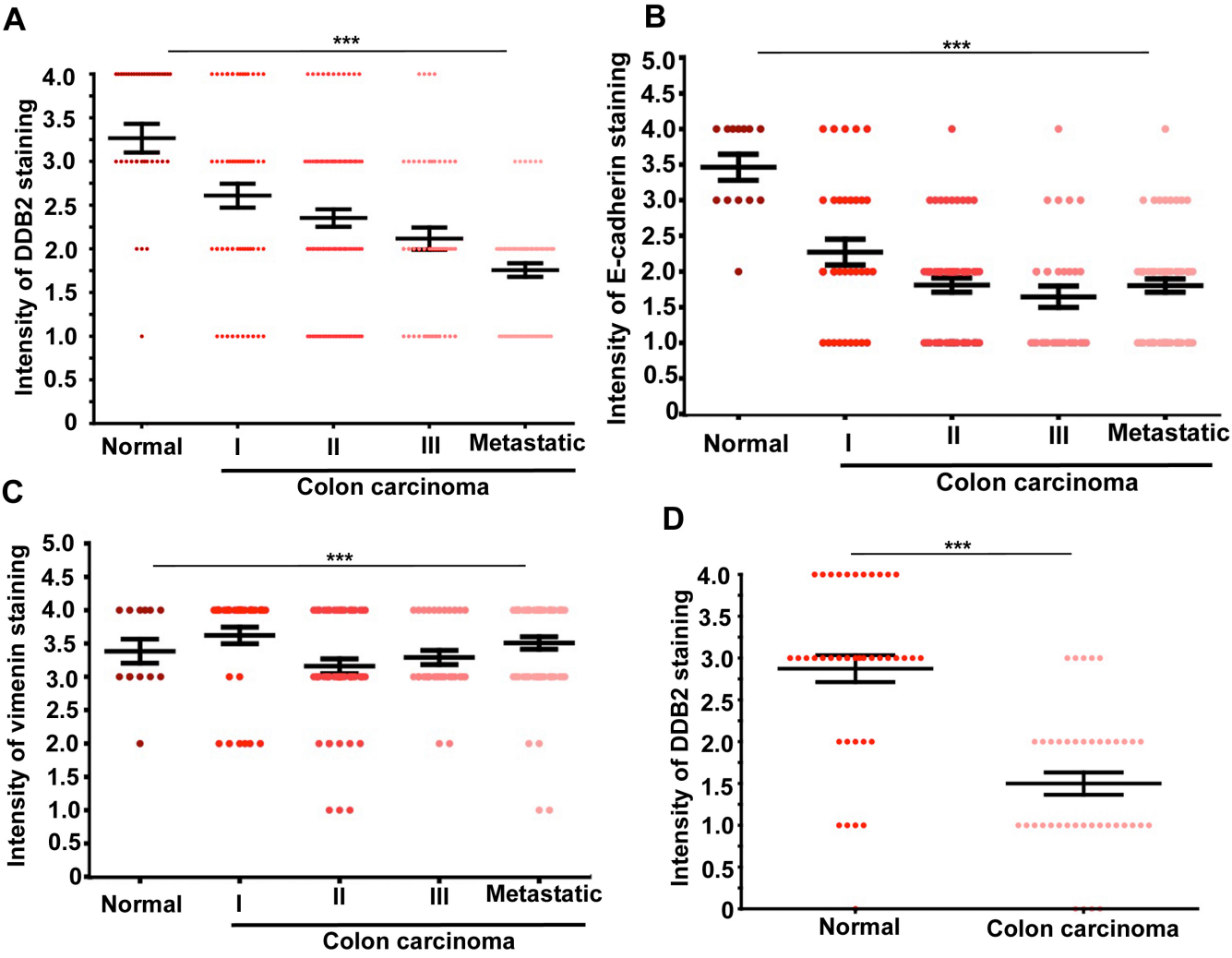
A
***
Intensity of DDB2 staining
4.0
3.5
3.0
2.5
2.0
1.5
1.0
0.5
0
Normal
I
II
III
Metastatic
Colon carcinoma
B
***
Intensity of E-cadherin staining
5.0
4.5
4.0
3.5
3.0
2.5
2.0
1.5
1.0
0.5
0
Normal
I
II
III
Metastatic
Colon carcinoma
C
***
Intensity of vimenin staining
5.0
4.5
4.0
3.5
3.0
2.5
2.0
1.5
1.0
0.5
0
Normal
I
II
III
Metastatic
Colon carcinoma
D
***
Intensity of DDB2 staining
4.0
3.5
3.0
2.5
2.0
1.5
1.0
0.5
0
Normal
Colon carcinoma

Figure 44: DDB2 deficiency increases invasiveness and tumorigenecity of colon cancer cells in vitro.
(A) and (B) Transwell invasion assay of HCT116 cells expressing control shRNA or DDB2 shRNA (mean +/- standard deviation; n=3). (C) HCT116 cells expressing control shRNA or DDB2 shRNA were grown on soft agar for 10 days. Top panel shows representative field of soft agar colonies. Bottom panel shows the bar graph representing quantification of soft agar colonies (mean +/- standard deviation; n=3).

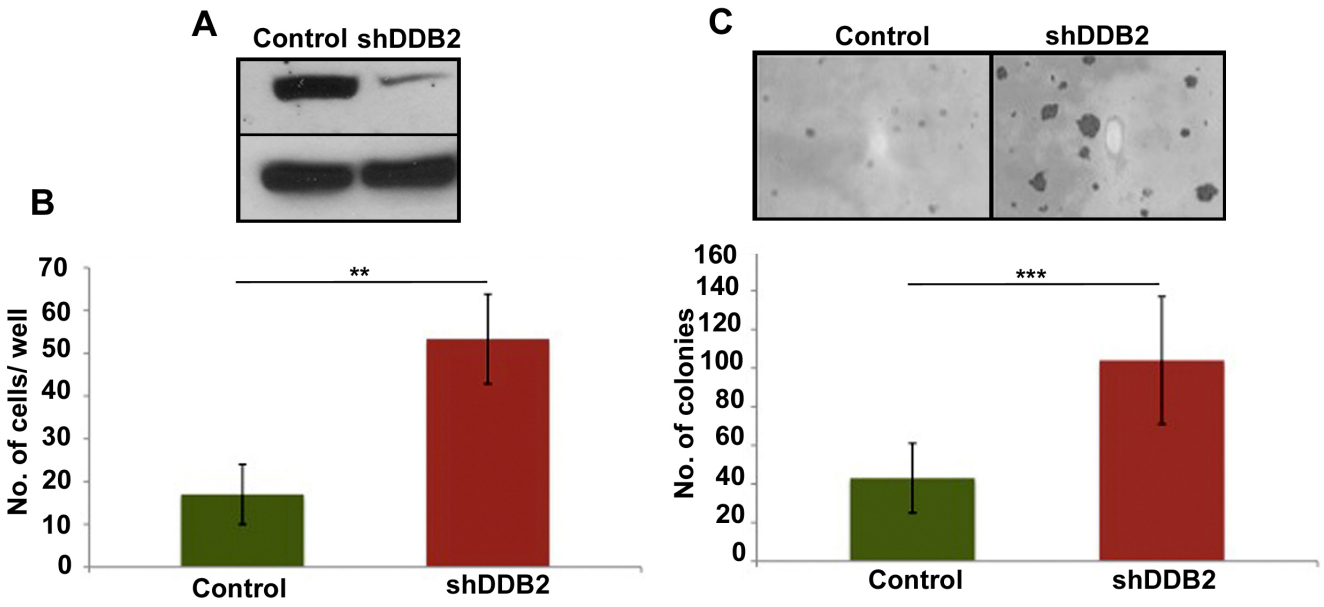
A
Control shDDB2
B
No. of cells/ well
70
60
50
40
30
20
10
0
**
Control
shDDB2
C
Control
shDDB2
No. of colonies
160
140
120
100
80
60
40
20
0
***
Control
shDDB2

EMT in HCT116 cells with loss in DDB2 expression, I found evidence that in colon carcinoma patient samples, low DDB2 expression indicates lower E-cadherin expression and subsequently worse outcome of the disease.

To investigate the significance of DDB2 down regulation in colon cancer, I compared the colon cancer cell line HCT116 with that stably expressing DDB2-shRNA (Fig.44 A). First, the DDB2 knockdown HCT116 cells were found to be significantly more invasive compared to the control cell line, as judged by matrigel migration assay (Fig.44 B). The invasiveness was confirmed also by scratch-healing assay (Fig.45 A). Moreover, in soft agar colony formation assay, the DDB2-shRNA expressing cells produced significantly more colonies than the control HCT116 cells (Fig.44 C). I explored the possibility that the DDB2 deficient cells might be resistant to anoikis. Control and DDB2 knock down cell lines were maintained in non-adherent culture condition (Poly-hema coated plates) and were harvested at 24h, 48h and 72h time points. Cleaved Caspase-3 levels were assayed at each time point. Control cell lines showed cleaved Caspase 3 expression as early as 48h, whereas the DDB2 deficient cells did not exhibit cleaved Caspase 3 even at 72h, confirming that these cells are resistant to matrix detachment induced cell death (Fig.45 B). Cells resistant to matrix detached cell death tend to form aggregate as a survival mechanism. Control and DDB2 knock down cells were plated as single cell suspension and were maintained up to 48h. DDB2 deficient cells clearly formed aggregate at the 48h time point, whereas the control cells remained mostly as single cells (Fig.45 C).

Figure 45: DDB2 deficient cells are deficient in anoikis.
(A) Wound healing assay of HCT 116 cells expressing control shRNA or DDB2 shRNA. Phase contrast images of wounded area of either cell line were recorded at indicated time points. (B) HCT 116 cells expressing control shRNA or DDB2 shRNA were cultured in suspension for 24, 48 or 72 hrs. Protein extracts for each time point from either cell line were subjected to Western blot analysis with cleaved caspase 3, p-AKT, p-ERK, total AKT, total ERK (50ug protein each). Actin was used as a loading control. (C) Cell aggregation in poly-HEMA coated dishes. HCT116 cells expressing control shRNA or DDB2 shRNA were cultured in 6 well poly-HEMA coated dishes for 48 hrs and photographed.

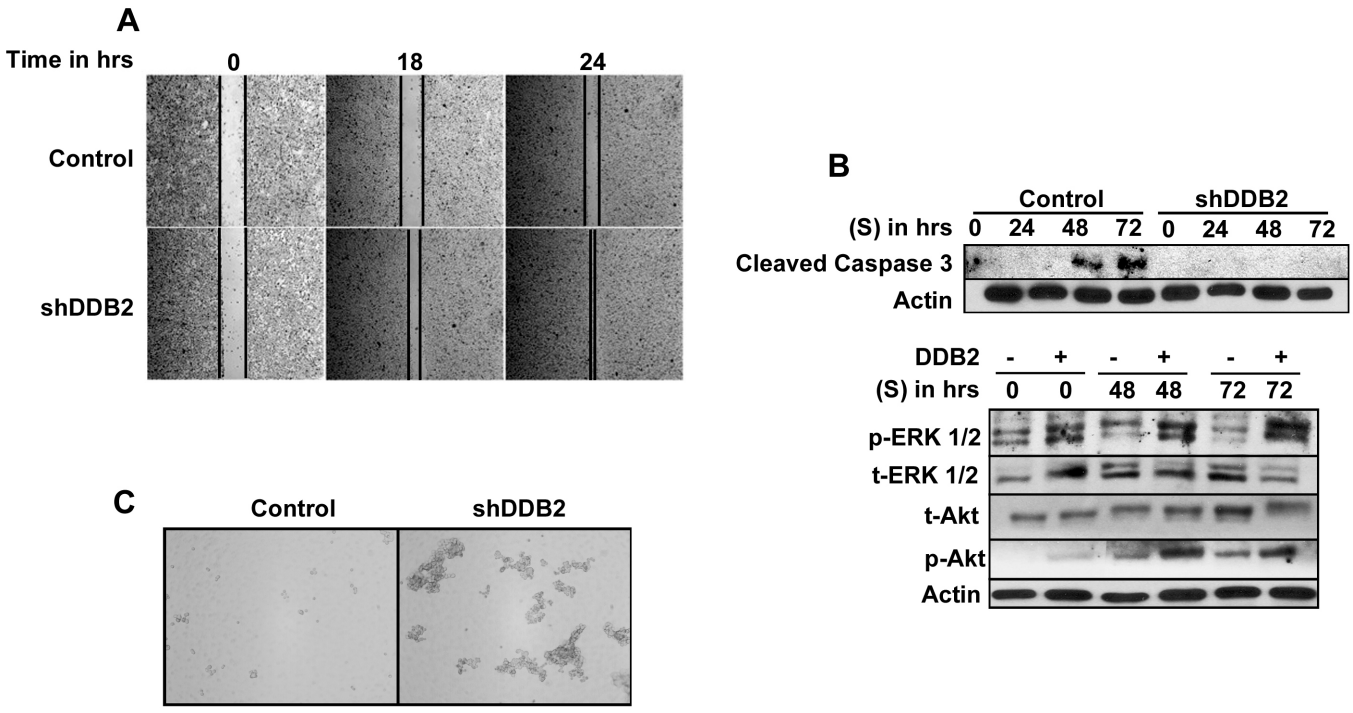
A
Time in hrs
0
18
24
Control
shDDB2
B
Control
shDDB2
(S) in hrs
0 24 48 72 0 24 48 72
Cleaved Caspase 3
Actin
DDB2 - + - + - +
(S) in hrs
0 0 48 48 72 72
p-ERK 1/2
t-ERK 1/2
t-Akt
p-Akt
Actin
C
Control
shDDB2

Figure 46: DDB2 deficiency increases invasiveness and tumorigenecity of colon cancer cells in vivo.
(A) HCT116 cells expressing control shRNA or DDB2 shRNA were injected subcutaneously into nude mice. Representative picture of xenograft tumors induced in nude mice by HCT 116 cells expressing control shRNA or DDB2 shRNA 7 weeks post-inoculation (n=5). (B) Bar graph representing tumor mass in nude mice from HCT 116 cells expressing control shRNA or DDB2 shRNA at the point of sacrifice of the mice (mean +/- standard error of mean; n=10). (C) Tumor volume induced in nude mice by HCT 116 cells expressing control shRNA or DDB2 shRNA (n=5).

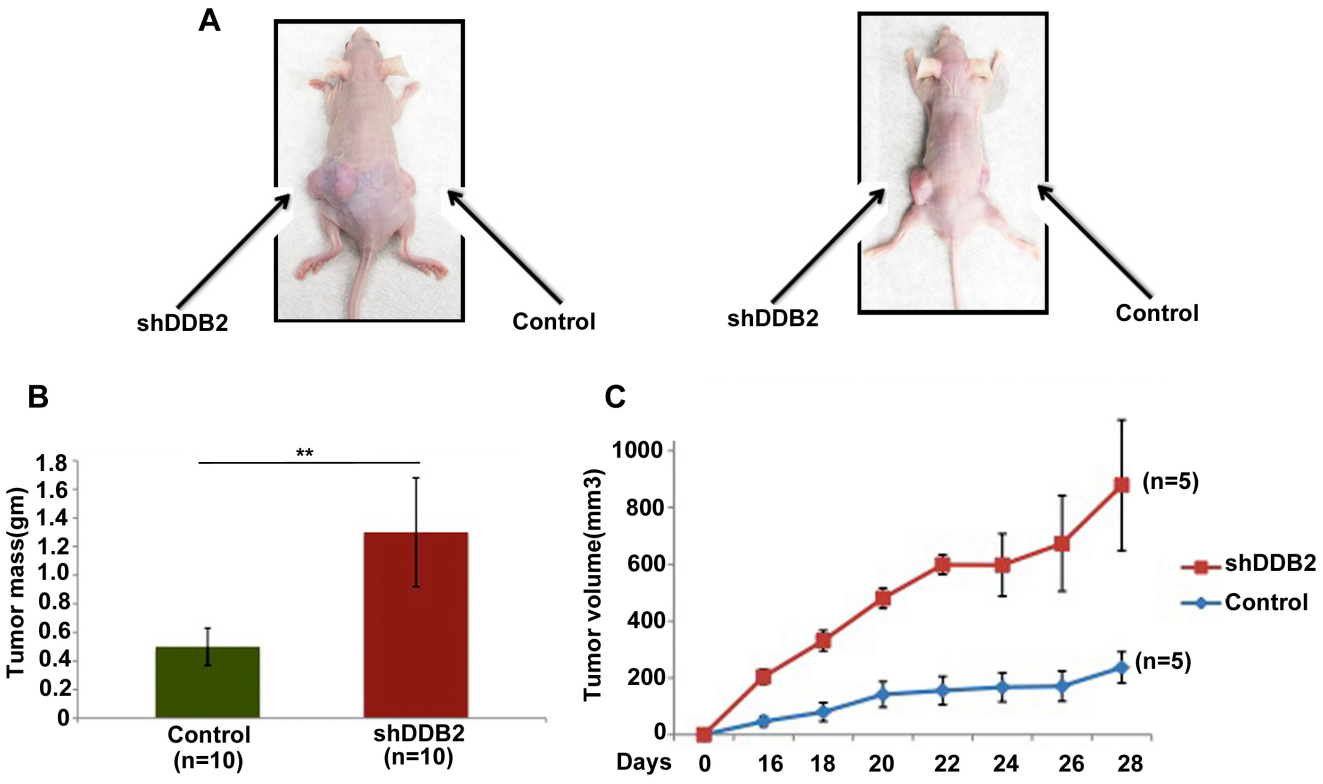
A
shDDB2
Control
shDDB2
Control
B
Tumor mass(gm)
1.8
1.6
1.4
1.2
1.0
0.8
0.6
0.4
0.2
0
**
Control
(n=10)
shDDB2
(n=10)
C
Tumor volume(mm3)
1000
800
600
400
200
0
Days
0
16
18
20
22
24
26
28
(n=5)
(n=5)
shDDB2
Control

Figure 47: Tumor from DDB2 deficient cells exhibit mesenchymal phenotype. HCT116 cells expressing control shRNA or DDB2 shRNA were injected subcutaneously into nude mice. Four weeks post inoculation mice were sacrificed and tumor sections were fixed in 10% Formalin, processed and embedded with paraffin for sectioning. Prepared tumor section slides were then subjected to immunohistochemical analysis using H & E staining, Smooth muscle actin, PCNA E-cadherin and Vimentin antibody. Representative images are shown.

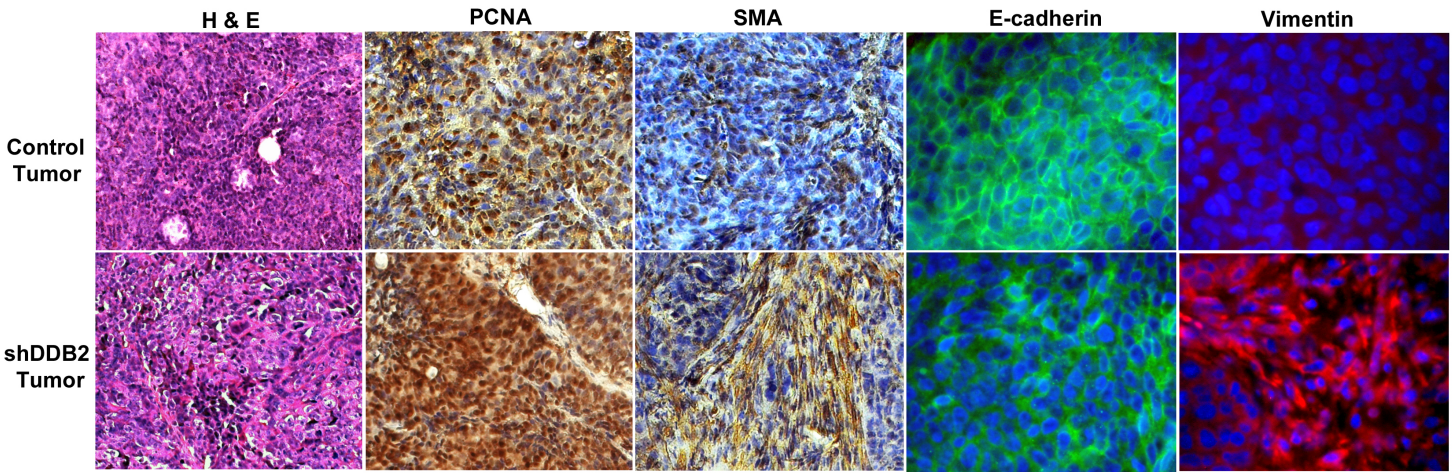
H & E
PCNA
SMA
E-cadherin
Vimentin
Control Tumor
shDDB2 Tumor

Consistent with the resistance to anoikis, the DDB2 deficient cells showed higher expression of p-ERK and p-AKT compared to the normal cells (Fig.45 B).

To confirm the increased tumorigenicity in the absence of DDB2, I compared tumor growth in mouse xenografts. Two million cells, HCT116 expressing control shRNA or DDB2-shRNA, were injected into nude mice subcutaneously and tumor growth was measured. Clearly, the DDB2-deficient cells generated a larger tumor mass in a much shorter time (Fig.46 A and B). That was evident also in a tumor growth curve analysis (Fig.46 C). Histology of the tumor specimen revealed aggressive nature of the tumor from DDB2 knockdown cells: increased Smooth Muscle Actin, PCNA expression (Fig.47). I further looked at E-cadherin and vimentin expression in these tumor samples. Consistent with my observation in vitro, I found evidence of reduced E-cadherin and increased vimentin expression in the xenograft tumors originating from DDB2 deficient cells (Fig.47). These studies collectively demonstrated that loss of DDB2 in colon cancer contributes to aggressive progression.

3.14 DDB2 IS A TRANSCRIPTIONAL REPRESSOR OF GENES THAT INDUCE EMT

RNA expression analyses confirmed that the DDB2 deficient cells express lower levels of the epithelial markers E-cadherin, Cytokeratin 18 and Cytokeratin 19, and increased expression of the mesenchymal markers Vimentin and N-cadherin (Fig.48). Several transcription factors, which have been implicated in the process of EMT such as Snail, Twist and Zeb 1, were up regulated at the mRNA-level in the absence of DDB2 (Fig.48). VEGF is also known to be an important player in the EMT

process [75, 119]. I observed that there was a significant increase in the levels of VEGF in DDB2 knocks down cells. Moreover, there was increased expression of Pinch 1, a protein that has been implicated in EMT and has the cognate binding element for DDB2 as described earlier [120]. I further looked at expression of VEGF, Snail1 and Zeb1 in SW480 and SW620 cells. siRNA mediated knock-down of DDB2 expression in the SW480 cells resulted attenuated expression of VEGF, Zeb1 and Snail1 (Fig.49 A and C). Next, I assayed for expression levels of them in SW620 cells following over-expression of DDB2. As expected, expression of DDB2 in SW620 cells inhibited expression of VEGF, Snail 1 and Zeb1 (Fig.49 B and D).

My previous studies on the regulation of the antioxidant genes by DDB2 identified a transcriptional repression function of DDB2. Therefore, I considered the possibility that the repression function of DDB2 might be linked to the EMT regulation. Because I observed a strong de-repression of VEGF expression, I considered that VEGF might be a direct repression target of DDB2. Also, there were strong increases in the expression of Zeb1 and Snail1, which are direct activator of EMT [64]. To examine whether DDB2 regulates expression of these genes directly, I performed Chromatin IP experiments to look at DDB2 occupancy at 3000 bp upstream from the start site of transcription. I observed an interaction of DDB2 with the VEGF promoter in ChIP) assays at two distinct sites (Fig.50 A). Moreover, DDB2 interacted with the Zeb1 and Snail promoters at specific sites (Fig.50 B and C). I also observed that loss of DDB2 leads to increased acetylation of the VEGF/Zeb1-chromatins that are conducive to

Figure 48: DDB2 acts as a transcriptional repressor of VEGF, Zeb1 and Snail.
Total RNA from HCT 116 cells expressing control shRNA or DDB2 shRNA was analyzed for the expression of E-cadherin, Cytokeratin 18, Cytokeratin 19, Vimentin, N-cadherin, Snail, Zeb1, Twist, VEGF, Pinch 1. Cyclophilin was used as a loading control.

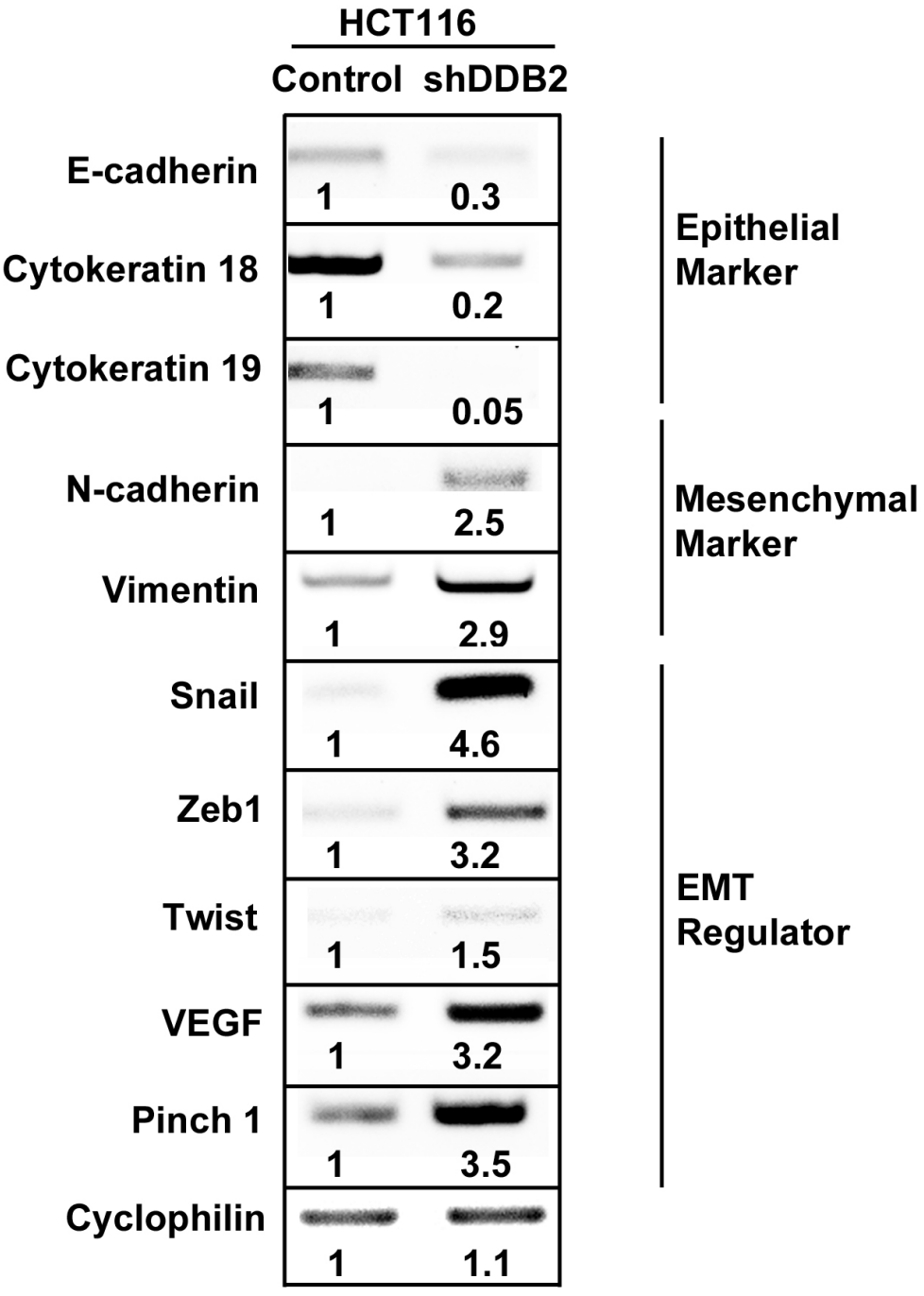
HCT116
Control
shDDB2
E-cadherin
1
0.3
Cytokeratin 18
1
0.2
Cytokeratin 19
1
0.05
N-cadherin
1
2.5
Vimentin
1
2.9
Snail
1
4.6
Zeb1
1
3.2
Twist
1
1.5
VEGF
1
3.2
Pinch 1
1
3.5
Cyclophilin
1
1.1
Epithelial Marker
Mesenchymal Marker
EMT Regulator

Figure 49: Overexpression of DDB2 in mesenchymal cells attenuates VEGF, Snail and Zeb1 expression.
(A) Total RNA from SW480 cells expressing control siRNA or DDB2 siRNA was analyzed for VEGF expression. Cyclophilin was used as a loading control. (B) Total RNA from SW620 cells expressing empty vector or DDB2 expressing vector was analyzed for VEGF expression. Cyclophilin was used as a loading control. (C) Protein extracts were made from SW480 cells expressing control siRNA or DDB2 siRNA and Western blot analysis was performed with Zeb1 (20ug protein), Snail (100ug protein) and DDB2 (50ug protein) antibody. Actin was used as a loading control. (D) Protein extracts were made from SW620 cells expressing empty vector or DDB2 expressing vector and Western blot analysis was performed with Zeb1 (20ug protein), Snail (100ug protein) and DDB2 (50ug protein) antibody. Actin was used as a loading control.

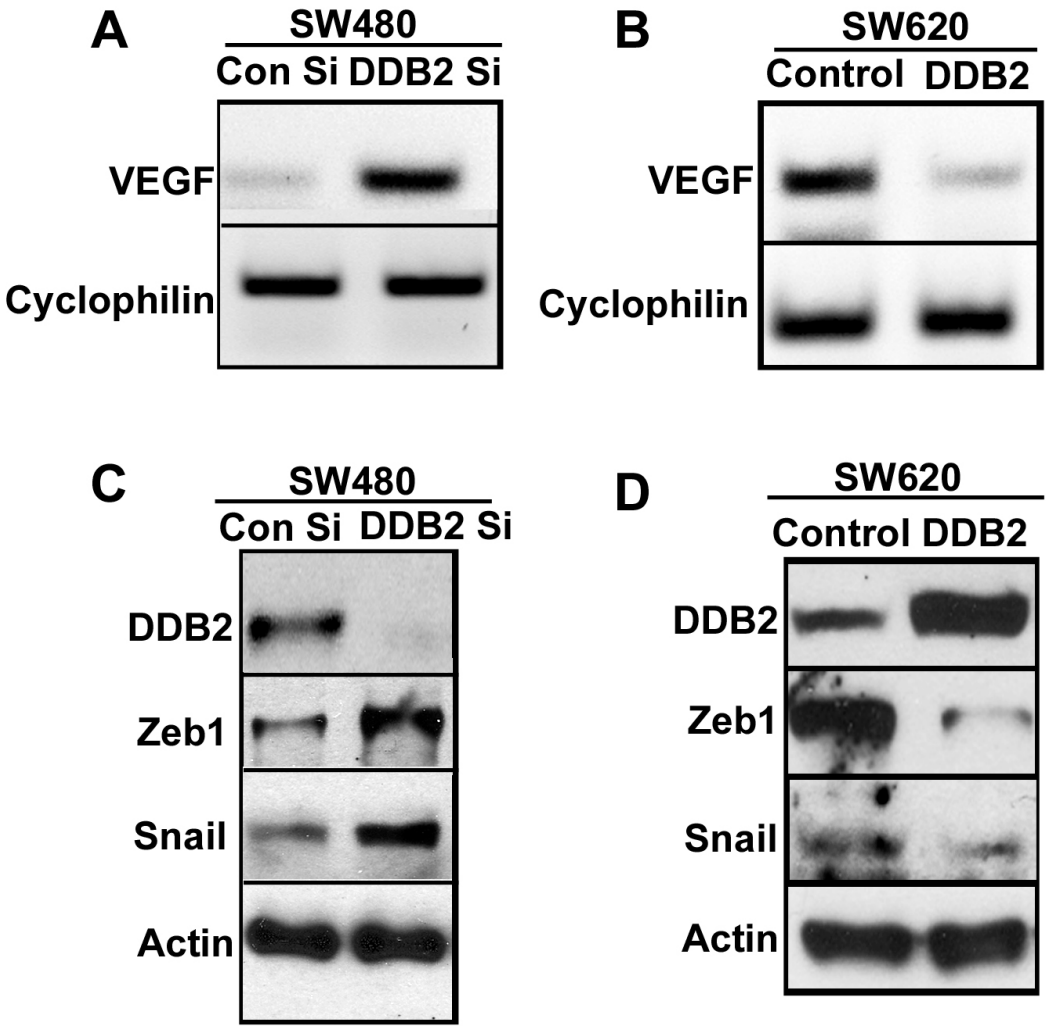
A
SW480
Con Si
DDB2 Si
VEGF
Cyclophilin
B
SW620
Control
DDB2
VEGF
Cyclophilin
C
SW480
Con Si
DDB2 Si
DDB2
Zeb1
Snail
Actin
D
SW620
Control
DDB2
DDB2
Zeb1
Snail
Actin

Figure 50: DDB2 binds to the promoter region of VEGF, Snail and Zeb1.
(A), (B) and (C) HCT 116 cells were subjected to ChIP assay on VEGF, Zeb1 or Snail promoter as described in materials and methods. Antibody against DDB2 or IgG was used for Immunoprecipitation.

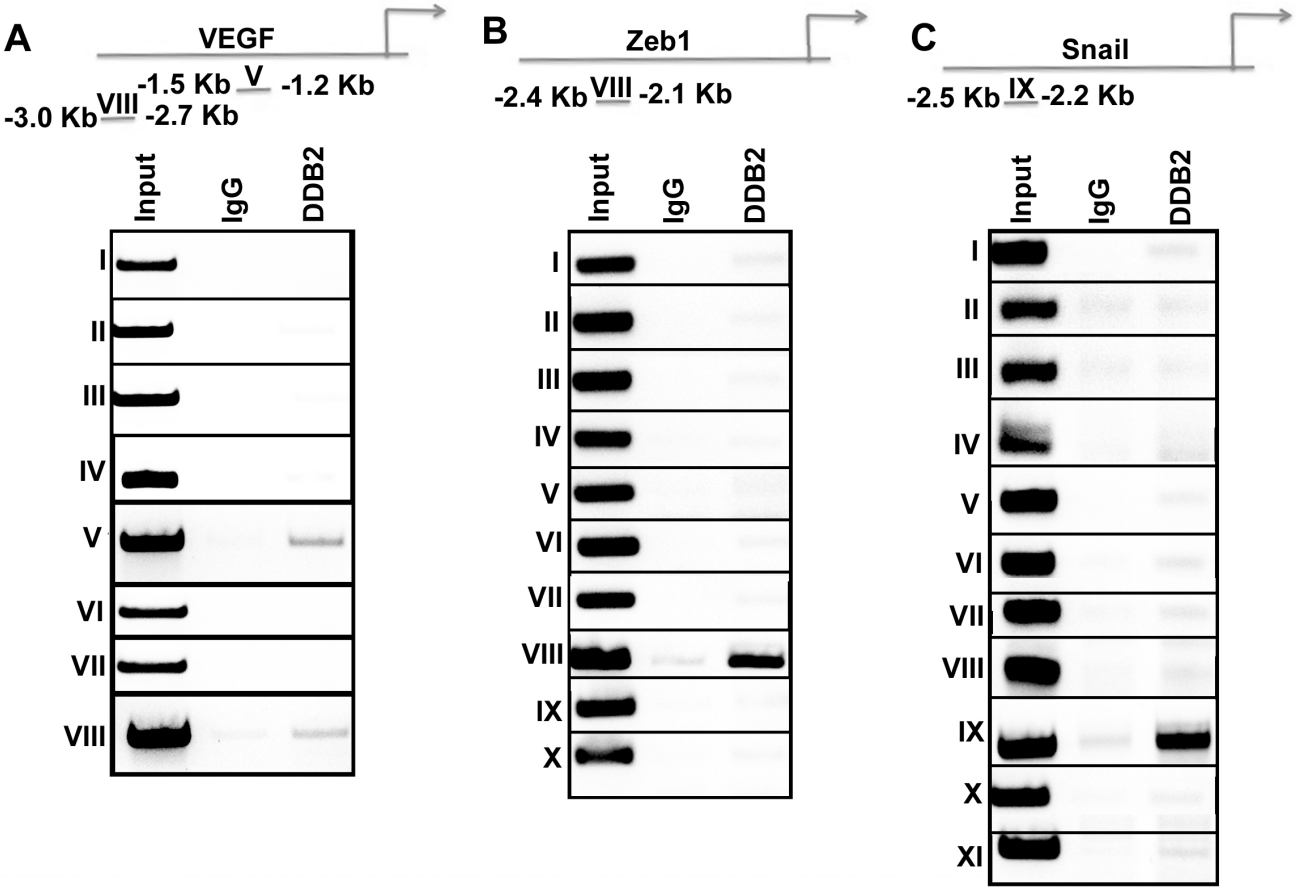
A
VEGF
-1.5 Kb
V
-1.2 Kb
-3.0 Kb
VIII
-2.7 Kb
Input
IgG
DDB2
I
II
III
IV
V
VI
VII
VIII
B
Zeb1
-2.4 Kb
VIII
-2.1 Kb
Input
IgG
DDB2
I
II
III
IV
V
VI
VII
VIII
IX
X
C
Snail
-2.5 Kb
IX
-2.2 Kb
Input
IgG
DDB2
I
II
III
IV
V
VI
VII
VIII
IX
X
XI

Figure 51: DDB2 is an epigenetic regulator of VEGF, Snail and Zeb1.
(A) HCT 116 cells expressing control shRNA or DDB2 shRNA were subjected to ChIP assay as described in materials and methods. Antibody against DDB1, Cul4a, Suv39h, H3K9Me3 or IgG was used for Immunoprecipitation. The VEGF, Zeb1 and Snail promoter fragments in the immunoprecipitated chromatin were quantified by semi-quantitative PCR with the primer pairs V (for VEGF), VIII (for Zeb1) and IX (for Snail). Bar graph represents percentage of immunoprecipitation versus input material (mean +/- standard deviation; n=3). (B) HCT 116 cells expressing control shRNA or DDB2 shRNA were subjected to ChIP assay as described in materials and methods. Antibody against H3Ac, H4Ac, H3K14Ac or IgG was used for Immunoprecipitation. The VEGF, Zeb1 and Snail promoter fragments in the immunoprecipitated chromatin were quantified by semi-quantitative PCR with the primer pairs V (for VEGF), VIII (for Zeb1) and IX (for Snail). Bar graph represents percentage of immunoprecipitation versus input material (mean +/- standard deviation; n=3). (C) HCT 116 cells were subjected to ChIP assay as described in materials and methods. Antibody against XPC or IgG was used for Immunoprecipitation. The VEGF, Zeb1 and Snail promoter fragments in the immunoprecipitated chromatin were quantified by semi-quantitative PCR with the primer pairs V (for VEGF), VIII (for Zeb1) and IX (for Snail). Occupancy on RAR promoter has been examined with or with out all-trans Retinoic Acid treatment. Bar graph represents percentage of immunoprecipitation versus input material (mean +/- standard deviation; n=3).

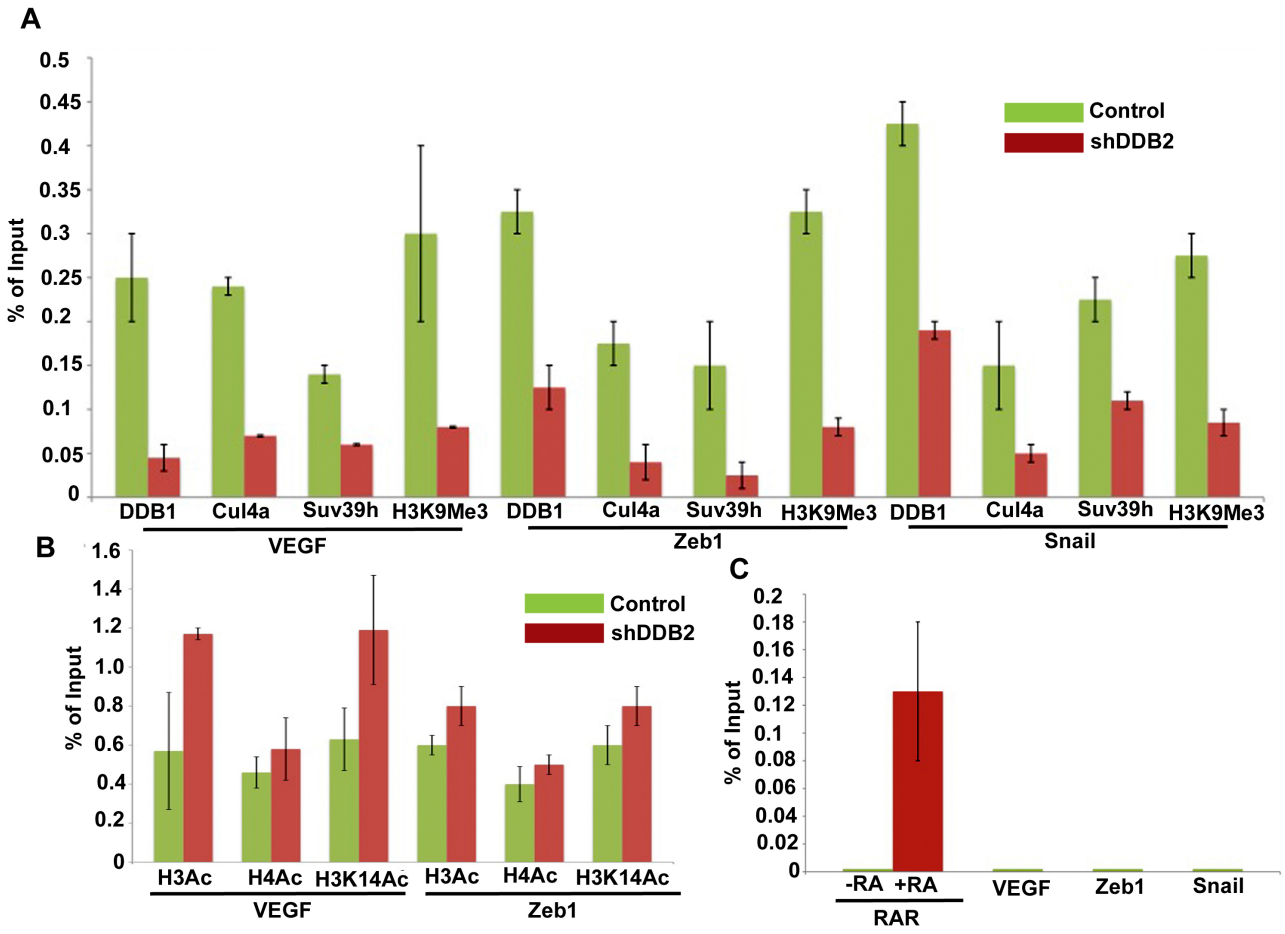
A
% of Input
0.5
0.45
0.4
0.35
0.3
0.25
0.2
0.15
0.1
0.05
0
Control
shDDB2
DDB1
Cul4a
Suv39h
H3K9Me3
VEGF
Zeb1
Snail
B
% of Input
1.6
1.4
1.2
1.0
0.8
0.6
0.4
0.2
0
H3Ac
H4Ac
H3K14Ac
VEGF
Zeb1
C
% of Input
0.2
0.18
0.16
0.14
0.12
0.1
0.08
0.06
0.04
0.02
0
-RA
+RA
RAR
VEGF
Zeb1
Snail

increased expression. My earlier observation implicated DDB2 as an epigenetic regulator of SOD2 and catalase genes. I next examined whether DDB2 is acting as a transcriptional repressor for VEGF, Zeb1 and Snail1 as well. Towards that, I performed chromatin IP with antibodies against DDB1, Cul4a, Suv39h and H3K9Me3 and compared binding of these repressors within the promoter of these 3 genes in HCT116 cells with shDDB2 expressing cells. Similar to my observation with the SOD2/ catalase genes, I observed reduced occupancy of DDB1, Cul4a in the promoter of all three genes in the cells expressing shRNA for DDB2 (Fig.51 A). I also observed reduced Suv39h and H3K9Me3 interaction with the promoter (Fig.51 A). Thus, in the context of EMT genes also, DDB2 causes Suv39h mediated methylation of H3K9 with the help of DDB1-Cul4a complex, leading to heterochromatinization. In agreement with that I observed increased H3 and H4 acetylation on the promoter of VEGF and Zeb1 in HCTshDDB2 cells (Fig.51 B). Together, the results suggest that DDB2 epigenetically repress expression of VEGF, Zeb1 and Snail, thereby inhibits the EMT process. Loss of DDB2 results in de-repression of these master regulators of EMT, leading to the epithelial to mesenchymal transition of the colon cancer cells. It has been shown previously that upon gene activation NER factors assemble with RNA polymerase II on the promoter. The XPC protein is particularly important for this assembly [121]. The NER factors help to achieve optimal DNA demthylation and histone post-translational modifications for efficient transcription process. This led me to investigate XPC occupancy on the promoter region of these genes. Towards that, I performed chromatin IP on VEGF, Snail1 and Zeb1. I did not find XPC binding

on the promoter of these genes (Fig.51 C). However, consistent with earlier report I did observe XPC binding on the promoter of RARβ2 upon AtRA treatment.

3.15 DDB2 REGULATES METASTASIS OF COLON CANCER CELLS

EMT in tumor cells is an early event in metastasis, where tumor cells detach from its primary site, travel through blood stream or lymph node and colonize to a distant organ. Since I observed evidence of EMT with loss of DDB2, functional metastasis assays, in vivo, were performed to examine whether DDB2 knock down cells are more metastatic. First, I carried out metastasis experiment using an orthotopic mouse model. Control HCT116 or the DDB2 knockdown HCT116 cells were subcutaneously injected in SCID beige mice. Once the tumors reached 0.5 mm in size, the tumors were excised and pieces of tumors were surgically implanted onto the cecum of host mice. Four weeks following implantation, the mice were analyzed for metastatic growth in the liver. I observed extensive metastasis with the tumor generated from DDB2 knock down cells in the liver. The tumor implant generated with the control HCT116 cells did not undergo any visible metastasis in any organ under these experimental conditions (Fig.52 A). To further confirm the observation, I performed tail vein injection of the DDB2-depleted cells in athymic nude mice. The parental or the DDB2 knock down cells were injected into the tail vein of mice. HCT116 cells were reported to form lung metastasis by four weeks [122]. To detect acceleration of metastasis by the loss of DDB2, I looked at the lung tumor metastasis after 4 weeks. The mice were sacrificed and examined for lung nodules. The mice injected with DDB2 knockdown cell line clearly exhibited evidence of lung tumor

Figure 52: DDB2 regulates metastasis of colon cancer cells.
(A) HCT116 cells expressing control shRNA or DDB2 shRNA were injected subcutaneously into SCID beige mice. Once xenografts were established, they were excised and orthotopically implanted into other SCID beige mice using microsurgical techniques (n=4). Animals were sacrificed 4 weeks post-implantation and examined for liver metastasis. Representative H & E staining of liver sections from mice injected with HCT 116 cells expressing control shRNA or DDB2 shRNA are shown (left panel). Quantification of percentage of metastasis occurrence in mice injected with HCT116 cells expressing control shRNA or DDB2 shRNA (right panel). (B) HCT116 cells expressing control shRNA or DDB2 shRNA were injected into 8 weeks old male nude mice intravenously via the tail vein (n=6). Mice were sacrificed after four weeks and lung tissues were harvested. Representative H & E staining of lung from mice injected with HCT 116 cells expressing control shRNA or DDB2 shRNA (left panel). Quantification of percentage of micro-metastasis occurrence in mice injected with HCT116 cells expressing control shRNA or DDB2 shRNA (right panel). (C) SW620 cells expressing empty vector or DDB2 expressing vector were injected into 8 weeks old male nude mice intravenously via tail vein (n=6). Mice were sacrificed after six weeks and lung tissues were harvested. Representative H & E staining of lung from mice injected with SW620 cells expressing empty vector or DDB2 expressing vector (left panel). Quantification of percentage of metastasis occurrence in mice injected with SW620 cells expressing empty vector or DDB2 expressing vector (right panel).

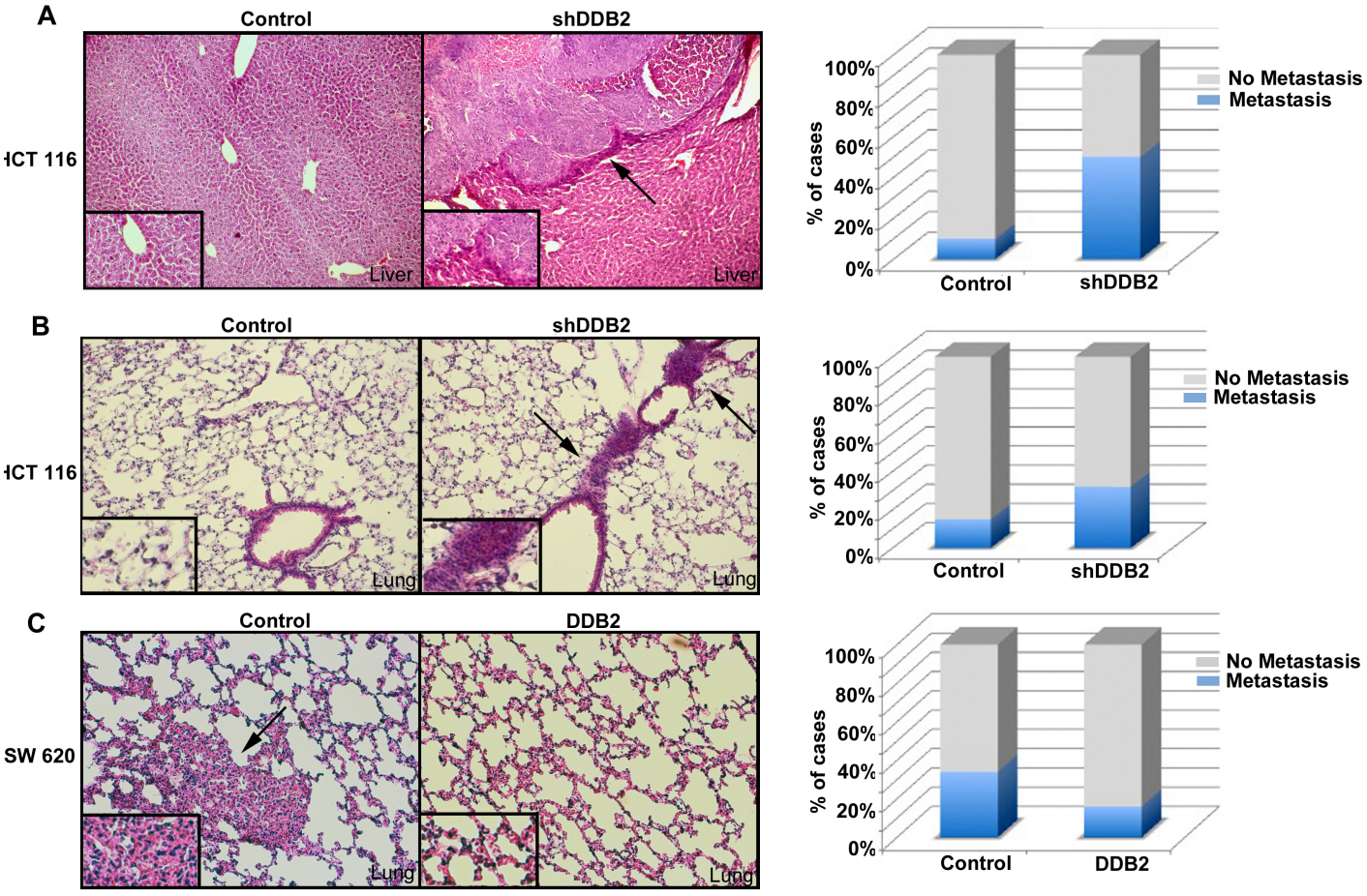
A
Control
shDDB2
HCT 116
Liver
Liver
100%
80%
60%
40%
20%
0%
% of cases
Control
shDDB2
No Metastasis
Metastasis
B
Control
shDDB2
HCT 116
Lung
Lung
100%
80%
60%
40%
20%
0%
% of cases
Control
shDDB2
No Metastasis
Metastasis
C
Control
DDB2
SW 620
Lung
Lung
100%
80%
60%
40%
20%
0%
% of cases
Control
DDB2
No Metastasis
Metastasis

micro-metastasis within that time, whereas the control HCT116 injected mice exhibited fewer micro-metastatic nodules (Fig.52 B). Because expression of DDB2 inhibited expression of the EMT genes and blocked EMT, I sought to determine. whether expression of DDB2 inhibits metastasis. To investigate that, I compared the metastatic line SW620 with SW620 stably expressing DDB2. Two million cells were injected in nude mice via tail vein. Six-weeks following injection, the mice were sacrificed and the metastatic colonies in the lung were compared. There was a significant reduction in the metastatic colonies in the lung tissue from mice injected with DDB2-expressing SW620 cells (Fig.52 C). These observations provide evidence that DDB2 is a potent inhibitor of colon cancer metastasis.

Tumor regression by PEITC involves DDB2

3.16 PEITC MEDIATED APOPTOSIS AND SENESCENCE REQUIRES DDB2

DDB2-/- mice are prone to spontaneous tumor development. Moreover, database research revealed loss of DDB2 expression in different forms of solid cancer including colon cancer. In the protein level as well there is evidence of reduction in DDB2 expression in colon carcinoma samples compared to the normal tissue. DDB2 is an essential mediator of apoptosis and senescence, two major tumor suppressor processes. Also, DDB2 inhibits EMT and consequently metastasis of colon carcinoma cells. Therefore, therapeutically targeting up-regulation of DDB2 can be beneficial to treat cancer patients with loss of DDB2 expression. Moreover, ROS increases DDB2 expression, which can be exploited to induce DDB2 expression as compound like PEITC increases ROS level in the cell [123]. PEITC increases ROS level in the cell and selectively kills the transformed cells. Increased DDB2 expression will be conducive for the cell to undergo senescence/ apoptosis.

First, I investigated whether PEITC increases DDB2 level. Towards that, HCT 116 cells were treated with PEITC and DDB2 level was examined at different time points both at protein and RNA level. Consistent with hydrogen peroxide mediated DDB2 response, PEITC was found to increase the level of DDB2 at the RNA and level (Fig.53 A). Moreover, this is p53 independent as PEITC can up-regulate DDB2 in HCT p53-/- cells (Fig.53 B).

Figure 53: PEITC induces expression of DDB2 independent of p53.
(A) HCT116 cells were treated with PEITC for indicated time point. Total RNA was analyzed by Semi-quantitative PCR for the level of DDB2. Cyclophlin was used as a loading control. (B) HCT116 p53-/- cells were treated with PEITC for indicated time points. Total RNA was analyzed by Semi-quantitative PCR for the level of DDB2. Cyclophlin was used as a loading control.

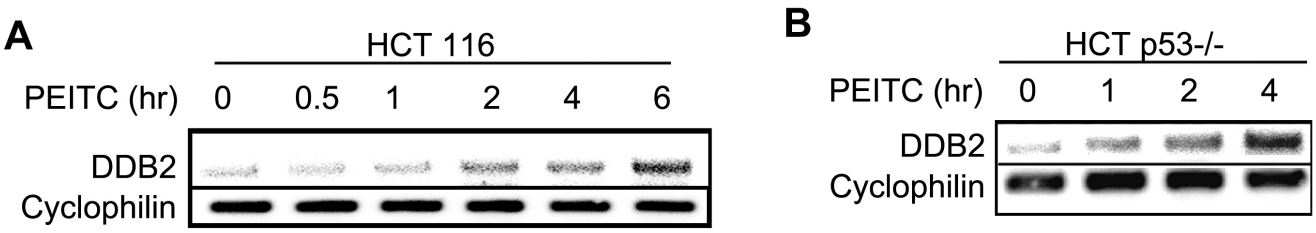
A
HCT 116
PEITC (hr) 0 0.5 1 2 4 6
DDB2
Cyclophilin
B
HCT p53-/-
PEITC (hr) 0 1 2 4
DDB2
Cyclophilin

Figure 54: PEITC mediated apoptosis and senescence requires DDB2.
HCT116 cells expressing control shRNA or DDB2 shRNA were treated with PEITC for 12 hrs. Next day, cells were analyzed for apoptosis by TUNEL assay. Representative images of HCT116 cells expressing LacZ shRNA or DDB2 shRNA stained for TUNEL assay after PEITC treatment. (A and B) TUNEL positive cells were counted from at least ten fields of triplicate plates. A quantification of TUNEL positive HCT116 cells after PEITC treatment is shown. (C and D) HCT116 cells expressing control shRNA or DDB2 shRNA were treated with PEITC for 4 hrs. After 48 hrs, cells were analyzed for SA β gal activity. Representative images of HCT116 cell expressing control shRNA or DDB2 shRNA stained for SA β gal after PEITC treatment. SA β gal positive cells were counted from at least ten fields of triplicate plates. A quantification of SA β gal positive HCT116 cells after PEITC treatment is shown.

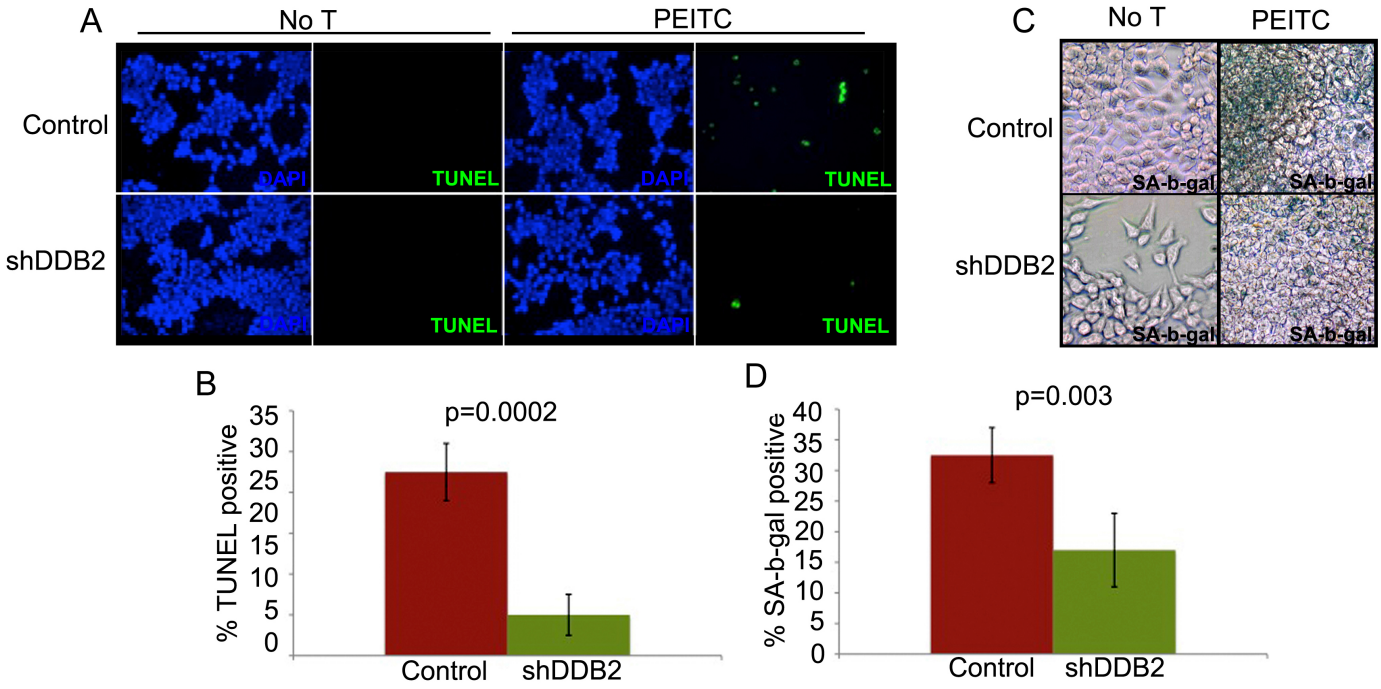
A
No T
PEITC
Control
shDDB2
DAPI
TUNEL
C
No T
PEITC
Control
shDDB2
SA-b-gal
B
p=0.0002
% TUNEL positive
35
30
25
20
15
10
5
0
Control
shDDB2
D
p=0.003
% SA-b-gal positive
40
35
30
25
20
15
10
5
0
Control
shDDB2

Figure 55: DDB2 deficient cells are drug resistant.
(A) HCT116 cells expressing control shRNA or DDB2 shRNA were seeded (500 cells) in 6 well plates. Next day cells were treated with PEITC for 12 hrs followed by wash with PBS twice. Cells were grown for 12 days. Colonies with more than 50 cells were counted from triplicate plates. Representative images of colonies from HCT116 cell expressing control shRNA or DDB2 shRNA stained with crystal violet are shown. (B) A quantification of colonies formed after PEITC treatment is shown. Colonies with more than 50 cells were counted from triplicate plates.

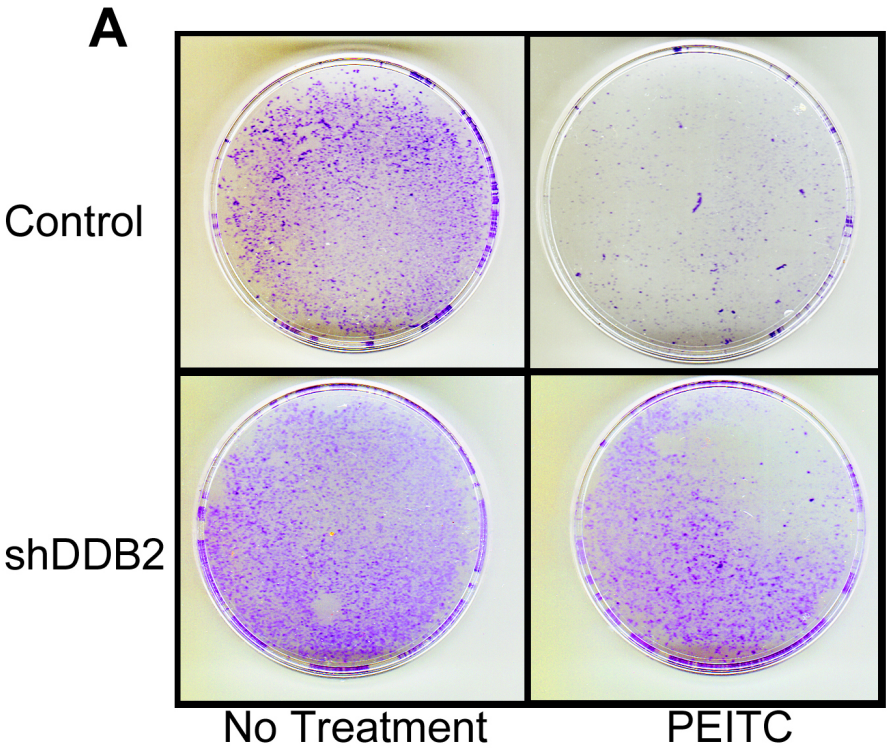
A
Control
shDDB2
No Treatment
PEITC

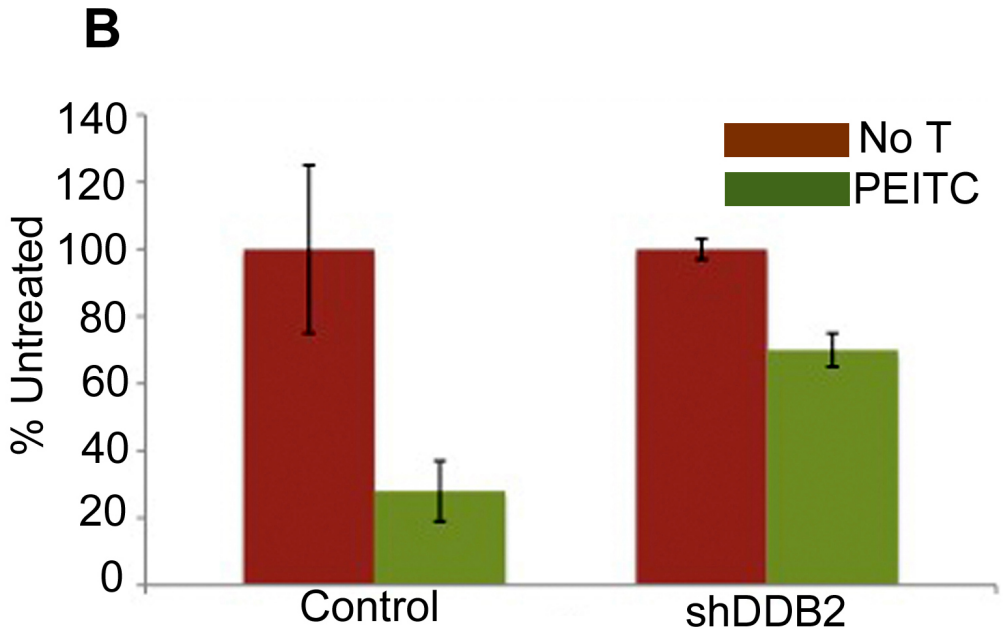
B
% Untreated
140
120
100
80
60
40
20
0
No T
PEITC
Control
shDDB2

PEITC has been reported to induce apoptosis and cell cycle arrest in colon carcinoma cell, HT29 [124]. In HCT 116 cells I investigated whether PEITC induces apoptosis or senescence and whether that is dependent on DDB2. HCT 116 cellsexpressing control shRNA or cells expressing DDB2 shRNA were treated with PEITC and TUNEL assay was performed to measure apoptosis response. Cells expressing DDB2 shRNA was significantly deficient in apoptosis response compared to the control shRNA expressing cells, suggesting that DDB2 is required for PEITC mediated apoptosis (Fig.54 A and B). Next, I looked at senescence response with PEITC treatment. HCT 116 cells expressing control shRNA or DDB2 shRNA were treated with PEITC for 6 hours and stained with SA-beta-gal after 48 hours. Cells expressing control shRNA underwent senescence after PEITC treatment, which was clearly deficient in DDB2 shRNA expressing cells (Fig.54 C and D). Hence, PEITC mediated apoptosis/ senescence response require DDB2 activity. Furthermore, to confirm this observation clonogenecity assay was performed with HCT 116 cells expressing control shRNA or DDB2 shRNA. Compared with the untreated cells, PEITC treated control shRNA expressing cells generated fewer colonies (Fig.55 A and B). However, DDB2 shRNA expressing cells developed significantly higher number of colonies following PEITC treatment (Fig.55 A and B). This further strengthens the observation that PEITC mediated drug response required efficient DDB2 activity. I also investigated whether DDB2 is important particularly for PEITC mediated drug action, or it plays a general role for other chemotherapeutic agent that increases ROS.

Figure 56:In vivo therapeutic activity of PEITC requires DDB2.
(A) and (B) HCT116 cells expressing control shRNA or DDB2 shRNA were injected subcutaneously into nude mice. Mice were divided randomly in two groups for each cell line for treatment with PEITC (n=5) or vehicle control (n=3). Graph represents the tumor mass from control or DDB2 deficient cells line treated with PEITC or left untreated along with percent reduction in tumor mass. (C) HCT116 cells expressing control shRNA or DDB2 shRNA were injected subcutaneously into nude mice. Mice were divided randomly in two groups for each cell line for treatment with PEITC or vehicle control. Four weeks post treatment mice were sacrificed and tumor sections were fixed in 10% Formalin, processed and embedded with paraffin for sectioning. Prepared tumor section slides were then subjected to immunohistochemical analysis using DDB2 antibody. Representative images from two different tumors are shown.

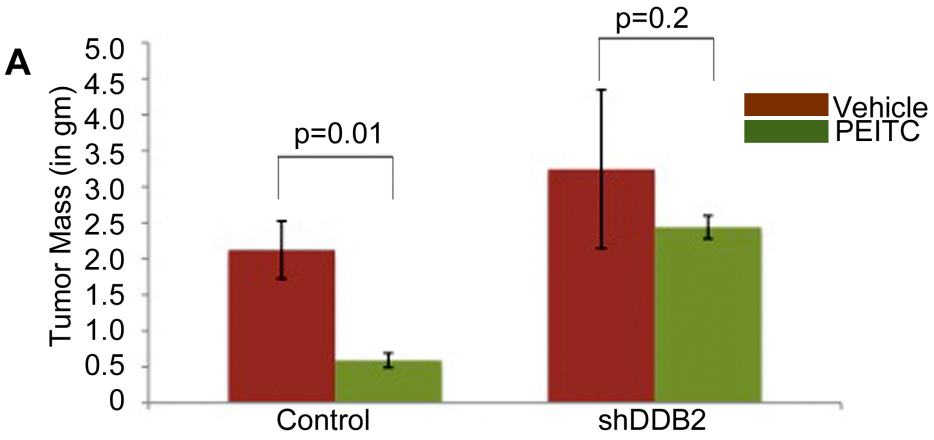
A
Tumor Mass (in gm)
5.0
4.5
4.0
3.5
3.0
2.5
2.0
1.5
1.0
0.5
0
p=0.01
p=0.2
Vehicle
PEITC
Control
shDDB2

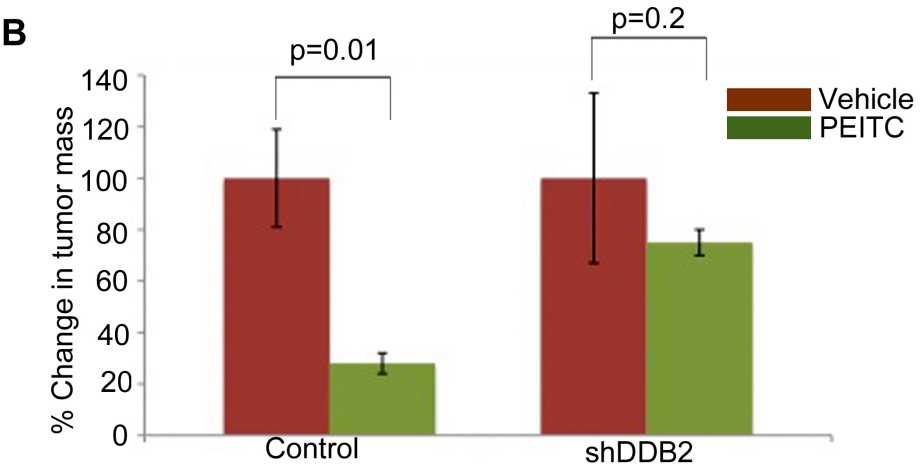
B
% Change in tumor mass
140
120
100
80
60
40
20
0
p=0.01
p=0.2
Vehicle
PEITC
Control
shDDB2

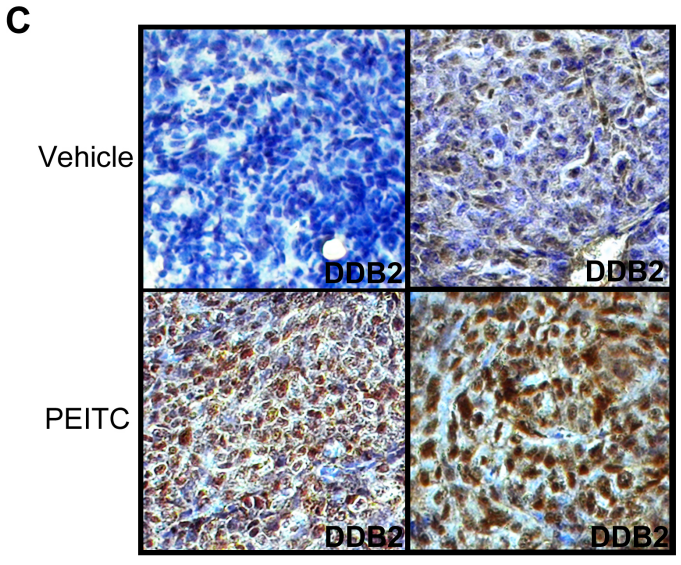
C
Vehicle
PEITC
DDB2
DDB2
DDB2
DDB2

Figure 57: DDB2 deficiency abrogates PEITC mediated regression in tumor aggressiveness.
HCT116 cells expressing control shRNA or DDB2 shRNA were injected subcutaneously into nude mice. Mice were divided randomly in two groups for each cell line for treatment with PEITC or vehicle control. Four weeks post treatment mice were sacrificed and tumor sections were fixed in 10% Formalin, processed and embedded with paraffin for sectioning. Prepared tumor section slides were then subjected to immunohistochemical analysis using H& E, PCNA or SMA antibody. Representative images (20X magnification) are shown. (B) PCNA positive cells per 40x magnification field were counted. 6 random fields were chosen for quantification. (C) SMA positive area was quantified by ImageJ. 6 random fields were chosen.

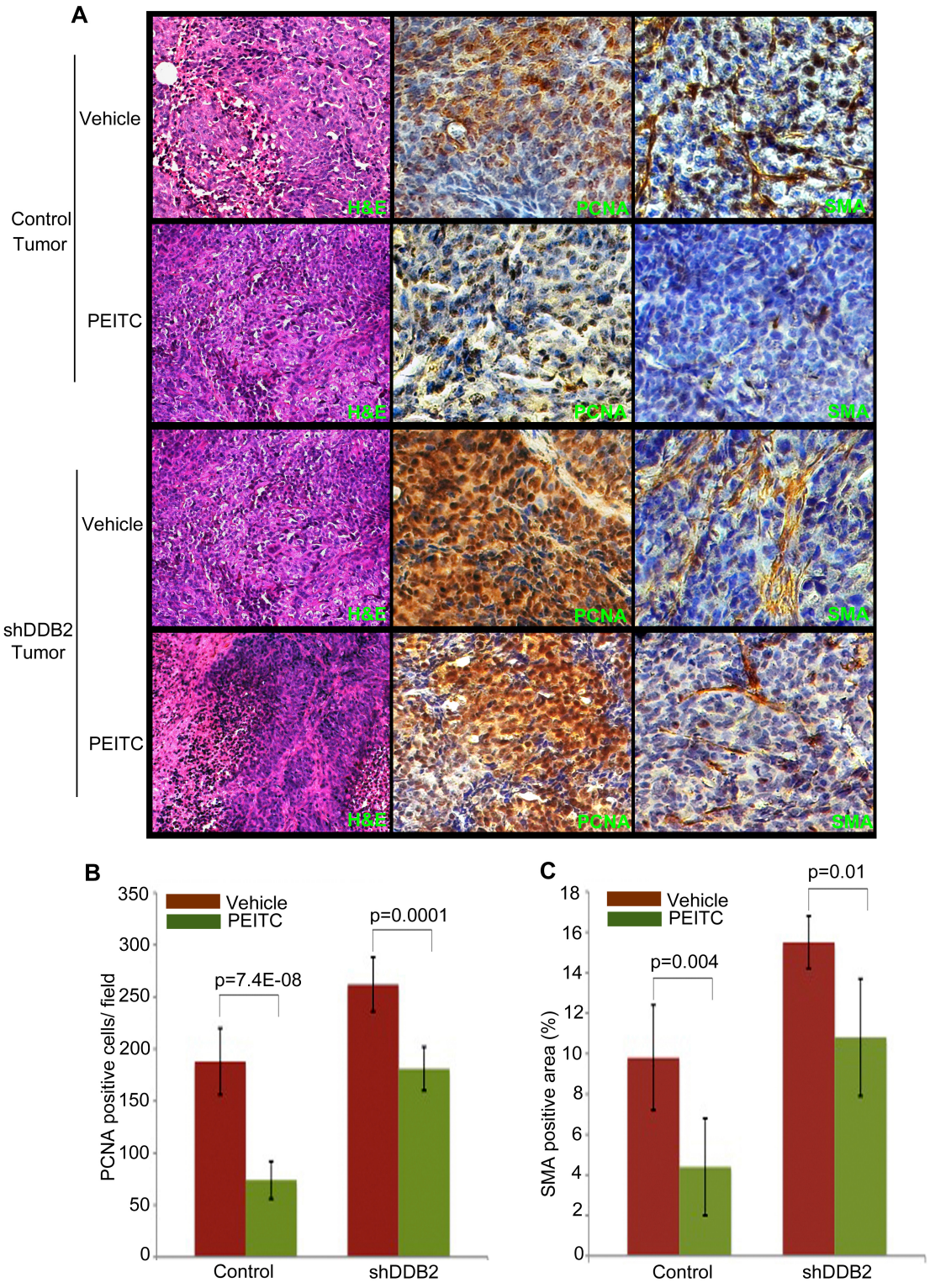
A
Vehicle
Control Tumor
PEITC
shDDB2 Tumor
Vehicle
PEITC
H&E
PCNA
SMA
B
PCNA positive cells/ field
Vehicle
PEITC
p=7.4E-08
p=0.0001
Control
shDDB2
C
SMA positive area (%)
Vehicle
PEITC
p=0.004
p=0.01
Control
shDDB2

Figure 58: DDB2 deficiency abrogates PEITC mediated apoptosis and senescence in vivo.
(A) HCT116 cells expressing control shRNA or DDB2 shRNA were injected subcutaneously into nude mice. Mice were divided randomly in two groups for each cell line for treatment with PEITC or vehicle control. Four weeks post treatment mice were sacrificed and tumor sections were fixed in 10% Formalin, processed and embedded with paraffin for sectioning. Prepared tumor section slides were then subjected to immunohistochemical analysis using Cleaved caspase3 or p16INK4a antibody. Representative images (at 20X magnification) are shown. (B) Cleaved caspase 3 positive cells per 40x magnification field were counted. 6 random fields were chosen for quantification. (C) p16INK4a positive cells per 40x magnification field were counted. 6 random fields were chosen for quantification.

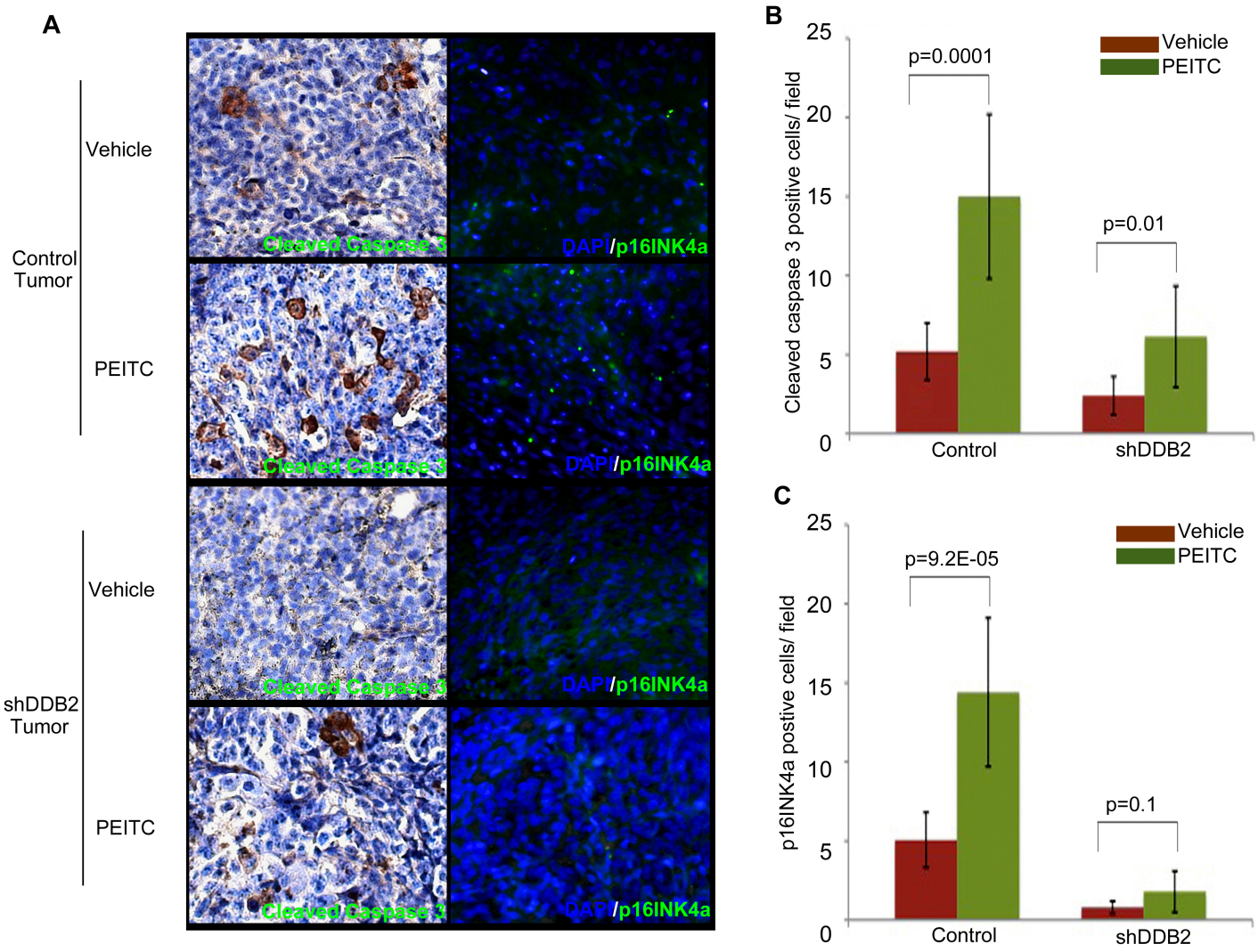
A
Control Tumor
Vehicle
PEITC
shDDB2 Tumor
Vehicle
PEITC
Cleaved Caspase 3
DAPI/p16INK4a
B
Cleaved caspase 3 positive cells/ field
p=0.0001
p=0.01
Vehicle
PEITC
Control
shDDB2
C
p16INK4a postive cells/ field
p=9.2E-05
p=0.1
Vehicle
PEITC
Control
shDDB2

3.17 PEITC MEDIATED TUMOR REGRESSION REQUIRES DDB2

I next investigated whether PEITC mediated tumor regression in vivo also requires DDB2 expression. First, HCT116 cells expressing control shRNA or DDB2 shRNA were subjected to sub-cutaneous injection in nude mice. Once the tumor reached 10-15 mm3, mice were subjected to PEITC or vehicle treatment up to 4 weeks. For the control cells, tumor was regressed by almost 50% consistent with earlier reports [87]. Interestingly, tumors developed from DDB2 shRNA expressing cells were significantly less responsive to PEITC treatment, providing evidence that PEITC treatment in vivo requires expression of DDB2 (Fig.56 A and B). I also looked at DDB2 expression in PEITC treated tumor from control shRNA cells. DDB2 expression was found to be elevated in the PEITC treated tumors compared to the vehicle treated tumor (Fig.56 C), which correlates with our in vitro observation that increased DDB2 expression is required for PEITC mediated apoptosis and senescence response. I also examined PCNA and smooth muscle actin expression between treated and untreated tumor from control or DDB2 deficient cells. There was higher expression of PCNA and smooth muscle actin in tumors from DDB2 deficient cells suggesting more aggressive nature of the tumor (Fig.57). I also looked at apoptosis and senescence response in the tissue sections from PEITC or vehicle treated tumor. There was a clear accumulation of apoptotic cells as suggested by cleaved caspase 3 expression in the tumor from control shRNA cells. However, in the tumor from DDB2 shRNA cells there was significantly less accumulation of apoptotic cells (Fig.58 A and B). I also looked at senescence response by p16INK4a staining in tissue sections from tumor. Consistent with my in vitro observation, tumor from

control cells exhibited increased p16INK4a expression, a hallmark of senescence, which was significantly less in tumors from DDB2 shRNA cells (Fig.58 A and C). Collectively, I provide evidence that in vivo, PEITC treated tumor regression requires DDB2 expression.

4.DISCUSSION:

In my thesis work, I provide new insights on role of DDB2 as a tumor suppressor. I show that DDB2 plays an important role to induce premature senescence. I further provide evidence that DDB2 inhibits EMT and metastasis of colon carcinoma cells. The aforementioned functions of DDB2 are related to its role as a transcription repressor. DDB2 acts as an epigenetic regulator of SOD2 and catalase that is related to its senescence function. Similarly, epigenetic repression of VEGF, Snail1 and Zeb1 by DDB2 is linked to its role as a suppressor of EMT. I further show that function of DDB2 as a tumor suppressor can be exploited for therapeutic purpose where I use PEITC to induce expression of DDB2. Collectively, my findings demonstrate DDB2 as a key factor to inhibit tumorigenesis and metastasis.

My initial observations are surprising with regard to p21. Several studies implicated p21 as an important component in the senescence pathway [125, 126]. For example, there is clear accumulation of p21 in senescence induced by telomere erosion [127]. Also, DNA damage-induced senescence was suggested to involve p21. The DNA damage response pathway activates p53 to induce expression of p21. A high level of p21 following extensive DNA damage has been implicated in premature senescence [105, 128, 129]. DDB2$^{-/-}$ mouse cells or DDB2-deficient human cells accumulate p21 at higher levels following DNA damage. The increase in accumulation of p21 prevents the DDB2-deficient cells from undergoing apoptosis after DNA damage. The lack of apoptosis following DNA damage and the increased accumulation of p21 prompted me to look at premature senescence. I observed that, compared to DDB2-

proficient cells, the DDB2-deficient cells are significantly impaired in undergoing premature senescence. Therefore, in the DDB2-deficient cells, the downstream effectors of p21 in senescence are disabled.

The DDB2$^{-/-}$ MEFs escape senescence at high frequencies, and they fail to maintain expression of p19Arf, especially at the late passages. The DDB2$^{-/-}$ MEFs also can be immortalized very easily. Expression of p19Arf in late passages or immortal DDB2$^{-/-}$ MEFs restored senescence, suggesting that lack of p19Arf expression is the main cause of the deficiency in senescence in those MEFs. However, at this point I do not know whether DDB2 plays any direct role in the expression of p19Arf. It was shown previously that senescence of MEFs, which depends on p19Arf, is a result of oxidative stress under the culture conditions [45, 130]. Consistent with that notion, I observed that the DDB2-deficient cells do not exhibit significant premature senescence when treated with hydrogen peroxide, an oxidative stress. The DDB2-deficient cells are impaired in premature senescence induced by oncogenic stress, which also involves oxidative stress [52, 131]. The DNA-damaging agents are also known to induce oxidative stress [132]. Therefore, oxidative stress appears to be the common denominator in the pathways to premature senescence. That is interesting because I found that DDB2 is required for ROS accumulation and for oxidative stress following treatments with DNA-damaging agents.

ROS are generated in cells by both enzymatic and nonenzymatic pathways. For example, the superoxide anion radical is generated by reduction of molecular

oxygen by NAD(P)H oxidase. It is generated also by leaking of electrons in the mitochondrial electron transport (complexes I and III) to oxygen [133]. Superoxide is dismutated by the superoxide dismutase to hydrogen peroxide, which in turn is scavenged by peroxidases, catalase, or other molecule scavengers. The activated Ras oncogene stimulates expression of NAD(P)H oxidase to increase the level of ROS in cells [134]. Apoptotic pathways can increase ROS production by disrupting the electron transport chain in mitochondrial membrane [135]. The ROS levels are attenuated by the scavengers, which are also carefully regulated in cells in order to maintain the optimum level of ROS required for cell proliferation [136]. Recently, it has been shown that in proliferating cells and in tumor cells, the transcription factor FoxM1 plays a significant role in attenuating the levels of ROS by stimulating expression of MnSOD, glutathione peroxidase, and catalase [86]. It is noteworthy that FoxM1 can be downregulated by p21, as they require phosphorylation by the cyclin-dependent kinases (CDKs) for their transcriptional activity [137, 138]. Consistently, it was shown that p21 could increase cellular levels of ROS, suggesting the possibility that ROS is the downstream mediator of p21 [102]. That would explain also why I do not see premature senescence in the presence of high-level p21 in the DDB2-deficient cells, because those cells do not accumulate ROS.

I found that in the DDB2-deficient cells MnSOD and catalase are expressed at a very high level. Expression of DDB2 repressed expression of those antioxidant genes. Coincidentally, a recent study indicated that DDB2 could constitutively repress expression of the MnSOD gene [93]. That study identified a sequence element in the

MnSOD promoter, which the authors claimed as a cognate element for DDB2. My observations are somewhat different in that I did not see binding of DDB2 with that region of the promoter of MnSOD in the HCT116 cells. Also, the catalase gene promoter, which apparently lacks that cognate element, could interact with DDB2. Given the difference, I think that DDB2 interacts with the MnSOD and catalase promoters through its interactions with other DNA binding proteins. Irrespective of the mechanism by which DDB2 interacts with the MnSOD or catalase promoter, the observations suggest that DDB2 is a dominant repressor of MnSOD and catalase expression. DDB2 associates with the Cul4A-DDB1 E3 ligase complex [14]. Interestingly, several studies implicated Cul4 also in methylation of histones in chromatin. In fission yeast Cul4 associates with the histone H3K9 methyltransferase Clr4 and Rik1 (a DDB1-like protein) to generate heterochromatin [94]. In mammalian cells, Cul4A has been shown to recruit H3K4 methyltransferase MLL1 onto the p16Ink4a promoter to stimulate expression during oncogenic stress [95]. I observed that DDB2 could recruit Cul4A and the Clr4 homolog Suv39h onto the promoters of the MnSOD and the catalase genes. Moreover, I observed increased H3K9 trimethylation in those promoter regions. The increase in association with Suv39h and H3K9 trimethylation in the presence of DDB2 suggests that DDB2 represses expression of MnSOD and catalase by altering chromatin conformation.

I observed that in the wild-type MEFs expression of DDB2 coincides with initiation of the senescence program. DDB2 in mouse cells is not induced by p53 [32]. It was suggested that the MEFs are sensitive to oxidative stress in the culture [45].

Figure 59: Schematic diagram depicting DDB2 mediated senescence induction. DDB2 amplifies ROS accumulation, ROS in turn increase DDB2 expression in positive feedback loop leading to premature senescence.

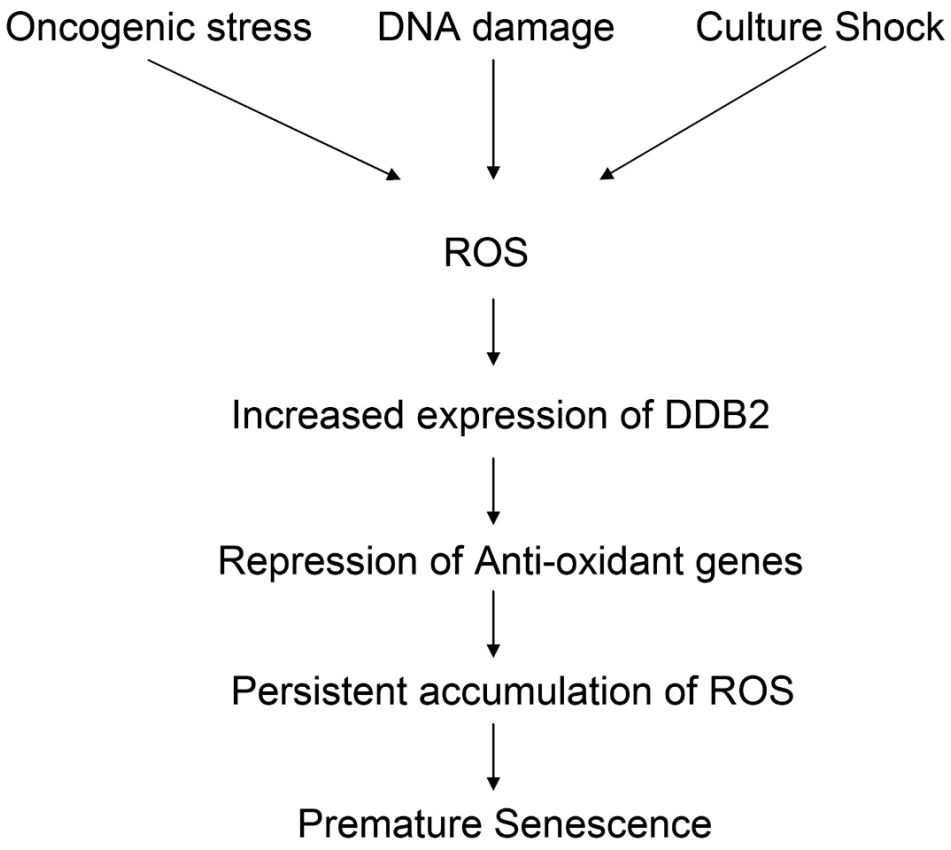
Oncogenic stress
DNA damage
Culture Shock
ROS
Increased expression of DDB2
Repression of Anti-oxidant genes
Persistent accumulation of ROS
Premature Senescence

Interestingly, I found that the DDB2 expression can be activated by ROS. Thus, it appears that DDB2, after being induced by ROS, causes repression of the ROS scavenger genes, such as MnSOD and catalase genes, to cause a persistent accumulation of ROS. A persistent accumulation of ROS could be the major reason for the induction of premature senescence. In the absence of DDB2, the antioxidant ROS scavenger genes are derepressed, causing high-level constitutive expression, which precludes persistent accumulation of ROS and thus prevents premature senescence (Fig.59).

DNA damage-induced premature senescence is a significant tumor suppression mechanism that would prevent UV-induced skin carcinogenesis. The DDB2$^{-/-}$ mice are susceptible to UV-induced skin carcinogenesis. Previous studies indicated that, in addition to NER, DDB2 is important for DNA damage-induced apoptosis, which is also an important tumor suppression mechanism. My study demonstrated premature senescence as an additional mechanism of tumor suppression supported by DDB2. I think that DDB2's role in the repression of MnSOD and catalase is distinct from its role in nucleotide excision repair (NER), which is linked to the phenotype of xeroderma pigmentosum (XP). The NER deficiency in the DDB2$^{-/-}$ MEFs is related to its ability to regulate the levels of p21, and that deficiency could be reversed by deletion of p21. However, deletion of p21 did not restore premature senescence in DDB2$^{-/-}$ MEFs. It is likely that DDB2 has evolved to participate in transcriptional repression of the antioxidant genes to ensure that cells harboring DNA damage do not replicate.

Although it is generally believed that DNA repair and apoptosis are important for preventing development of cancer cells, my results suggest a critical role of premature senescence in inhibiting UV-induced skin cancer. I show that premature senescence is more important than NER and apoptosis in inhibiting UV-induced skin cancer. In addition, I show that the p53-induced genes p21 and DDB2 play significant roles in that process. p21 and DDB2 cause accumulation of ROS to a high level following UV irradiation, leading to senescence.

UV skin carcinogenesis protocol involves irradiation of mice with high doses of UV-B, leading to extensive DNA damage that overwhelms the repair machinery. In the DDB2-/- background the repair capacity becomes further limiting because of high levels of p21. The high level of p21 also inhibits apoptosis of the cells harboring irreparable DNA damages. Deletion of p21 restored repair and apoptosis but did not restore premature senescence in DDB2-/- mice. However, there was a stronger inhibition of premature senescence in the DDB2-/- p21-/- mice compared with the single knock-outs. In addition, there was a huge increase in proliferation in the skin of the UV-irradiated DDB2-/- p21-/- mice. It is likely that the increased proliferation and the lack of premature senescence of the UV-irradiated cells are responsible for acceleration of the tumor development in the DDB2-/- p21-/- mice. My findings are consistent with a study demonstrating that p21 anti-proliferative function is indispensable for inhibition of tumorigenesis in the liver. It was observed that induction of p21 in Fah-/- mice, a mouse model of hereditary tyrosinemia type I, a human disorder characterized by accumulation of toxic metabolites that causes

chronic DNA damage leading to hepatocellular carcinoma. Fah-/- hepatocytes also exhibit cell cycle arrest and deficiency in apoptosis [139]. Apoptosis resistance in Fah-/- mice was found to be due to accumulation of p21, because its depletion restored apoptosis. Despite efficient apoptosis, deletion of p21 in Fah-/- background resulted in rapid proliferation and cancer formation.

p21 inhibits cell proliferation and supports premature senescence through its ability to inhibit the CYCLIN-CDK kinases [140]. The CYCLIN-CDK inhibitory function supports premature senescence by activation of the cell cycle inhibitory pathways of the retinoblastoma protein. The DDB2-/- p21-/- cells possess higher CYCLIN-CDK kinase activity, which is therefore expected to contribute to the lack of senescence in the double knock-out cells through inhibition of the retinoblastoma protein [16]. Interestingly, consistent with a previous report, I observed a role of p21 in the ROS accumulation [102], a mechanism that contributes to senescence [48]. In UV-irradiated skin, both DDB2-/- and p21-/- mice accumulated much lower levels of ROS compared with that in the wild type mice. The levels of ROS in the double knock-outs were significantly lower than the levels observed in the single knock-outs, suggesting that p21 and DDB2 regulate ROS through distinct mechanisms. Consistent with that, there was a higher expression of catalase in the double knock-out skin samples compared with that in the single knock-outs. However, in the skin samples, MnSOD expression was not increased significantly in the absence of DDB2. It is likely that other mechanisms overcome the DDB2-mediated repression of MnSOD in skin. The increase was observed also in the p21-/-

background, suggesting that p21 also represses Catalase expression. Interestingly, p21 was shown to repress expression of FoxM1, a proliferation-associated transcription factor, is also an activator of Catalase [86, 106]. Interestingly, FoxM1 activates its own expression [141]. But the activity of FoxM1 requires phosphorylation by CYCLIN-CDK [142]. Therefore, it is possible that p21 inhibits FoxM1 expression by inhibiting its activation by the CYCLIN-CDK kinases. A reduced FoxM1 activity will reduce its own expression. Consistent with that, I observed a significantly higher expression of FoxM1 in the p21-/- background. High level of FOXM1 is known to inhibit premature senescence by attenuating oxidative stress or ROS [86]. FoxM1 reduces oxidative stress by stimulating expression of several antioxidant genes, including Catalase.

The deficiency in premature senescence is expected to increase the proliferation, and therefore it could explain the high level proliferation in the DDB2-/- p21-/- background. The lack of p21 will increase CYCLIN-CDK activities, contributing to a higher rate of proliferation. In addition, the increased expression of FoxM1, a pro-proliferation transcription factor, is expected to contribute to proliferation significantly because it stimulates expression of SKP2 and CKS1 to promote G_1/S progression and stimulates a number of mitotic genes to promote G_2/M transition [107]. Therefore, the high expression of FoxM1 in the DDB2-/- p21-/- background is expected to promote proliferation through activation of the cell cycle genes. FoxM1 is a target of the DNA damage checkpoint effectors, and its reduced expression has been implicated in the G_2/M delay following exposure to DNA-damaging agents

Figure 60: Model depicting role of p21 and DDB2 in inhibiting UV induced skin carcinogenesis.
p21 and DDB2 co-operates with each other to inhibit UV induced skin carcinoma formation by accumulation of catalase and increased ROS level.

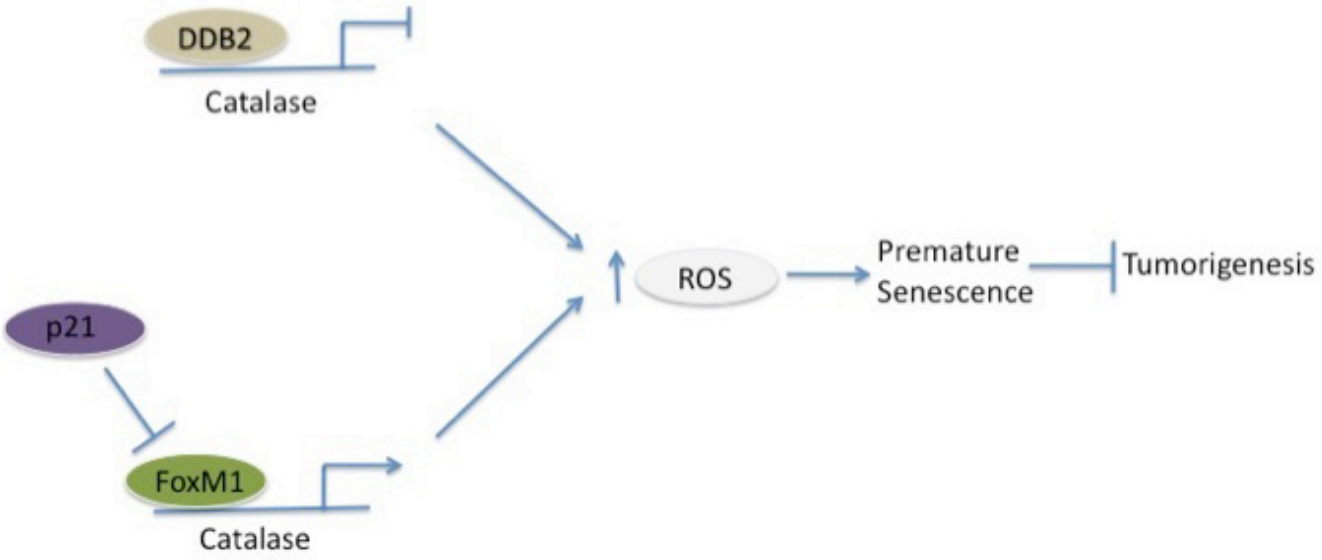
DDB2
Catalase
p21
FoxM1
Catalase
ROS
Premature
Senescence
Tumorigenesis

[143]. High expression of FoxM1 in p21-/- background is expected to overcome the checkpoints in cells harboring irreparable DNA damage and therefore is expected to support accumulation of mutant cells. The DDB2-/- cells to do not arrest after DNA damage. Therefore, the DDB2-/- p21-/- cells are expected to generate mutant cells at much higher rates, which is likely the basis for the acceleration of skin cancer development (Fig.60).

I further show that ROS can activate DDB2 expression in a p53 independent manner. Along the same line, PEITC also increases DDB2 expression independently of p53. PEITC induces apoptosis and senescence of colon carcinoma cells in vitro and in vivo. Moreover, the effectiveness of the PEITC-induced apoptosis and senescence depends upon DDB2. DDB2 is a p53-induced gene in human. Because p53 is mutated in over 50% of cancers, it is likely that the loss of p53 function would cause a deficiency in the expression of DDB2 [144, 145]. p53 is a major player in the induction of apoptosis and senescence. Hence, loss of p53 function renders the carcinoma cells refractory to apoptosis, senescence and cell cycle arrest following chemotherapy. Therefore, there is an urgent need to find out chemotherapeutic targets which acts in a p53 independent way. DDB2 seems to fit that function. I provide evidence that ROS mediated induction of DDB2 is not mediated by p53; rather it depends on the stress activated protein kinase pathways. Moreover, PEITC also augments DDB2 expression independent of p53 function. Use of PEITC, exploiting the fact the ROS induces DDB2 expression, is an attractive choice.

I provided evidence that the PEITC-induced expression of DDB2 enhances apoptosis and senescence response that lead to tumor regression by PEITC. Patients with loss of p53 function exhibit compromised apoptosis and senescence response following chemotherapy [146-148]. These patients can be potentially treated by PEITC to induce DDB2 expression. There is evidence for a crosstalk between DDB2 and p53. p53 stimulates DDB2 expression both at the basal level as well as following DNA damage. On the other hand, it was reported that in XP-E cells with mutated DDB2 there was deficiency in UV induced apoptosis due to reduced basal and UV induced p53 level [33]. Moreover, apoptosis function in DDB2 deficient XP-E cells were restored with expression of p53 cDNA construct indicating that DDB2 can participate in DNA damage induced apoptosis through p53 regulation. However, DDB2 participates in apoptosis also by down-regulation of p21, a cyclin dependent kinase inhibitor [16]. p21 exhibits anti-apoptotic activity, as the activity of caspases requires cdk activity. Here, I show that ROS and PEITC both can activate DDB2 expression independent of p53, and that these mechanisms would be significant in therapy of tumors harboring mutation in p53.

I provide evidence that ROS induced DDB2 expression involves up-regulated MAPK/JNK activity. Interestingly, a previous report suggested that p38MAPK mediated degradation of DDB2 following UV irradiation [34]. In contrast, I find ROS induce DDB2 expression through activated p38MAPK. This apparent discrepancy possibly results from the choice of treatment and the cell fate associated with it. Cells preferably attempt to repair the DNA damage following UV irradiation. p38

Figure 61: Schematic diagram showing role of DDB2 in PEITC mediated tumor regression.

PEITC mediates apoptosis and senescence response to inhibit tumor growth by augmenting DDB2 expression.

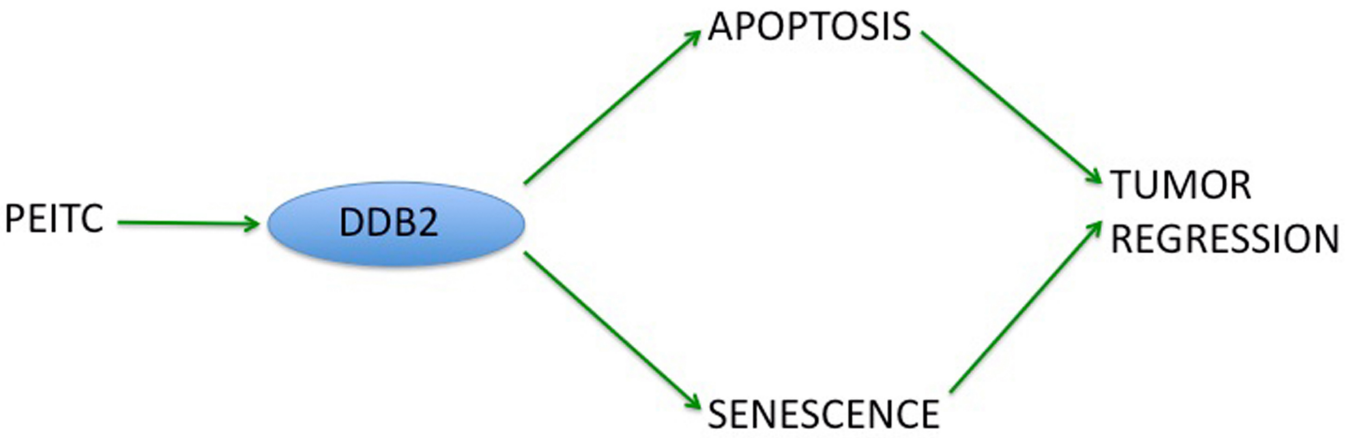
APOPTOSIS
PEITC
DDB2
TUMOR
REGRESSION
SENESCENCE

MAPK is an important player in UV induced DNA damage response. p38MAPK has been reported to facilitate nucleotide excision repair following UV irradiation through its phosphorylation of Histone H3 at serine 10 and subsequent alteration of chromatin condensation [149, 150]. Similarly, p38MAPK mediated phosphorylation of DDB2 leads to its degradation that in turn facilitate in the recruitment of XPC in the DNA damage lesions and initiate DNA repair. The oxidative stress treatment I employed mostly leads to apoptosis or senescence induction. In that scenario, DDB2 up-regulation is important to facilitate these tumor suppressor pathways. Thus, it appears that depending upon the context, p38MAPK either inhibits or augments DDB2 expression. Therefore, my data indicates potential usability of DDB2 expression as a chemotherapeutic target. As a proof of principle, I have provided evidence of PEITC induced expression of DDB2 is critical for induction of apoptosis and senescence in tumors, as well as for PEITC-mediated regression of tumors (Fig.61).

My work further demonstrate role of DDB2 in the regulation of colon cancer metastasis. I show that it is a potent regulator of EMT, as it transcriptionally inhibits expression of the key genes required for EMT and tumor invasion. Moreover, I show that DDB2 stands as a barrier downstream of the signaling pathways that induce EMT. DNA repair proteins have been previously been implicated in colon cancer. For example, about 15% of all colorectal cancers (CRC) exhibit microsatellite instability, a marker for impaired mismatch repair function. Germline mutations in the mismatch repair (MMR) genes MLH1, MSH2, MSH6 and

PMS2 have been detected in CRC [117]. In addition to mutations, epigenetic silencing occurs to the MLH1 gene. Mutations in the nucleotide repair genes are rare in CRC. However, in a study with small groups of CRC patients, it was shown that 25% (2/8) exhibited LOH at the XPE loci, 11q12-13 [151]. My analyses of the publicly available database indicated a reduced expression of DDB2 in a much greater population of the CRC patients. Moreover, the reduction of DDB2 expression coincides with the appearance of high-grade colon cancers. Therefore, progression of colon cancer associates with the activation of mechanisms that reduce DDB2 expression. It is noteworthy that DDB2 is a p53-induced gene, and p53 mutations are common in colon cancer, and that might explain the loss of expression [152]. However, other possibilities exist. For example, the DDB2 promoter region contains CpG islands [38]. Epigenetic mechanisms that regulate CpG islands are often deregulated in colon cancer [153]. The loss of DDB2 expression is expected also to reduce the repair (NER) activity, which is likely to contribute to the evolution of the high-grade colon cancer. However, my results indicate that a transcriptional repressor function of DDB2 is the predominant mechanism by which DDB2 inhibits EMT and metastasis of the colon cancers. The roles of DDB2 in the accumulation of ROS and inhibition of EMT are unexpected because it was shown that, in mammary epithelial cells, MMP3 could induce EMT through an increase in ROS that leads to increased Snail1 expression [77]. However, I observed that the loss of DDB2 expression caused a huge increase in the expression of Snail1 and Zeb1, both of which are pro-EMT. These observations suggest that DDB2 directly represses expression of these EMT genes, and that the

Figure 62: Schematic diagram indicating the mechanism by which DDB2 inhibits EMT.

EMT inducing signals (hypoxia or TGF-b) increases expression of VEGF, Snail1 and Zeb1 to reduce expression of E-cadherin and bring about EMT-like changes in colon cancer cells. The XPE gene product DDB2, on the other hand, binds to the promoters of VEGF, Snail1 and Zeb1 to inhibit their expression, and thus, supports MET.

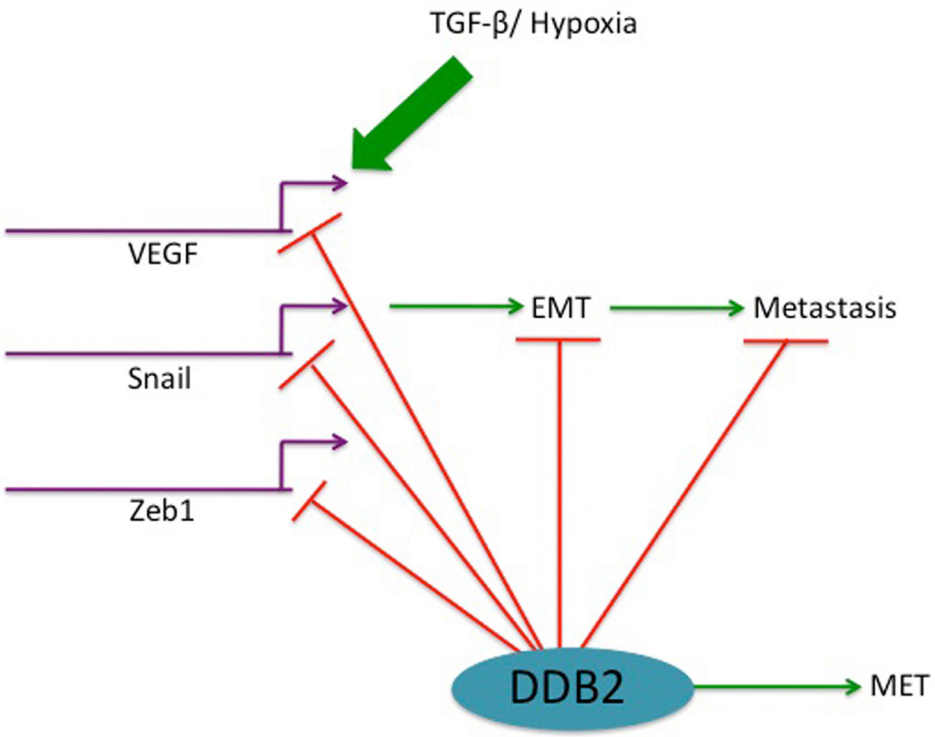
TGF-β/ Hypoxia
VEGF
Snail
Zeb1
EMT
Metastasis
DDB2
MET

mechanism is independent of its role in ROS accumulation. It is also consistent with a much greater increase in Snail1 expression through de-repression in the DDB2 knockdown cells, as compared to a relatively smaller increase observed with increased ROS by MMP3 expression. Since several microRNAs have been shown to regulate EMT by inhibiting the levels of Zeb1 and Zeb2 [154], it is a possibility that DDB2 regulates EMT through expression of the regulatory microRNAs. However, increased mRNA expression of Snail and Zeb1 in DDB2-depleted cells along with interactions of DDB2 with the Zeb1 and Snail promoters will be consistent with a direct repression of these genes by DDB2. Also, I show that DDB2 binds to the promoter of VEGF-A, a factor that is important in EMT and tumor invasion. Because VEGF-A can stimulate expression of Zeb1 and Snail1, it is unclear whether or not part of the increase in Zeb1 and Snail in the DDB2-deficient colon cancer cells resulted also from an increased VEGF-A expression [119, 155].

In addition to increased VEGF-A expression, I observed evidence for increased activation of the Akt-pathway. Thus, in the absence of DDB2, multiple pathways that induce EMT are activated. These pathways activate EMT by inducing Snail1 and Zeb1 that are repressors of E-cadherin expression. Interestingly, over-expression of DDB2 in the epithelial type colon cancer line SW480 blocked EMT as judged by a loss of the E-cadherin expression. These observations are consistent with the notion that DDB2 is a major player in suppressing EMT of the colon cancer cells.

The decrease in expression of DDB2 was observed also in colon cancer cell line SW620 compared to SW480. These two lines are derived from one patient at an early point in the tumor progression, SW480, and at a later metastatic stage of progression, SW620 [114]. Consistent with a role of DDB2 in inhibition of EMT, the mesenchymal-like SW620 cells expressed much lower level of DDB2. Moreover, re-expression of DDB2 in the SW620 cells induced expression of the epithelial markers and inhibition of the mesenchymal morphology. These observations also indicate that DDB2 is one of the major regulators in epithelial tumor cells that resist conversion to a mesenchymal-like morphology, and that induction of EMT occurs mainly after a loss of DDB2 expression. Consistent with that we show depletion of DDB2 induces EMT of the colon cancer cells that is associated with increased invasiveness and accelerated growth of tumors in xenografts. Moreover, a reduced expression of DDB2 enhances metastasis of colon cancer cells in both experimental metastasis assays and in an orthotopic xenograft model. Moreover, re-expression of DDB2 inhibits metastasis. These results explain why loss of DDB2 expression coincides with the high-grade progression of colon cancers. These results, for the first time, demonstrate an important tumor suppression function of the xeroderma pigmentosum gene DDB2 in colon cancer metastasis (Fig.62).

EMT, a pro-tumorigenic pathway and senescence, an anti-tumorigenic pathway, have several common factors playing dominant roles. For example, transcription factor Twist has been shown as a critical factor to induce EMT [66]. However, Twist has also been shown to inhibit expression of Arf, a gene that is highly induced

during senescence [156]. Furthermore, Twist has also been reported to affect transcriptional regulation on p16INK4a and p21, two other mediators of cell cycle arrest and senescence [110]. These lines of evidence clearly demonstrate that Twist can simultaneously deregulate p53 and Rb pathway, both of which have been heavily implicated in the senescence process. The presumption that activation of EMT is related to suppression of cellular senescence has been proposed also in the context of another EMT regulator, Zeb1 [67]. Zeb1 induces EMT by down-regulation of E-cadherin expression. On the other hand, Zeb1 inhibits senescence by regulating gene expression of CDKN1A and INK4B locus [157]. However, there is evidence of EMT regulators, which can induce cell cycle arrest as well. For example, Snail induces cell cycle arrest by induction of p21 in MDCK epithelial cells [158]. Snail has been shown to induce cell cycle arrest also by up-regulation of p15INK4B in HEPG2 cells [159]. Another EMT regulator, Zeb2 has also been shown to reduce proliferation of cells by attenuating expression of CyclinD1 [160].

Conversely, a number of key senescence effector molecules have been implicated in EMT. Retinoblastoma protein Rb, a critical regulator of cellular senescence has been linked to EMT. For example, viral oncoprotein SV40 large T antigen suppress E-cadherin expression and induce EMT, which is dependent on Rb inactivation [161]. Also, in MCF10A cells, EMT induced by TGF-β/ TNF-α is related to attenuated expression of Rb [111]. Furthermore, Rb has been shown to bind the CDH1 promoter, thereby suppressing its transcription [162, 163]. p53, a critical senescence effector molecule has been suggested to inhibit EMT by attenuating

expression of transcription factor Slug [164]. p21, another factor associated with cellular senescence has been shown to attenuate Ras and c-myc dependent EMT in vivo [112].

These observations clearly suggest that common effector molecules link EMT and senescence, two important processes involved in cancer progression. This can be particularly interesting from a therapeutic perspective. Attenuated senescence response gives the carcinoma cells the liberty to proliferate indefinitely. Towards their clonal expansion, EMT induction will allow them to metastasize to a distant organ. Hence, targeting the common factors playing role in either of these processes might be particularly beneficial. This will result a double impact on carcinoma progression by induction of senescence and attenuation of metastasis related to EMT. Towards that, my results on DDB2 are interesting. DDB2 induces senescence, an anti-tumorigenic pathway and inhibits EMT, a pro-tumorigenic pathway. Therefore, activation or re-expression of DDB2 has dual benefit: DDB2 will induce senescence to impede tumorigenesis and inhibit EMT to prevent metastatic dissemination of the tumor from the primary site. In conclusion, the discoveries on DDB2's transcriptional function have revealed several interesting possibilities that can be explored in designing novel therapeutics for the treatment of cancer (Fig.63 and Fig.64).

One important question that still needs to be addressed is whether DDB2 mediated inhibition of EMT and induction of senescence only involves its transcriptional repressor function. I found increased expression of several other proteins related to

EMT and senescence in the absence of DDB2. For example, there is up-regulation of Akt and ERK activity in the absence of DDB2.Therefore, it is important to investigate whether DDB2 regulates the expression of these proteins. If it does so, then, the relative contribution of that regulation to the functions of DDB2 needs to be tested. Also, DDB2 mediated transcriptional regulation can be achieved by other means. DDB2 has been found to be in a complex with STAGA, a chromatin acetylating transcriptional co-activator. DDB2 also acts as a co-factor for E2F1 transcription factor. Therefore, investigation of other possible modes of transcriptional regulation by DDB2 might divulge important facts regarding DDB2's role in transcription.

Figure 63: Schematic diagram depicting role of DDB2 as a tumor suppressor.
DDB2 acts as a tumor suppressor by regulation of nucleotide excision repair, apoptosis and senescence.

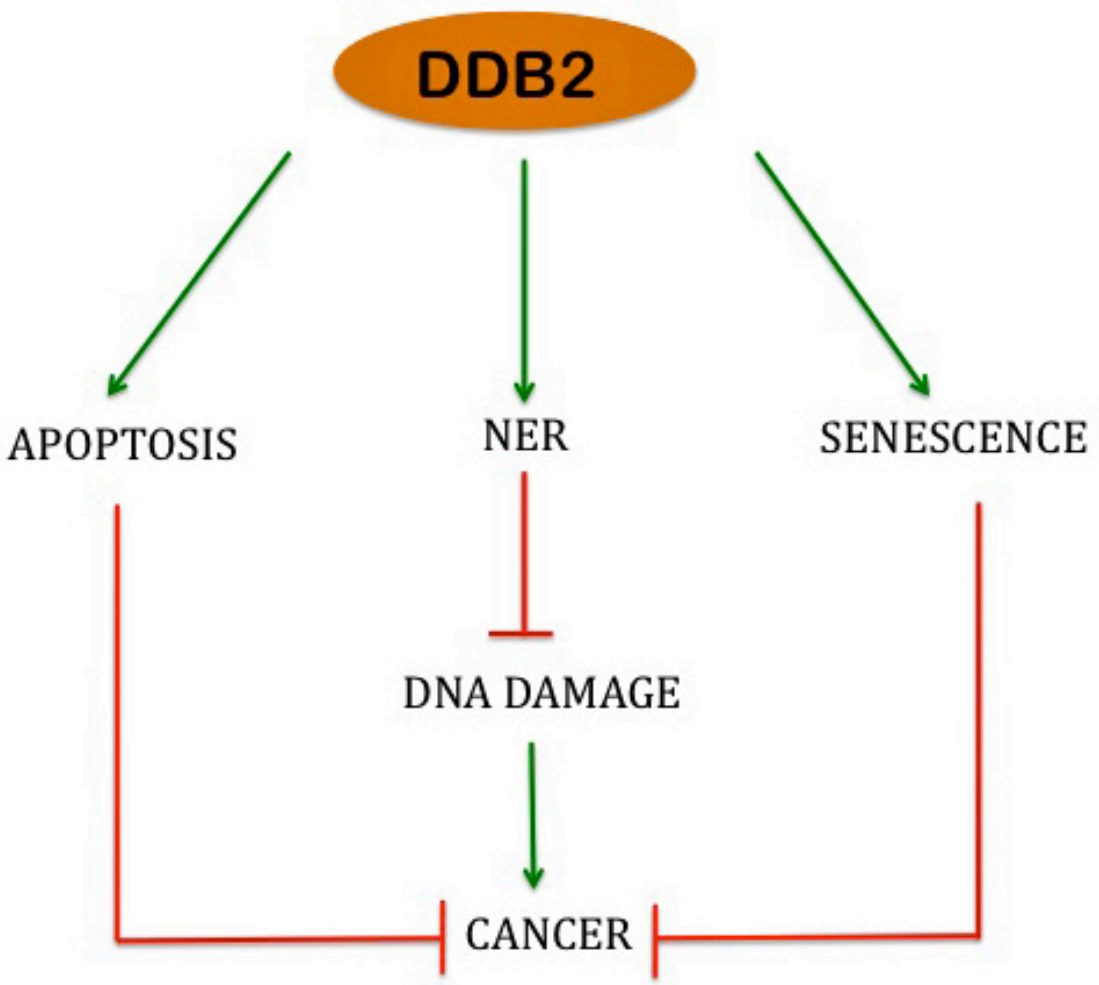
DDB2
APOPTOSIS
NER
SENESCENCE
DNA DAMAGE
CANCER

Figure 64: Schematic diagram depicting how DDB2 can be targeted therapeutically for the treatment of cancer and aging.
DDB2 expression is lost during carcinoma progression. DDB2 up-regulation can be therapeutically achieved to induce senescence and apoptosis response to inhibit tumorigenesis. In contrast, DDB2 expression is augmented with aging. Hence, attenuation of DDB2 expression might prove to be beneficial to inhibit aging and age related disorders.

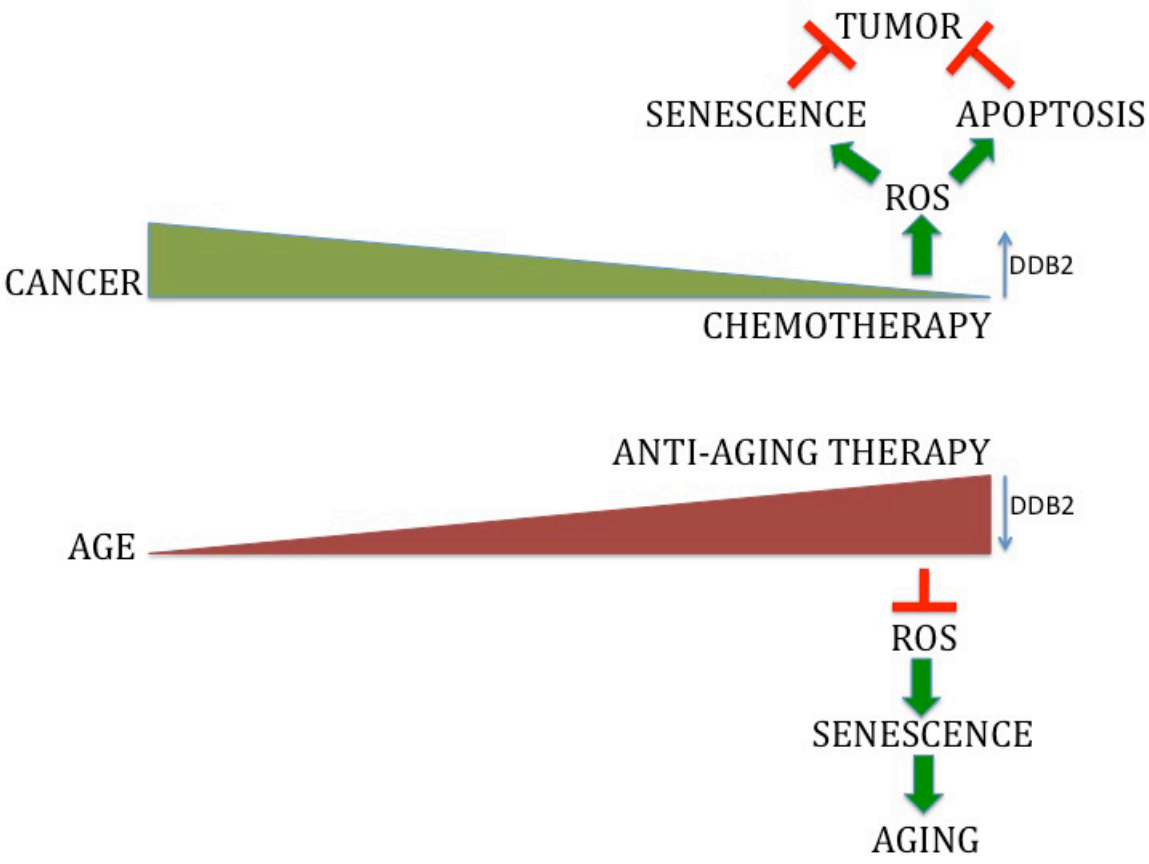
TUMOR
SENESCENCE
APOPTOSIS
ROS
DDB2
CANCER
CHEMOTHERAPY
ANTI-AGING THERAPY
DDB2
AGE
ROS
SENESCENCE
AGING

CITED LITERATURE

1. Tang, J.; Chu, G., Xeroderma pigmentosum complementation group E and UV-damaged DNA-binding protein. *DNA Repair (Amst)* **2002,** 1, (8), 601-16.

2. Sancar, A.; Lindsey-Boltz, L. A.; Unsal-Kacmaz, K.; Linn, S., Molecular mechanisms of mammalian DNA repair and the DNA damage checkpoints. *Annu Rev Biochem* **2004,** 73, 39-85.

3. Cleaver, J. E., Cancer in xeroderma pigmentosum and related disorders of DNA repair. *Nat Rev Cancer* **2005,** 5, (7), 564-73.

4. Friedberg, E. C., How nucleotide excision repair protects against cancer. *Nat Rev Cancer* **2001,** 1, (1), 22-33.

5. Masutani, C.; Kusumoto, R.; Yamada, A.; Dohmae, N.; Yokoi, M.; Yuasa, M.; Araki, M.; Iwai, S.; Takio, K.; Hanaoka, F., The XPV (xeroderma pigmentosum variant) gene encodes human DNA polymerase eta. *Nature* **1999,** 399, (6737), 700-4.

6. Tang, J. Y.; Hwang, B. J.; Ford, J. M.; Hanawalt, P. C.; Chu, G., Xeroderma pigmentosum p48 gene enhances global genomic repair and suppresses UV-induced mutagenesis. *Mol Cell* **2000,** 5, (4), 737-44.

7. Hwang, B. J.; Toering, S.; Francke, U.; Chu, G., p48 Activates a UV-damaged-DNA binding factor and is defective in xeroderma pigmentosum group E cells that lack binding activity. *Mol Cell Biol* **1998,** 18, (7), 4391-9.

8. Keeney, S.; Eker, A. P.; Brody, T.; Vermeulen, W.; Bootsma, D.; Hoeijmakers, J. H.; Linn, S., Correction of the DNA repair defect in xeroderma pigmentosum group E by injection of a DNA damage-binding protein. *Proc Natl Acad Sci U S A* **1994,** 91, (9), 4053-6.

9. Itoh, T.; Cado, D.; Kamide, R.; Linn, S., DDB2 gene disruption leads to skin tumors and resistance to apoptosis after exposure to ultraviolet light but not a chemical carcinogen. *Proc Natl Acad Sci U S A* **2004,** 101, (7), 2052-7.

10. Yoon, T.; Chakrabortty, A.; Franks, R.; Valli, T.; Kiyokawa, H.; Raychaudhuri, P., Tumor-prone phenotype of the DDB2-deficient mice. *Oncogene* **2005,** 24, (3), 469-78.

11. Alekseev, S.; Kool, H.; Rebel, H.; Fousteri, M.; Moser, J.; Backendorf, C.; de Gruijl, F. R.; Vrieling, H.; Mullenders, L. H., Enhanced DDB2 expression

protects mice from carcinogenic effects of chronic UV-B irradiation. *Cancer Res* **2005,** 65, (22), 10298-306.

12. Itoh, T.; Iwashita, S.; Cohen, M. B.; Meyerholz, D. K.; Linn, S., Ddb2 is a haploinsufficient tumor suppressor and controls spontaneous germ cell apoptosis. *Hum Mol Genet* **2007,** 16, (13), 1578-86.

13. Lee, J.; Zhou, P., DCAFs, the missing link of the CUL4-DDB1 ubiquitin ligase. *Mol Cell* **2007,** 26, (6), 775-80.

14. Shiyanov, P.; Nag, A.; Raychaudhuri, P., Cullin 4A associates with the UV-damaged DNA-binding protein DDB. *J Biol Chem* **1999,** 274, (50), 35309-12.

15. Nag, A.; Bondar, T.; Shiv, S.; Raychaudhuri, P., The xeroderma pigmentosum group E gene product DDB2 is a specific target of cullin 4A in mammalian cells. *Mol Cell Biol* **2001,** 21, (20), 6738-47.

16. Stoyanova, T.; Roy, N.; Kopanja, D.; Bagchi, S.; Raychaudhuri, P., DDB2 decides cell fate following DNA damage. *Proc Natl Acad Sci U S A* **2009,** 106, (26), 10690-5.

17. Sugasawa, K.; Okuda, Y.; Saijo, M.; Nishi, R.; Matsuda, N.; Chu, G.; Mori, T.; Iwai, S.; Tanaka, K.; Hanaoka, F., UV-induced ubiquitylation of XPC protein mediated by UV-DDB-ubiquitin ligase complex. *Cell* **2005,** 121, (3), 387-400.

18. Nag, A.; Datta, A.; Yoo, K.; Bhattacharyya, D.; Chakrabortty, A.; Wang, X.; Slagle, B. L.; Costa, R. H.; Raychaudhuri, P., DDB2 induces nuclear accumulation of the hepatitis B virus X protein independently of binding to DDB1. *J Virol* **2001,** 75, (21), 10383-92.

19. Shiyanov, P.; Hayes, S. A.; Donepudi, M.; Nichols, A. F.; Linn, S.; Slagle, B. L.; Raychaudhuri, P., The naturally occurring mutants of DDB are impaired in stimulating nuclear import of the p125 subunit and E2F1-activated transcription. *Mol Cell Biol* **1999,** 19, (7), 4935-43.

20. Liu, W.; Nichols, A. F.; Graham, J. A.; Dualan, R.; Abbas, A.; Linn, S., Nuclear transport of human DDB protein induced by ultraviolet light. *J Biol Chem* **2000,** 275, (28), 21429-34.

21. Kapetanaki, M. G.; Guerrero-Santoro, J.; Bisi, D. C.; Hsieh, C. L.; Rapic-Otrin, V.; Levine, A. S., The DDB1-CUL4ADDB2 ubiquitin ligase is deficient in xeroderma pigmentosum group E and targets histone H2A at UV-damaged DNA sites. *Proc Natl Acad Sci U S A* **2006,** 103, (8), 2588-93.

22. Wang, H.; Zhai, L.; Xu, J.; Joo, H. Y.; Jackson, S.; Erdjument-Bromage, H.; Tempst, P.; Xiong, Y.; Zhang, Y., Histone H3 and H4 ubiquitylation by the

CUL4-DDB-ROC1 ubiquitin ligase facilitates cellular response to DNA damage. *Mol Cell* **2006,** 22, (3), 383-94.

23. Datta, A.; Bagchi, S.; Nag, A.; Shiyanov, P.; Adami, G. R.; Yoon, T.; Raychaudhuri, P., The p48 subunit of the damaged-DNA binding protein DDB associates with the CBP/p300 family of histone acetyltransferase. *Mutat Res* **2001,** 486, (2), 89-97.

24. Martinez, E.; Palhan, V. B.; Tjernberg, A.; Lymar, E. S.; Gamper, A. M.; Kundu, T. K.; Chait, B. T.; Roeder, R. G., Human STAGA complex is a chromatin-acetylating transcription coactivator that interacts with pre-mRNA splicing and DNA damage-binding factors in vivo. *Mol Cell Biol* **2001,** 21, (20), 6782-95.

25. Luijsterburg, M. S.; Lindh, M.; Acs, K.; Vrouwe, M. G.; Pines, A.; van Attikum, H.; Mullenders, L. H.; Dantuma, N. P., DDB2 promotes chromatin decondensation at UV-induced DNA damage. *J Cell Biol* **2012**.

26. Abraham, R. T., Cell cycle checkpoint signaling through the ATM and ATR kinases. *Genes Dev* **2001,** 15, (17), 2177-96.

27. Zhou, B. B.; Elledge, S. J., The DNA damage response: putting checkpoints in perspective. *Nature* **2000,** 408, (6811), 433-9.

28. Chao, C.; Hergenhahn, M.; Kaeser, M. D.; Wu, Z.; Saito, S.; Iggo, R.; Hollstein, M.; Appella, E.; Xu, Y., Cell type- and promoter-specific roles of Ser18 phosphorylation in regulating p53 responses. *J Biol Chem* **2003,** 278, (42), 41028-33.

29. Stoyanova, T.; Yoon, T.; Kopanja, D.; Mokyr, M. B.; Raychaudhuri, P., The xeroderma pigmentosum group E gene product DDB2 activates nucleotide excision repair by regulating the level of p21Waf1/Cip1. *Mol Cell Biol* **2008,** 28, (1), 177-87.

30. el-Deiry, W. S.; Tokino, T.; Velculescu, V. E.; Levy, D. B.; Parsons, R.; Trent, J. M.; Lin, D.; Mercer, W. E.; Kinzler, K. W.; Vogelstein, B., WAF1, a potential mediator of p53 tumor suppression. *Cell* **1993,** 75, (4), 817-25.

31. Hwang, B. J.; Ford, J. M.; Hanawalt, P. C.; Chu, G., Expression of the p48 xeroderma pigmentosum gene is p53-dependent and is involved in global genomic repair. *Proc Natl Acad Sci U S A* **1999,** 96, (2), 424-8.

32. Tan, T.; Chu, G., p53 Binds and activates the xeroderma pigmentosum DDB2 gene in humans but not mice. *Mol Cell Biol* **2002,** 22, (10), 3247-54.

33. Itoh, T.; O'Shea, C.; Linn, S., Impaired regulation of tumor suppressor p53 caused by mutations in the xeroderma pigmentosum DDB2 gene: mutual regulatory interactions between p48(DDB2) and p53. *Mol Cell Biol* **2003,** 23, (21), 7540-53.

34. Zhao, Q.; Barakat, B. M.; Qin, S.; Ray, A.; El-Mahdy, M. A.; Wani, G.; Arafa el, S.; Mir, S. N.; Wang, Q. E.; Wani, A. A., The p38 mitogen-activated protein kinase augments nucleotide excision repair by mediating DDB2 degradation and chromatin relaxation. *J Biol Chem* **2008,** 283, (47), 32553-61.

35. Cong, F.; Tang, J.; Hwang, B. J.; Vuong, B. Q.; Chu, G.; Goff, S. P., Interaction between UV-damaged DNA binding activity proteins and the c-Abl tyrosine kinase. *J Biol Chem* **2002,** 277, (38), 34870-8.

36. Groisman, R.; Polanowska, J.; Kuraoka, I.; Sawada, J.; Saijo, M.; Drapkin, R.; Kisselev, A. F.; Tanaka, K.; Nakatani, Y., The ubiquitin ligase activity in the DDB2 and CSA complexes is differentially regulated by the COP9 signalosome in response to DNA damage. *Cell* **2003,** 113, (3), 357-67.

37. El-Mahdy, M. A.; Zhu, Q.; Wang, Q. E.; Wani, G.; Praetorius-Ibba, M.; Wani, A. A., Cullin 4A-mediated proteolysis of DDB2 protein at DNA damage sites regulates in vivo lesion recognition by XPC. *J Biol Chem* **2006,** 281, (19), 13404-11.

38. Nichols, A. F.; Itoh, T.; Zolezzi, F.; Hutsell, S.; Linn, S., Basal transcriptional regulation of human damage-specific DNA-binding protein genes DDB1 and DDB2 by Sp1, E2F, N-myc and NF1 elements. *Nucleic Acids Res* **2003,** 31, (2), 562-9.

39. Stoyanova, T.; Roy, N.; Kopanja, D.; Raychaudhuri, P.; Bagchi, S., DDB2 (damaged-DNA binding protein 2) in nucleotide excision repair and DNA damage response. *Cell Cycle* **2009,** 8, (24), 4067-71.

40. Gartel, A. L.; Tyner, A. L., The role of the cyclin-dependent kinase inhibitor p21 in apoptosis. *Mol Cancer Ther* **2002,** 1, (8), 639-49.

41. Barakat, B. M.; Wang, Q. E.; Han, C.; Milum, K.; Yin, D. T.; Zhao, Q.; Wani, G.; Arafa el, S. A.; El-Mahdy, M. A.; Wani, A. A., Overexpression of DDB2 enhances the sensitivity of human ovarian cancer cells to cisplatin by augmenting cellular apoptosis. *Int J Cancer* **2010,** 127, (4), 977-88.

42. Sun, N. K.; Sun, C. L.; Lin, C. H.; Pai, L. M.; Chao, C. C., Damaged DNA-binding protein 2 (DDB2) protects against UV irradiation in human cells and Drosophila. *J Biomed Sci* **2010,** 17, 27.

43. Campisi, J.; d'Adda di Fagagna, F., Cellular senescence: when bad things happen to good cells. *Nat Rev Mol Cell Biol* **2007,** 8, (9), 729-40.

44. Dimri, G. P.; Lee, X.; Basile, G.; Acosta, M.; Scott, G.; Roskelley, C.; Medrano, E. E.; Linskens, M.; Rubelj, I.; Pereira-Smith, O.; et al., A biomarker that identifies senescent human cells in culture and in aging skin in vivo. *Proc Natl Acad Sci U S A* **1995,** 92, (20), 9363-7.

45. Parrinello, S.; Samper, E.; Krtolica, A.; Goldstein, J.; Melov, S.; Campisi, J., Oxygen sensitivity severely limits the replicative lifespan of murine fibroblasts. *Nat Cell Biol* **2003,** 5, (8), 741-7.

46. von Zglinicki, T.; Saretzki, G.; Ladhoff, J.; d'Adda di Fagagna, F.; Jackson, S. P., Human cell senescence as a DNA damage response. *Mech Ageing Dev* **2005,** 126, (1), 111-7.

47. Kuilman, T.; Michaloglou, C.; Mooi, W. J.; Peeper, D. S., The essence of senescence. *Genes Dev* **2010,** 24, (22), 2463-79.

48. Chen, Q.; Fischer, A.; Reagan, J. D.; Yan, L. J.; Ames, B. N., Oxidative DNA damage and senescence of human diploid fibroblast cells. *Proc Natl Acad Sci U S A* **1995,** 92, (10), 4337-41.

49. Serrano, M.; Lin, A. W.; McCurrach, M. E.; Beach, D.; Lowe, S. W., Oncogenic ras provokes premature cell senescence associated with accumulation of p53 and p16INK4a. *Cell* **1997,** 88, (5), 593-602.

50. Kamijo, T.; Zindy, F.; Roussel, M. F.; Quelle, D. E.; Downing, J. R.; Ashmun, R. A.; Grosveld, G.; Sherr, C. J., Tumor suppression at the mouse INK4a locus mediated by the alternative reading frame product p19ARF. *Cell* **1997,** 91, (5), 649-59.

51. Ben-Porath, I.; Weinberg, R. A., The signals and pathways activating cellular senescence. *Int J Biochem Cell Biol* **2005,** 37, (5), 961-76.

52. Lee, A. C.; Fenster, B. E.; Ito, H.; Takeda, K.; Bae, N. S.; Hirai, T.; Yu, Z. X.; Ferrans, V. J.; Howard, B. H.; Finkel, T., Ras proteins induce senescence by altering the intracellular levels of reactive oxygen species. *J Biol Chem* **1999,** 274, (12), 7936-40.

53. Furumoto, K.; Inoue, E.; Nagao, N.; Hiyama, E.; Miwa, N., Age-dependent telomere shortening is slowed down by enrichment of intracellular vitamin C via suppression of oxidative stress. *Life Sci* **1998,** 63, (11), 935-48.

54. Iwasa, H.; Han, J.; Ishikawa, F., Mitogen-activated protein kinase p38 defines the common senescence-signalling pathway. *Genes Cells* **2003,** 8, (2), 131-44.

55. Itahana, K.; Zou, Y.; Itahana, Y.; Martinez, J. L.; Beausejour, C.; Jacobs, J. J.; Van Lohuizen, M.; Band, V.; Campisi, J.; Dimri, G. P., Control of the replicative life span of human fibroblasts by p16 and the polycomb protein Bmi-1. *Mol Cell Biol* **2003,** 23, (1), 389-401.

56. Sherr, C. J., The INK4a/ARF network in tumour suppression. *Nat Rev Mol Cell Biol* **2001,** 2, (10), 731-7.

57. Thiery, J. P.; Acloque, H.; Huang, R. Y.; Nieto, M. A., Epithelial-mesenchymal transitions in development and disease. *Cell* **2009,** 139, (5), 871-90.

58. Huber, M. A.; Kraut, N.; Beug, H., Molecular requirements for epithelial-mesenchymal transition during tumor progression. *Curr Opin Cell Biol* **2005,** 17, (5), 548-58.

59. Yang, J.; Weinberg, R. A., Epithelial-mesenchymal transition: at the crossroads of development and tumor metastasis. *Dev Cell* **2008,** 14, (6), 818-29.

60. Bolos, V.; Peinado, H.; Perez-Moreno, M. A.; Fraga, M. F.; Esteller, M.; Cano, A., The transcription factor Slug represses E-cadherin expression and induces epithelial to mesenchymal transitions: a comparison with Snail and E47 repressors. *J Cell Sci* **2003,** 116, (Pt 3), 499-511.

61. Cano, A.; Perez-Moreno, M. A.; Rodrigo, I.; Locascio, A.; Blanco, M. J.; del Barrio, M. G.; Portillo, F.; Nieto, M. A., The transcription factor snail controls epithelial-mesenchymal transitions by repressing E-cadherin expression. *Nat Cell Biol* **2000,** 2, (2), 76-83.

62. Comijn, J.; Berx, G.; Vermassen, P.; Verschueren, K.; van Grunsven, L.; Bruyneel, E.; Mareel, M.; Huylebroeck, D.; van Roy, F., The two-handed E box binding zinc finger protein SIP1 downregulates E-cadherin and induces invasion. *Mol Cell* **2001,** 7, (6), 1267-78.

63. Eger, A.; Aigner, K.; Sonderegger, S.; Dampier, B.; Oehler, S.; Schreiber, M.; Berx, G.; Cano, A.; Beug, H.; Foisner, R., DeltaEF1 is a transcriptional repressor of E-cadherin and regulates epithelial plasticity in breast cancer cells. *Oncogene* **2005,** 24, (14), 2375-85.

64. Peinado, H.; Olmeda, D.; Cano, A., Snail, Zeb and bHLH factors in tumour progression: an alliance against the epithelial phenotype? *Nat Rev Cancer* **2007,** 7, (6), 415-28.

65. Vandewalle, C.; Comijn, J.; De Craene, B.; Vermassen, P.; Bruyneel, E.; Andersen, H.; Tulchinsky, E.; Van Roy, F.; Berx, G., SIP1/ZEB2 induces EMT by

repressing genes of different epithelial cell-cell junctions. *Nucleic Acids Res* **2005,** 33, (20), 6566-78.

66. Yang, J.; Mani, S. A.; Donaher, J. L.; Ramaswamy, S.; Itzykson, R. A.; Come, C.; Savagner, P.; Gitelman, I.; Richardson, A.; Weinberg, R. A., Twist, a master regulator of morphogenesis, plays an essential role in tumor metastasis. *Cell* **2004,** 117, (7), 927-39.

67. Liu, Y.; El-Naggar, S.; Darling, D. S.; Higashi, Y.; Dean, D. C., Zeb1 links epithelial-mesenchymal transition and cellular senescence. *Development* **2008,** 135, (3), 579-88.

68. Postigo, A. A., Opposing functions of ZEB proteins in the regulation of the TGFbeta/BMP signaling pathway. *EMBO J* **2003,** 22, (10), 2443-52.

69. Postigo, A. A.; Depp, J. L.; Taylor, J. J.; Kroll, K. L., Regulation of Smad signaling through a differential recruitment of coactivators and corepressors by ZEB proteins. *EMBO J* **2003,** 22, (10), 2453-62.

70. Xu, J.; Lamouille, S.; Derynck, R., TGF-beta-induced epithelial to mesenchymal transition. *Cell Res* **2009,** 19, (2), 156-72.

71. Peinado, H.; Quintanilla, M.; Cano, A., Transforming growth factor beta-1 induces snail transcription factor in epithelial cell lines: mechanisms for epithelial mesenchymal transitions. *J Biol Chem* **2003,** 278, (23), 21113-23.

72. Yook, J. I.; Li, X. Y.; Ota, I.; Hu, C.; Kim, H. S.; Kim, N. H.; Cha, S. Y.; Ryu, J. K.; Choi, Y. J.; Kim, J.; Fearon, E. R.; Weiss, S. J., A Wnt-Axin2-GSK3beta cascade regulates Snail1 activity in breast cancer cells. *Nat Cell Biol* **2006,** 8, (12), 1398-406.

73. Forsythe, J. A.; Jiang, B. H.; Iyer, N. V.; Agani, F.; Leung, S. W.; Koos, R. D.; Semenza, G. L., Activation of vascular endothelial growth factor gene transcription by hypoxia-inducible factor 1. *Mol Cell Biol* **1996,** 16, (9), 4604-13.

74. Imai, T.; Horiuchi, A.; Wang, C.; Oka, K.; Ohira, S.; Nikaido, T.; Konishi, I., Hypoxia attenuates the expression of E-cadherin via up-regulation of SNAIL in ovarian carcinoma cells. *Am J Pathol* **2003,** 163, (4), 1437-47.

75. Mak, P.; Leav, I.; Pursell, B.; Bae, D.; Yang, X.; Taglienti, C. A.; Gouvin, L. M.; Sharma, V. M.; Mercurio, A. M., ERbeta impedes prostate cancer EMT by destabilizing HIF-1alpha and inhibiting VEGF-mediated snail nuclear localization: implications for Gleason grading. *Cancer Cell* **2010,** 17, (4), 319-32.

76. Yang, M. H.; Wu, M. Z.; Chiou, S. H.; Chen, P. M.; Chang, S. Y.; Liu, C. J.; Teng, S. C.; Wu, K. J., Direct regulation of TWIST by HIF-1alpha promotes metastasis. *Nat Cell Biol* **2008,** 10, (3), 295-305.

77. Radisky, D. C.; Levy, D. D.; Littlepage, L. E.; Liu, H.; Nelson, C. M.; Fata, J. E.; Leake, D.; Godden, E. L.; Albertson, D. G.; Nieto, M. A.; Werb, Z.; Bissell, M. J., Rac1b and reactive oxygen species mediate MMP-3-induced EMT and genomic instability. *Nature* **2005,** 436, (7047), 123-7.

78. Wright, J. A.; Richer, J. K.; Goodall, G. J., microRNAs and EMT in mammary cells and breast cancer. *J Mammary Gland Biol Neoplasia* **2010,** 15, (2), 213-23.

79. Zhang, H.; Li, Y.; Lai, M., The microRNA network and tumor metastasis. *Oncogene* **2010,** 29, (7), 937-48.

80. Chaveroux, C.; Jousse, C.; Cherasse, Y.; Maurin, A. C.; Parry, L.; Carraro, V.; Derijard, B.; Bruhat, A.; Fafournoux, P., Identification of a novel amino acid response pathway triggering ATF2 phosphorylation in mammals. *Mol Cell Biol* **2009,** 29, (24), 6515-26.

81. Krizhanovsky, V.; Yon, M.; Dickins, R. A.; Hearn, S.; Simon, J.; Miething, C.; Yee, H.; Zender, L.; Lowe, S. W., Senescence of activated stellate cells limits liver fibrosis. *Cell* **2008,** 134, (4), 657-67.

82. Franken, N. A.; Rodermond, H. M.; Stap, J.; Haveman, J.; van Bree, C., Clonogenic assay of cells in vitro. *Nat Protoc* **2006,** 1, (5), 2315-9.

83. Benhar, M.; Engelberg, D.; Levitzki, A., ROS, stress-activated kinases and stress signaling in cancer. *EMBO Rep* **2002,** 3, (5), 420-5.

84. Benkoussa, M.; Brand, C.; Delmotte, M. H.; Formstecher, P.; Lefebvre, P., Retinoic acid receptors inhibit AP1 activation by regulating extracellular signal-regulated kinase and CBP recruitment to an AP1-responsive promoter. *Mol Cell Biol* **2002,** 22, (13), 4522-34.

85. Zhou, X. F.; Shen, X. Q.; Shemshedini, L., Ligand-activated retinoic acid receptor inhibits AP-1 transactivation by disrupting c-Jun/c-Fos dimerization. *Mol Endocrinol* **1999,** 13, (2), 276-85.

86. Park, H. J.; Carr, J. R.; Wang, Z.; Nogueira, V.; Hay, N.; Tyner, A. L.; Lau, L. F.; Costa, R. H.; Raychaudhuri, P., FoxM1, a critical regulator of oxidative stress during oncogenesis. *EMBO J* **2009,** 28, (19), 2908-18.

87. Nogueira, V.; Park, Y.; Chen, C. C.; Xu, P. Z.; Chen, M. L.; Tonic, I.; Unterman, T.; Hay, N., Akt determines replicative senescence and oxidative or oncogenic

premature senescence and sensitizes cells to oxidative apoptosis. *Cancer Cell* **2008,** 14, (6), 458-70.

88. Chung, Y. M.; Lee, S. B.; Kim, H. J.; Park, S. H.; Kim, J. J.; Chung, J. S.; Yoo, Y. D., Replicative senescence induced by Romo1-derived reactive oxygen species. *J Biol Chem* **2008,** 283, (48), 33763-71.

89. Dolado, I.; Swat, A.; Ajenjo, N.; De Vita, G.; Cuadrado, A.; Nebreda, A. R., p38alpha MAP kinase as a sensor of reactive oxygen species in tumorigenesis. *Cancer Cell* **2007,** 11, (2), 191-205.

90. Talotta, F.; Cimmino, A.; Matarazzo, M. R.; Casalino, L.; De Vita, G.; D'Esposito, M.; Di Lauro, R.; Verde, P., An autoregulatory loop mediated by miR-21 and PDCD4 controls the AP-1 activity in RAS transformation. *Oncogene* **2009,** 28, (1), 73-84.

91. Chen, J. H.; Hales, C. N.; Ozanne, S. E., DNA damage, cellular senescence and organismal ageing: causal or correlative? *Nucleic Acids Res* **2007,** 35, (22), 7417-28.

92. Rowe, L. A.; Degtyareva, N.; Doetsch, P. W., DNA damage-induced reactive oxygen species (ROS) stress response in Saccharomyces cerevisiae. *Free Radic Biol Med* **2008,** 45, (8), 1167-77.

93. Minig, V.; Kattan, Z.; van Beeumen, J.; Brunner, E.; Becuwe, P., Identification of DDB2 protein as a transcriptional regulator of constitutive SOD2 gene expression in human breast cancer cells. *J Biol Chem* **2009,** 284, (21), 14165-76.

94. Jia, S.; Kobayashi, R.; Grewal, S. I., Ubiquitin ligase component Cul4 associates with Clr4 histone methyltransferase to assemble heterochromatin. *Nat Cell Biol* **2005,** 7, (10), 1007-13.

95. Kotake, Y.; Zeng, Y.; Xiong, Y., DDB1-CUL4 and MLL1 mediate oncogene-induced p16INK4a activation. *Cancer Res* **2009,** 69, (5), 1809-14.

96. Issa, R.; Williams, E.; Trim, N.; Kendall, T.; Arthur, M. J.; Reichen, J.; Benyon, R. C.; Iredale, J. P., Apoptosis of hepatic stellate cells: involvement in resolution of biliary fibrosis and regulation by soluble growth factors. *Gut* **2001,** 48, (4), 548-57.

97. Oh, K. S.; Emmert, S.; Tamura, D.; DiGiovanna, J. J.; Kraemer, K. H., Multiple skin cancers in adults with mutations in the XP-E (DDB2) DNA repair gene. *J Invest Dermatol* 131, (3), 785-8.

98. Bagchi, S.; Raychaudhuri, P., Damaged-DNA Binding Protein-2 Drives Apoptosis Following DNA Damage. *Cell Div* **2010,** 5, 3.

99. Kim, M. Y.; Park, H. J.; Baek, S. C.; Byun, D. G.; Houh, D., Mutations of the p53 and PTCH gene in basal cell carcinomas: UV mutation signature and strand bias. *J Dermatol Sci* **2002,** 29, (1), 1-9.

100. Shea, C. R.; McNutt, N. S.; Volkenandt, M.; Lugo, J.; Prioleau, P. G.; Albino, A. P., Overexpression of p53 protein in basal cell carcinomas of human skin. *Am J Pathol* **1992,** 141, (1), 25-9.

101. Stoyanova, T.; Roy, N.; Bhattacharjee, S.; Kopanja, D.; Valli, T.; Bagchi, S.; Raychaudhuri, P., p21 cooperates with DDB2 protein in suppression of ultraviolet ray-induced skin malignancies. *J Biol Chem* **2012,** 287, (5), 3019-28.

102. Macip, S.; Igarashi, M.; Fang, L.; Chen, A.; Pan, Z. Q.; Lee, S. W.; Aaronson, S. A., Inhibition of p21-mediated ROS accumulation can rescue p21-induced senescence. *Embo J* **2002,** 21, (9), 2180-8.

103. Bunz, F.; Dutriaux, A.; Lengauer, C.; Waldman, T.; Zhou, S.; Brown, J. P.; Sedivy, J. M.; Kinzler, K. W.; Vogelstein, B., Requirement for p53 and p21 to sustain G2 arrest after DNA damage. *Science* **1998,** 282, (5393), 1497-501.

104. Di Leonardo, A.; Linke, S. P.; Clarkin, K.; Wahl, G. M., DNA damage triggers a prolonged p53-dependent G1 arrest and long-term induction of Cip1 in normal human fibroblasts. *Genes Dev* **1994,** 8, (21), 2540-51.

105. Waldman, T.; Kinzler, K. W.; Vogelstein, B., p21 is necessary for the p53-mediated G1 arrest in human cancer cells. *Cancer Res* **1995,** 55, (22), 5187-90.

106. Barsotti, A. M.; Prives, C., Pro-proliferative FoxM1 is a target of p53-mediated repression. *Oncogene* **2009,** 28, (48), 4295-305.

107. Wang, I. C.; Chen, Y. J.; Hughes, D.; Petrovic, V.; Major, M. L.; Park, H. J.; Tan, Y.; Ackerson, T.; Costa, R. H., Forkhead box M1 regulates the transcriptional network of genes essential for mitotic progression and genes encoding the SCF (Skp2-Cks1) ubiquitin ligase. *Mol Cell Biol* **2005,** 25, (24), 10875-94.

108. Wierstra, I.; Alves, J., FOXM1, a typical proliferation-associated transcription factor. *Biol Chem* **2007,** 388, (12), 1257-74.

109. Janda, E.; Lehmann, K.; Killisch, I.; Jechlinger, M.; Herzig, M.; Downward, J.; Beug, H.; Grunert, S., Ras and TGF[beta] cooperatively regulate epithelial cell

plasticity and metastasis: dissection of Ras signaling pathways. *J Cell Biol* **2002,** 156, (2), 299-313.

110. Ansieau, S.; Bastid, J.; Doreau, A.; Morel, A. P.; Bouchet, B. P.; Thomas, C.; Fauvet, F.; Puisieux, I.; Doglioni, C.; Piccinin, S.; Maestro, R.; Voeltzel, T.; Selmi, A.; Valsesia-Wittmann, S.; Caron de Fromentel, C.; Puisieux, A., Induction of EMT by twist proteins as a collateral effect of tumor-promoting inactivation of premature senescence. *Cancer Cell* **2008,** 14, (1), 79-89.

111. Smit, M. A.; Peeper, D. S., Epithelial-mesenchymal transition and senescence: two cancer-related processes are crossing paths. *Aging (Albany NY)* **2010,** 2, (10), 735-41.

112. Liu, M.; Casimiro, M. C.; Wang, C.; Shirley, L. A.; Jiao, X.; Katiyar, S.; Ju, X.; Li, Z.; Yu, Z.; Zhou, J.; Johnson, M.; Fortina, P.; Hyslop, T.; Windle, J. J.; Pestell, R. G., p21CIP1 attenuates Ras- and c-Myc-dependent breast tumor epithelial mesenchymal transition and cancer stem cell-like gene expression in vivo. *Proc Natl Acad Sci U S A* **2009,** 106, (45), 19035-9.

113. Ohashi, S.; Natsuizaka, M.; Wong, G. S.; Michaylira, C. Z.; Grugan, K. D.; Stairs, D. B.; Kalabis, J.; Vega, M. E.; Kalman, R. A.; Nakagawa, M.; Klein-Szanto, A. J.; Herlyn, M.; Diehl, J. A.; Rustgi, A. K.; Nakagawa, H., Epidermal growth factor receptor and mutant p53 expand an esophageal cellular subpopulation capable of epithelial-to-mesenchymal transition through ZEB transcription factors. *Cancer Res* **2010,** 70, (10), 4174-84.

114. Leibovitz, A.; Stinson, J. C.; McCombs, W. B., 3rd; McCoy, C. E.; Mazur, K. C.; Mabry, N. D., Classification of human colorectal adenocarcinoma cell lines. *Cancer Res* **1976,** 36, (12), 4562-9.

115. Kubens, B. S.; Zanker, K. S., Differences in the migration capacity of primary human colon carcinoma cells (SW480) and their lymph node metastatic derivatives (SW620). *Cancer Lett* **1998,** 131, (1), 55-64.

116. Sahlgren, C.; Gustafsson, M. V.; Jin, S.; Poellinger, L.; Lendahl, U., Notch signaling mediates hypoxia-induced tumor cell migration and invasion. *Proc Natl Acad Sci U S A* **2008,** 105, (17), 6392-7.

117. Pino, M. S.; Kikuchi, H.; Zeng, M.; Herraiz, M. T.; Sperduti, I.; Berger, D.; Park, D. Y.; Iafrate, A. J.; Zukerberg, L. R.; Chung, D. C., Epithelial to mesenchymal transition is impaired in colon cancer cells with microsatellite instability. *Gastroenterology* **2010,** 138, (4), 1406-17.

118. Labianca, R.; Beretta, G. D.; Kildani, B.; Milesi, L.; Merlin, F.; Mosconi, S.; Pessi, M. A.; Prochilo, T.; Quadri, A.; Gatta, G.; de Braud, F.; Wils, J., Colon cancer. *Crit Rev Oncol Hematol* **2010,** 74, (2), 106-33.

119. Gonzalez-Moreno, O.; Lecanda, J.; Green, J. E.; Segura, V.; Catena, R.; Serrano, D.; Calvo, A., VEGF elicits epithelial-mesenchymal transition (EMT) in prostate intraepithelial neoplasia (PIN)-like cells via an autocrine loop. *Exp Cell Res* **2010,** 316, (4), 554-67.

120. Li, Y.; Dai, C.; Wu, C.; Liu, Y., PINCH-1 promotes tubular epithelial-to-mesenchymal transition by interacting with integrin-linked kinase. *J Am Soc Nephrol* **2007,** 18, (9), 2534-43.

121. Le May, N.; Mota-Fernandes, D.; Velez-Cruz, R.; Iltis, I.; Biard, D.; Egly, J. M., NER factors are recruited to active promoters and facilitate chromatin modification for transcription in the absence of exogenous genotoxic attack. *Mol Cell* **2010,** 38, (1), 54-66.

122. Spaderna, S.; Schmalhofer, O.; Wahlbuhl, M.; Dimmler, A.; Bauer, K.; Sultan, A.; Hlubek, F.; Jung, A.; Strand, D.; Eger, A.; Kirchner, T.; Behrens, J.; Brabletz, T., The transcriptional repressor ZEB1 promotes metastasis and loss of cell polarity in cancer. *Cancer Res* **2008,** 68, (2), 537-44.

123. Trachootham, D.; Zhou, Y.; Zhang, H.; Demizu, Y.; Chen, Z.; Pelicano, H.; Chiao, P. J.; Achanta, G.; Arlinghaus, R. B.; Liu, J.; Huang, P., Selective killing of oncogenically transformed cells through a ROS-mediated mechanism by beta-phenylethyl isothiocyanate. *Cancer Cell* **2006,** 10, (3), 241-52.

124. Hu, R.; Kim, B. R.; Chen, C.; Hebbar, V.; Kong, A. N., The roles of JNK and apoptotic signaling pathways in PEITC-mediated responses in human HT-29 colon adenocarcinoma cells. *Carcinogenesis* **2003,** 24, (8), 1361-7.

125. Berube, N. G.; Smith, J. R.; Pereira-Smith, O. M., The genetics of cellular senescence. *Am J Hum Genet* **1998,** 62, (5), 1015-9.

126. Roninson, I. B., Oncogenic functions of tumour suppressor p21(Waf1/Cip1/Sdi1): association with cell senescence and tumour-promoting activities of stromal fibroblasts. *Cancer Lett* **2002,** 179, (1), 1-14.

127. Preto, A.; Singhrao, S. K.; Haughton, M. F.; Kipling, D.; Wynford-Thomas, D.; Jones, C. J., Telomere erosion triggers growth arrest but not cell death in human cancer cells retaining wild-type p53: implications for antitelomerase therapy. *Oncogene* **2004,** 23, (23), 4136-45.

128. Wang, Y.; Blandino, G.; Givol, D., Induced p21waf expression in H1299 cell line promotes cell senescence and protects against cytotoxic effect of radiation and doxorubicin. *Oncogene* **1999,** 18, (16), 2643-9.

129. Chen, Q. M.; Bartholomew, J. C.; Campisi, J.; Acosta, M.; Reagan, J. D.; Ames, B. N., Molecular analysis of H2O2-induced senescent-like growth arrest in normal human fibroblasts: p53 and Rb control G1 arrest but not cell replication. *Biochem J* **1998,** 332 (Pt 1), 43-50.

130. Serrano, M.; Blasco, M. A., Putting the stress on senescence. *Curr Opin Cell Biol* **2001,** 13, (6), 748-53.

131. Yaswen, P.; Campisi, J., Oncogene-induced senescence pathways weave an intricate tapestry. *Cell* **2007,** 128, (2), 233-4.

132. Campisi, J.; Vijg, J., Does damage to DNA and other macromolecules play a role in aging? If so, how? *J Gerontol A Biol Sci Med Sci* **2009,** 64, (2), 175-8.

133. Starkov, A. A., The role of mitochondria in reactive oxygen species metabolism and signaling. *Ann N Y Acad Sci* **2008,** 1147, 37-52.

134. Irani, K.; Xia, Y.; Zweier, J. L.; Sollott, S. J.; Der, C. J.; Fearon, E. R.; Sundaresan, M.; Finkel, T.; Goldschmidt-Clermont, P. J., Mitogenic signaling mediated by oxidants in Ras-transformed fibroblasts. *Science* **1997,** 275, (5306), 1649-52.

135. Kroemer, G.; Reed, J. C., Mitochondrial control of cell death. *Nat Med* **2000,** 6, (5), 513-9.

136. Cadenas, E., Basic mechanisms of antioxidant activity. *Biofactors* **1997,** 6, (4), 391-7.

137. Park, H. J.; Costa, R. H.; Lau, L. F.; Tyner, A. L.; Raychaudhuri, P., Anaphase-promoting complex/cyclosome-CDH1-mediated proteolysis of the forkhead box M1 transcription factor is critical for regulated entry into S phase. *Mol Cell Biol* **2008,** 28, (17), 5162-71.

138. Park, H. J.; Wang, Z.; Costa, R. H.; Tyner, A.; Lau, L. F.; Raychaudhuri, P., An N-terminal inhibitory domain modulates activity of FoxM1 during cell cycle. *Oncogene* **2008,** 27, (12), 1696-704.

139. Willenbring, H.; Sharma, A. D.; Vogel, A.; Lee, A. Y.; Rothfuss, A.; Wang, Z.; Finegold, M.; Grompe, M., Loss of p21 permits carcinogenesis from chronically damaged liver and kidney epithelial cells despite unchecked apoptosis. *Cancer Cell* **2008,** 14, (1), 59-67.

140. Abbas, T.; Dutta, A., p21 in cancer: intricate networks and multiple activities. *Nat Rev Cancer* **2009,** 9, (6), 400-14.

141. Halasi, M.; Gartel, A. L., A novel mode of FoxM1 regulation: positive auto-regulatory loop. *Cell Cycle* **2009,** 8, (12), 1966-7.

142. Chen, Y. J.; Dominguez-Brauer, C.; Wang, Z.; Asara, J. M.; Costa, R. H.; Tyner, A. L.; Lau, L. F.; Raychaudhuri, P., A conserved phosphorylation site within the forkhead domain of FoxM1B is required for its activation by cyclin-CDK1. *J Biol Chem* **2009,** 284, (44), 30695-707.

143. Alvarez-Fernandez, M.; Halim, V. A.; Krenning, L.; Aprelia, M.; Mohammed, S.; Heck, A. J.; Medema, R. H., Recovery from a DNA-damage-induced G2 arrest requires Cdk-dependent activation of FoxM1. *EMBO Rep* **2010,** 11, (6), 452-8.

144. Soussi, T.; Lozano, G., p53 mutation heterogeneity in cancer. *Biochem Biophys Res Commun* **2005,** 331, (3), 834-42.

145. Vogelstein, B.; Lane, D.; Levine, A. J., Surfing the p53 network. *Nature* **2000,** 408, (6810), 307-10.

146. Schmitt, C. A.; Fridman, J. S.; Yang, M.; Lee, S.; Baranov, E.; Hoffman, R. M.; Lowe, S. W., A senescence program controlled by p53 and p16INK4a contributes to the outcome of cancer therapy. *Cell* **2002,** 109, (3), 335-46.

147. Vazquez, A.; Bond, E. E.; Levine, A. J.; Bond, G. L., The genetics of the p53 pathway, apoptosis and cancer therapy. *Nat Rev Drug Discov* **2008,** 7, (12), 979-87.

148. Vergel, M.; Marin, J. J.; Estevez, P.; Carnero, A., Cellular senescence as a target in cancer control. *J Aging Res* **2010,** 2011, 725365.

149. Cheung, P.; Allis, C. D.; Sassone-Corsi, P., Signaling to chromatin through histone modifications. *Cell* **2000,** 103, (2), 263-71.

150. Zhong, S. P.; Ma, W. Y.; Dong, Z., ERKs and p38 kinases mediate ultraviolet B-induced phosphorylation of histone H3 at serine 10. *J Biol Chem* **2000,** 275, (28), 20980-4.

151. Takebayashi, Y.; Nakayama, K.; Kanzaki, A.; Miyashita, H.; Ogura, O.; Mori, S.; Mutoh, M.; Miyazaki, K.; Fukumoto, M.; Pommier, Y., Loss of heterozygosity of nucleotide excision repair factors in sporadic ovarian, colon and lung carcinomas: implication for their roles of carcinogenesis in human solid tumors. *Cancer Lett* **2001,** 174, (2), 115-25.

152. Iacopetta, B., TP53 mutation in colorectal cancer. *Hum Mutat* **2003,** 21, (3), 271-6.

153. Borinstein, S. C.; Conerly, M.; Dzieciatkowski, S.; Biswas, S.; Washington, M. K.; Trobridge, P.; Henikoff, S.; Grady, W. M., Aberrant DNA methylation occurs in

colon neoplasms arising in the azoxymethane colon cancer model. *Mol Carcinog* **2010,** 49, (1), 94-103.

154. Kim, T.; Veronese, A.; Pichiorri, F.; Lee, T. J.; Jeon, Y. J.; Volinia, S.; Pineau, P.; Marchio, A.; Palatini, J.; Suh, S. S.; Alder, H.; Liu, C. G.; Dejean, A.; Croce, C. M., p53 regulates epithelial-mesenchymal transition through microRNAs targeting ZEB1 and ZEB2. *J Exp Med* **2011,** 208, (5), 875-83.

155. Shaheen, R. M.; Davis, D. W.; Liu, W.; Zebrowski, B. K.; Wilson, M. R.; Bucana, C. D.; McConkey, D. J.; McMahon, G.; Ellis, L. M., Antiangiogenic therapy targeting the tyrosine kinase receptor for vascular endothelial growth factor receptor inhibits the growth of colon cancer liver metastasis and induces tumor and endothelial cell apoptosis. *Cancer Res* **1999,** 59, (21), 5412-6.

156. Kwok, W. K.; Ling, M. T.; Yuen, H. F.; Wong, Y. C.; Wang, X., Role of p14ARF in TWIST-mediated senescence in prostate epithelial cells. *Carcinogenesis* **2007,** 28, (12), 2467-75.

157. Brabletz, S.; Brabletz, T., The ZEB/miR-200 feedback loop--a motor of cellular plasticity in development and cancer? *EMBO Rep* **2010,** 11, (9), 670-7.

158. Vega, S.; Morales, A. V.; Ocana, O. H.; Valdes, F.; Fabregat, I.; Nieto, M. A., Snail blocks the cell cycle and confers resistance to cell death. *Genes Dev* **2004,** 18, (10), 1131-43.

159. Hu, C. T.; Wu, J. R.; Chang, T. Y.; Cheng, C. C.; Wu, W. S., The transcriptional factor Snail simultaneously triggers cell cycle arrest and migration of human hepatoma HepG2. *J Biomed Sci* **2008,** 15, (3), 343-55.

160. Mejlvang, J.; Kriajevska, M.; Vandewalle, C.; Chernova, T.; Sayan, A. E.; Berx, G.; Mellon, J. K.; Tulchinsky, E., Direct repression of cyclin D1 by SIP1 attenuates cell cycle progression in cells undergoing an epithelial mesenchymal transition. *Mol Biol Cell* **2007,** 18, (11), 4615-24.

161. Martel, C.; Harper, F.; Cereghini, S.; Noe, V.; Mareel, M.; Cremisi, C., Inactivation of retinoblastoma family proteins by SV40 T antigen results in creation of a hepatocyte growth factor/scatter factor autocrine loop associated with an epithelial-fibroblastoid conversion and invasiveness. *Cell Growth Differ* **1997,** 8, (2), 165-78.

162. Batsche, E.; Muchardt, C.; Behrens, J.; Hurst, H. C.; Cremisi, C., RB and c-Myc activate expression of the E-cadherin gene in epithelial cells through interaction with transcription factor AP-2. *Mol Cell Biol* **1998,** 18, (7), 3647-58.

163. Arima, Y.; Inoue, Y.; Shibata, T.; Hayashi, H.; Nagano, O.; Saya, H.; Taya, Y., Rb depletion results in deregulation of E-cadherin and induction of cellular phenotypic changes that are characteristic of the epithelial-to-mesenchymal transition. *Cancer Res* **2008,** 68, (13), 5104-12.

164. Wang, S. P.; Wang, W. L.; Chang, Y. L.; Wu, C. T.; Chao, Y. C.; Kao, S. H.; Yuan, A.; Lin, C. W.; Yang, S. C.; Chan, W. K.; Li, K. C.; Hong, T. M.; Yang, P. C., p53 controls cancer cell invasion by inducing the MDM2-mediated degradation of Slug. *Nat Cell Biol* **2009,** 11, (6), 694-704.

VITA

NAME: NILOTPAL ROY

EDUCATION: B.Sc, Zoology, University of Calcutta, Calcutta, India ,2004

M. Sc, Biochemistry, University of Calcutta, India, 2006

HONORS: UIC Deans' Scholar Award, 2010

ABSTRACTS: 1. **Roy N**, Raychaudhuri P. Reduced expression of DDB2 promotes epithelial to mesenchymal transition in colon cancer. AACR Annual meeting, March31-April4, 2012.

2. **Roy N**, Raychaudhuri P. Reduced expression of DDB2 promotes epithelial to mesenchymal transition in colon cancer. University of Illinois cancer research forum, March 6, 2012.

3. **Roy N**, Stoyanova T, Bhattacharjee S, Kopanja D, Valli T, Bagchi S and Raychaudhuri P. p21 cooperates with DDB2 in suppression of UV- induced Skin Cancer. UIC College of Medicine Research Forum, Nov 11, 2011.

4. **Roy N**, Bhattacharjee S, Bhat UG, Kopanja D, Bagchi S and Raychaudhuri P. Role of DDB2 in Colon Cancer EMT. (*Oral Presentation) Annual Retreat, University of Illinois at Chicago, Oct 1-2, 2011.

5. **Roy N**, Stoyanova T, Bhattacharjee S, Kopanja D, Valli T, Bagchi S and Raychaudhuri P. p21 cooperates with DDB2 in suppression of UV- induced Skin Cancer. Mechanisms and Models of Cancer No 6, Salk Institute, August 10- August 14, 2011

6. **Roy N**, Stoyanova T, Kopanja D, Bagchi S and Raychaudhuri P. DDB2, a critical mediator of Reactive Oxygen Species. ASBMB Annual Meeting, April 9-April 13, 2011.

7. **Roy N**, Stoyanova T, Dominguez-Brauer C, Park HJ, Bagchi S and Raychaudhuri P.DDB2 plays critical role in apoptosis and Premature Senescence following DNA damage. The cell Cycle. Cold Spring Harbor symposia. May 18-May 22, 2010.

Vita (Continued)

8. **Roy N**, Stoyanova T, Dominguez-Brauer C, Park HJ, Bagchi S and Raychaudhuri P. DDB2, an Essential Mediator of Oxidative Stress and Premature Senescence. Graduate and Professional Research Forum. University of Illinois at Chicago. April 19, 2010.

9. **Roy N**, Stoyanova T, Dominguez-Brauer C, Park HJ, Bagchi S and Raychaudhuri P. DDB2, an Essential Mediator of Oxidative Stress and Premature Senescence. New Insights into Healthspan and Diseases of Aging: From Molecular to Functional Senescence. Keystone symposia. Jan 31- Feb 5, 2010.

10. **Roy N**, Stoyanova T, Dominguez-Brauer C, Park HJ, Bagchi S and Raychaudhuri P. DDB2, an Essential Mediator of Oxidative Stress and Premature Senescence. Annual retreat. University of Illinois at Chicago. October 17-18, 2009.

11. **Roy N**, Stoyanova T, Bardhan I, Bagchi S and Raychaudhuri P. Role of DDB2 in Replicative Senescence. Graduate and Professional Research Forum. University of Illinois at Chicago. April 18, 2008.

PUBLICATIONS: 1. **Roy, N.**; Bagchi, S. and Raychaudhuri, P., Damaged DNA Binding Protein 2 in ROS regulation and premature senescence. *Int J Mol Sc* **2012**, (in press)

2. **Roy. N.***; Stoyanova, T.*; Bhattacharjee, S.; Kopanja, D.; Valli, T.; Bagchi, S. and Raychaudhuri, P., p21 Co-operates with DDB2 in suppression of UV induced skin malignancies. *J Biol Chem* **2012**, Jan 27; 287 (5): 3019-28 (* equally contributed)

3. Kopanja, D.; **Roy, N.**; Stoyanova, T.; Hess, R.A.; Bagchi, S. and Raychaudhuri, P., Cul4a is essential for spermatogenesis and male fertility. *Dev Biol* **2011**, April 15; 352 (2): 278-87.

4. **Roy, N.**; Stoyanova, T.; Dominguez-Brauer, C.; Park, J.H.; Bagchi, S. and Raychaudhuri, P., DDB2, an essential mediator of Premature Senescence. *Mol Cell Biol* **2010** June 30; (11): 2681- 92 (Selected as MCB Spotlight)

5. Stoyanova, T.; **Roy, N.**; Kopanja, D.; Bagchi, S. and Raychaudhuri, P., DDB2 in nucleotide excision repair and DNA damage response. *Cell Cycle* **2009**, 8(24): 4067- 71.

Vita (Continued)

6. Stoyanova, T.; **Roy, N.**; Kopanja, D.; Bagchi, S. and Raychaudhuri, P., DDB2 decides cell fate following DNA damage. *Proc Natl Acad Sci USA* **2009**, 106(26): 10690-5.